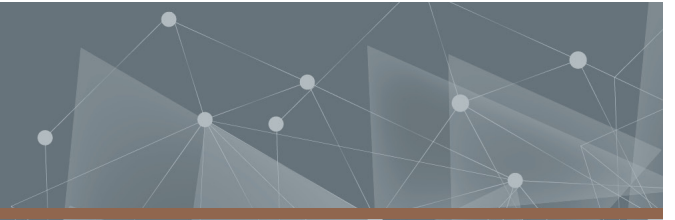




CHALMERS
UNIVERSITY OF TECHNOLOGY



Thermal Management of a Battery Electric Vehicle

How thermal management strategies can improve the performance of a battery electric vehicle for various driving cycles and conditions

Master's thesis in Automotive Engineering

JONATHAN LINDEROTH

DEPARTMENT OF MECHANICS AND MARITIME SCIENCES

CHALMERS UNIVERSITY OF TECHNOLOGY

Gothenburg, Sweden 2021

www.chalmers.se

MASTER'S THESIS 2021

Thermal Management of a Battery Electric Vehicle

How thermal management strategies can improve the performance of a battery electric vehicle for various driving cycles and conditions

JONATHAN LINDEROTH



CHALMERS
UNIVERSITY OF TECHNOLOGY

Department of Mechanics and Maritime Sciences
Division of Vehicle Engineering and Autonomous Systems
CHALMERS UNIVERSITY OF TECHNOLOGY
Gothenburg, Sweden 2021

Thermal management of a battery electric vehicle

JONATHAN LINDEROTH

© JONATHAN LINDEROTH, 2021

Supervisor and Examiner: Jelena Andric, VEAS

Industry Supervisor: Gunnar Latz, Siemens

Master's thesis in Automotive Engineering 2021:21

Department of Mechanical and Maritime Sciences

Division of Vehicle Engineering and Autonomous Systems

Chalmers University of Technology

SE-412 96 Göteborg

Sweden

Phone: +46 (0)31-772 1000

Abstract

The automotive industry is developing due to changes in climate, legislations and customer demands. Battery electric vehicles (BEVs) are becoming more important with their zero tailpipe emissions and their share is expected to rise in the future. A major problem concerning BEVs is the driving range which is affected by demanding ambient conditions and puts the thermal management system (TMS) in focus. The TMS has an important role to ensure that the battery, electric motor and cabin compartment are kept in certain temperature intervals where comfort, efficiency and safety are optimal.

In this thesis a complete system-level model for a BEV and its TMS is developed in Amesim simulation software. In Amesim vehicle-level simulations are performed to investigate different thermal management strategies to analyze vehicle energy efficiency. First the model validation is performed for different BEV models using their official data for driving range. The trends were well captured for WLTP, EPA, NYCC, Artemis highway and Artemis urban driving cycles at the ambient temperatures -15°C , 0°C , 20°C and 40°C .

The model is employed to analyze the effects of different TM strategies including preconditioning, heating the battery for regenerative braking, limiting the current-peaks and a holistic approach where the battery and electric motor share a common thermal management circuit. Simulation results show that preconditioning BEVs by heating up or cooling down the components provides a major difference compared to not precondition where range can drop significantly depending on driving cycle and ambient conditions. Using the energy from the battery to heat it up shows great potential, however, the outcome depends on initial and target temperatures, battery energy levels, battery size and the driving cycle. Provided this information the vehicle could estimate when to heat up the battery, which can result in between 10-250 % being recuperated of the invested energy for heating by regenerative braking. Limiting the current-peaks and using the holistic approach results in up to 2.5% energy savings increasing driving range in certain driving cycles and temperatures. A combination of limiting the current peaks and using the same thermal management circuit for the motor and battery results in increased range in all driving cycles and 4 temperature levels except EPA. The increased energy savings and range were below 1% in most scenarios but reached 2.1% in the best case.

By implementing these strategies the efficiency in BEVs can be increased by several percent, which if implemented at large scale can impact the total emissions and contribute to a better experience for customers especially in demanding conditions.

Keywords: Thermal management, thermal management strategy, battery electric vehicle, system simulation, Amesim, virtual testing.

Acknowledgements

While this Master's thesis only has my name as the author, it would never have been possible to write without the very generous and kind support I have received throughout the project and during my time as a student. Support can be provided in many different ways and in a year where the global pandemic has been the main topic with plenty of challenges along with it, this thesis is the work, both directly and indirectly, of many different people.

I would like to start by thanking my examiner and supervisor Jelena Andric for very helpful advice and support throughout the thesis. Receiving feedback, recommendations and direction while writing this thesis has been a large factor behind the results of this report and have made a big difference.

I want to thank Gunnar Latz, industrial supervisor from Siemens who been very helpful with providing valuable guidance how to work with the Amesim software with tips and advice that made the simulations possible.

I would also like to thank Lennart Löfdahl, Professor emeritus who provided advice with the report and how to proceed with the thesis based on his long experience within the subject. The thesis was on paper conducted alone but there are several more people who have been supporting me through discussions, opinions and company that indirectly have contributed to reaching better final result and they most likely know who they are.

Finally, I would like to thank my family for their unconditional support throughout my studies. For obvious reasons I would never be able to write this thesis without them and will always be grateful for the support I have received in many different ways. In moments of doubt, uncertainty and adversity it is comforting and important knowing that there always are people caring for you.

Abbreviations

BEV - Battery Electric Vehicle
EV - Electric Vehicle
PHEV - Plug-in Hybrid Electric Vehicle
ZLEV - Zero to Low Emission Vehicles
TM - Thermal Management
TMS - Thermal Management System
COP - Coefficient Of Performance
ICE - Internal Combustion Engine
GHG - GreenHouse Gas
ZEV - Zero Emission Vehicle
CO₂ - Carbon Dioxide
PM - Particulate Matter
LCA - Life Cycle Analysis
WTT - Well-To-Tank
TTW - Tank-To-Wheel
CoG - Center of Gravity
HVAC - Heating Ventilation and Air-Conditioning
SOC - State of Charge
NCA - Nickel-Cobalt-Aluminium (cell chemistry)
BMS - Battery Management System
PCM - Phase Change Material
PTC - Positive Temperature Coefficient
PMSM - Permanent Magnetic Synchronous Machine
VCU - Vehicle Control Unit
RPA - Relative Positive Acceleration

Symbols

P_{regen} - Regenerated Power [W]
 T_{wheel} - Torque at the wheel [Nm]
 Ω_{wheel} - Wheel angular velocity [rad/s]
 $F_{traction}$ - Traction force at the wheel [N]
 $F_{external}$ - External forces acting on the vehicle [N]
 F_{acc} - Force due to inertia while accelerating the vehicle [N]
 F_{air} - Force due to air resistance [N]
 F_{grade} - Force due to road gradient resistance [N]
 F_{roll} - Force due to rolling resistance [N]
 $m_{vehicle}$ - Mass of the vehicle [kg]
 $a_{vehicle}$ - Acceleration of the vehicle [m/s²]
 v_{start} - Vehicle's starting velocity [m/s]
 v_{final} - Vehicle's final velocity [m/s]
 C_d - Drag Coefficient []
 $A_{vehicle}$ - Frontal area of the vehicle [m²]
 ρ_{air} - Air density [kg/m³]
 V_{rel} - Relative velocity of the vehicle in relation to ambient air [m/s]
 FT_{amb} - Ambient air temperature [°C]
 g - Gravitational constant at 9.81 [m/s²]
 α - Road angle [°]

C_r - Rolling coefficient []
 S_x - Longitudinal wheel slip []
 r_{wheel} - Wheel radius [m]
 v_x - Longitudinal velocity [m/s]
 F_x - Maximum longitudinal wheel force [N]
 F_z - Vertical force acting on the wheel [N]
 μ - Friction coefficient []
 F_{AB} - Wheel force where A is direction and B position [N]
 h_{CoG} - CoG height from the ground [m]
 $l_{f/r}$ - Distance between front and rear axle to CoG (longitudinal) [m]
 h_{air} - Distance between ground and air resistance position [N]
 P_{rmax} - Maximum regenerative braking due to mechanical limits [W]
 P_{losses} - Power losses inside the battery [W]
 $P_{irreversible}$ - Irreversible power losses inside the battery [W]
 $P_{reversible}$ - Reversible power losses inside the battery [W]
 $I_{battery}$ - Battery current [A]
 $R_{internal}$ - Internal resistance inside the battery [Ω]
 $T_{battery}$ - Battery Temperature [K]
 $U_{battery}$ - Battery voltage [V]
 q_{cond} - Thermal conductivity [W/m²*K]
 $P_{reversible}$ - Reversible power losses inside the battery [W]
 T_{cell} - Cell temperature [$^{\circ}$ C]
 q_{conv} - Thermal convection [W]
 h - heat transfer coefficient [W/m²*K]
 C_p - Specific heat [W/kg*K]
 P_{EM} - Power of electric motor [W]
 T_{EM} - Torque of electric motor [Nm]
 Ω_{EM} - Angular velocity of electric motor [W]
 Ψ_d - d-axis flux linkage [Wb]
 Ψ_q - q-axis flux linkage [Wb]
 i_d - d-axis current [A]
 i_q - q-axis current [A]
 L_d - d-axis inductance [H]
 L_q - q-axis inductance [H]
 P_{wheel} - Power at wheel [W]
 $\eta_{gearbox}$ - gearbox efficiency []
 P_{cu} - Copper losses [W]
 $R_{winding}$ - Resistance in the electric motor winding [Ω]
 I_{em} - RMS current in the electric motor [A]
 R_0 - Reference resistance in the electric motor winding [Ω]
 α_0 - temperature coefficient []
 T_{wire} - Copper winding temperature [$^{\circ}$ C]
 T_{ref} - Reference temperature of the winding [$^{\circ}$ C]
 P_{fe} - Iron losses [W]
 P_h - Hysteresis losses [W]
 P_e - Eddy current losses [W]
 K_h - Hysteresis parameter []
 K_e - Eddy current parameter []
 $Q_{evap,cond}$ - Combined output from evaporator and condenser in HVAC [J]
 $Q_{compressor}$ - Energy used by the compressor [J]

List of Figures

1	Scenarios for different increases in earth's temperature [85]	5
2	Global greenhouse gas emissions and warming scenarios [29]	6
3	Carbon dioxide budget [103]	6
4	Global GHG emissions by sector [81]	7
5	LCA of BEV from IEA [10]	8
6	Polestar 2 LCA [24]	8
7	AAA range losses [8]	10
8	Temperature effects on range[58]	10
9	Energy flow within a battery electric vehicle	11
10	Regenerative braking in UDDS driving cycle compared to mechanical braking	13
11	Longitudinal vehicle model with external forces	14
12	Max regen power from veh. dyn.	18
13	Comparison between external forces	18
14	Battery during discharging and charging	19
15	Internal resistance in various temperatures and SOC from Amesim	20
16	Battery capacity in different temperatures [68]	20
17	Battery aging for 30, 40, 48°C [115]	21
18	SEI layer	21
19	Illustration of different cooling methods [105]	22
20	PMSM losses [118]	24
21	Electric motor cooling [60]	24
22	Energy consumption of different system in a BEV in summer, spring and winter [64]	25
23	PH-diagram R134a Carnot cycle	26
24	Flow scheme for a Carnot cycle	26
25	Thermal management layouts. a) Passengers compartment, b) Battery, c) Electric motor	27
26	Cooling mode with super bottle tesla model 3 (based on [7])	28
27	Heating mode with super bottle tesla model 3 (based on [7])	28

28	V5-model showing the V1-part	29
29	V1-model	29
30	Driver submodel in Amesim	30
31	Driver control from Amesim	30
32	Battery loop in the model	31
33	Battery TM strategy	31
34	Electric motor loop from model	32
35	Motor control from Amesim	32
36	Compressor control from model	33
37	HVAC loop from model	33
38	HV and LV auxiliary load system	34
39	TM strategy used in the model	34
40	WLTP driving cycle profile	35
41	NYCC driving cycle profile	35
42	FTP75 driving cycle profile	36
43	HWFET driving cycle profile	36
44	Artemis highway drive cycle profile	37
45	Artemis urban drive cycle profile	37
46	AAA range for different vehicles and operating scenarios	40
47	Amesim Peak-I model	43
48	Cabin cooling - block diagram	43
49	Regenerative braking control module in Amesim	44
50	Regen-map from Tesla Model 3 [72]	45
51	3D-plane from data points	45
52	Series and parallel TM circuit	47
53	Amesim BEM model	47
54	Model verification - range in WLTP and EPA from official data and simulation	49
55	Model TMS verification - comparison of range with AAA study	50

56	Average power in different driving cycles and conditions	51
57	Energy per distance in different driving cycles and conditions	52
58	WLTP and EPA range	53
59	Normalized range with geotab	53
60	Reduced range in cold conditions	54
61	Reduced range in warm conditions	54
62	Temperature and power consumption with and without preconditioning	55
63	Range difference with Peak-I	56
64	Battery losses difference with Peak-I	56
65	Cabin temperature with Peak-I	56
66	Current form battery with Peak-I	56
67	Invested energy with pre-heating	57
68	Transfer efficiency with pre-heating	57
69	COP for WLTP and 30% SOC	58
70	COP for WLTP and 70% SOC	58
71	COP for HWFET and 30% SOC	58
72	COP for HWFET and 70% SOC	58
73	Range difference with BEM concept	59
74	Artemis Highway average power with BEM	59
75	Artemis highway temp. with BEM	60
76	Copper-losses difference with BEM	60
77	Range difference using a combination of Peak-I and BEM	60
78	WLTP simulation result parameters from Amesim	75
79	Amesim model V.5	76

List of Tables

1	Total life cycle emissions in different countries [109]	8
2	Drag coefficients for battery electric vehicles [47]	16
3	Driver and vehicle parameters for the standard vehicle	30
4	Battery model specifications	31
5	Electric motor characteristics from the model	32
6	HVAC characteristics from the model	33
7	Auxiliary loads characteristics from the model	34
8	Driving cycles parameters	37
9	Small city and large premium BEV range parameters	38
10	Mid-size BEV range parameters	39
11	Polestar 2 dual motor parameters	39
12	Parameters in preconditioning concept	42
13	Regenerative braking various driving cycles	45
14	Model verification difference and standard deviation	50
15	Mazda mx30 parameters	77
16	Honda e parameters	77
17	Peugeot 208e parameters	77
18	Renault zoe parameters	78
19	Volkswagen ID.3 parameters	78
20	Volvo xc40 recharge parameters	78
21	Tesla model 3 SR+ parameters	78
22	Tesla model Y LR parameters	79
23	Volkswagen ID.4 parameters	79
24	Hyundai kona parameters	79
25	Audi e-tron parameters	79
26	Tesla model X parameters	80
27	Mercedes EQS 450+ parameters	80

Contents

1	Introduction	1
1.1	Background	1
1.2	Virtual testing through Amesim simulations	2
1.3	Aim and purpose of thesis	2
1.4	Ethical perspective	3
2	General background	5
2.1	The environmental background	5
2.1.1	Emissions from battery electric vehicles	6
2.1.2	Life cycle of electric vehicles	7
2.2	Policies, legislation and market	8
2.2.1	Electric vehicles post 2030	9
2.2.2	Demands on electric vehicles	9
2.3	The importance of thermal management for performance	10
3	Theoretical background	11
3.1	Basics of a battery electric vehicle	11
3.1.1	Regenerative braking	12
3.2	Vehicle dynamics and external forces	13
3.2.1	Inertia forces	15
3.2.2	Air resistance	15
3.2.3	Road grade resistance	16
3.2.4	Rolling resistance	17
3.2.5	Limiting vehicle dynamics	17
3.3	Lithium-ion battery	19
3.3.1	Battery thermal management	20
3.3.2	Thermal management methods	22
3.4	Electric motor	23

3.4.1	Losses in electric motors	23
3.4.2	Electric motor thermal management	25
3.5	Passenger compartment	25
3.5.1	Cooling passengers compartment	25
3.5.2	Heating of passengers compartment	26
3.6	Holistic thermal management system	27
4	Modeling and simulation methodology	29
4.1	Methodology	29
4.2	The Amesim model of a BEV	30
4.2.1	Driver and vehicle	30
4.2.2	Battery loop	31
4.2.3	Electric motor loop	32
4.2.4	HVAC and control system	32
4.2.5	High and low voltage auxiliary	33
4.3	Driving cycles and ambient conditions	34
4.3.1	WLTP and NYCC driving cycles	35
4.3.2	UDDS and HWFET driving cycles	35
4.3.3	Real world based driving cycles	36
4.4	Driving conditions	37
4.5	Verification of Amesim model	38
4.5.1	Verification of TMS	40
5	Thermal management simulations and concepts	41
5.1	Driving cycles and conditions in simulations	41
5.2	Preconditioning - the effect of initial temperatures	41
5.3	Peak I - minimizing the peak currents	42
5.4	Re-gen - heating up battery for regenerative braking	43
5.5	BEM - connecting components in a holistic approach	46

6	Results	49
6.1	Amesim model verification results	49
6.2	Driving cycles and ambient temperatures results	51
6.3	Preconditioning concept results	54
6.4	Peak-I concept results	55
6.5	Heating for re-gen concept results	57
6.6	BEM concept results	59
7	Discussion	61
7.1	Background and validation of the Amesim model	61
7.2	Cycles, conditions and concepts	62
8	Conclusion	65

1 Introduction

In this chapter an introduction to the thesis will be presented including background, virtual testing, aim, purpose and ethical perspective. In the background a brief introduction to the subject is provided including the role of vehicle thermal management system. The importance of virtual testing and model-based approach for vehicle development are described and the questions intended to be answered throughout the thesis are presented. Finally, the ethical perspective brings some additional background which should be included while working within the subject.

1.1 Background

The automotive sector is developing at rapid pace with electromobility as a large focus area. Electromobility is a paradigm-shift in the industry with a shift from conventional propulsion technologies to electric vehicles. The market grows fast and manufacturers already have or are about to launch new models equipped with electric propulsion [19]. A large driving force behind this development comes from the environmental crisis where emissions from, amongst others, the transportation sector lead to global warming. Electric vehicles bring advantages with their high efficiency and zero emissions during driving. With increasing demands from legislators, awareness from customers and a changing climate these advantages make manufacturers head towards battery electric vehicles (BEVs).

BEVs use a battery as energy storage and electric motors for propulsion as main components. Compared to conventional vehicles running on fossil fuels, BEVs are more efficient and emit no emissions while driving. The emissions occur mostly during manufacturing and electricity production and analysis of the complete life cycle can be utilized. However one main drawback is typically the range anxiety from customers which is an obstacle for adapting to BEVs. BEVs are extra sensitive to extreme temperatures, experiencing reduced driving range especially in colder climates. In order to mitigate this issue, a thermal management system (TMS) is often used. The TMS also affects overall safety by keeping components cool, comfort by providing optimal temperature for passengers and costs by prolonging components life by avoiding overheating and wear. A well designed TMS for BEVs is therefore of high importance and relevance.

A wider market around the world living in different climates and conditions requires a TMS designed to keep its sensitive components within certain temperature range. The battery operates within a specific temperature range, the motors and electronics within another and similar for the passenger cabin. Keeping these vehicle components within their respective operating temperature range increases both efficiency and the overall safety. Demanding ambient conditions with sub-zero and hot temperatures result in using a lot of energy from the battery to control the temperatures, affecting the driving range of the BEV. Combustion engine have a substantially lower efficiency with high heat losses which can be used to heat the passenger compartment and power the auxiliary loads. In BEVs with its high efficiency and low heat losses the traction battery provides the energy, making it more sensitive to external factors compared to conventional vehicles. A TMS designed with this in mind can increase the driving range at demanding conditions by optimising energy flow considering holistic effects and utilize efficient components. A trend within the industry is to connect the components and transfer energy between them to either cool or heat them to desired temperatures, thus saving energy and increasing driving range. By investigating various thermal management strategies in real-life scenarios, a better understanding and improved total efficiency can be achieved.

A wide range of strategies for thermal management can be used to optimize the energy flow, leading to an increased efficiency and range of a BEV in varying conditions and scenarios. By improving its thermal management system and reducing the impact of ambient temperatures, the emissions from the electricity production and the vehicle manufacturing process can be decreased and more people can take advantage of the many benefits of BEVs.

1.2 Virtual testing through Amesim simulations

Siemens Amesim is a simulation software that is used for modeling and analysis of multidomain systems and is well-adapted for simulations of vehicles with electrified drivetrains. In this thesis a complete model of a BEV together with its TMS was built from the system perspective and simulated in different driving conditions and driving scenarios.

In this thesis a simulation model of a BEV with a TMS is built in Amesim. A step-by-step methodology with gradual improvements was generated, resulting in a complete vehicle model used for performing simulations to virtually test TM strategies. Due to lack of experimental data, vehicle data and information about control strategies, the models could not undergo rigorous validation procedures. Nevertheless, the simulation results were compared to the official data for the purpose of capturing and identifying the trends.

A model with correct specifications, input data and test data can be used in virtual testing. Virtual testing is a growing concept within the automotive industry where performance of a vehicle can be tested in shorter time and at lower cost compared to physical testing. In a world where new technologies such as electromobility are emerging with high demands in time-to-market deliveries, virtual testing is highly compelling. In the initial design phase such models can be used to understand the interaction between vehicle subsystems and investigate different concepts. By utilizing virtual models the cost can also decrease since the need for physical testing is reduced.

Once the Amesim vehicle model was validated, it could be used as a base-model to construct concepts for different thermal management strategies. These concept-models were used for further simulations to investigate the performance of the thermal management strategies.

1.3 Aim and purpose of thesis

The aim of this thesis is to investigate how a TMS in a BEV affects its performance and how it can be designed to increase the overall efficiency of the vehicle. The goal was to build a model of a BEV in Amesim with a complete TMS, perform simulations in transient driving cycles and other situations common for a vehicle. Several TM concepts are developed based on the trends within the automotive industry and from research within the topic and then tested and evaluated for the overall efficiency. The following questions are answered by this thesis:

- How do various ambient temperatures affect efficiency of a BEV and why?
- In different driving cycles, how does the electric vehicle perform and why?
- How well does the model correlate with the official data?
- Which holistic effects and TM strategies can be utilized within the TMS to achieve greater efficiency?
- Which strategy achieves the best result and what is the theoretical background explaining the findings?
- How can the TMS in a BEV affect the overall performance?

1.4 Ethical perspective

Sustainable future should not be valid if it is built by neglecting human rights or moving hazardous emissions to another place on the planet. This thesis concerns BEVs and the major discussion point within the subject is the emissions caused by manufacturing and the well-to-tank emissions. BEVs emit no CO₂-emissions while driving, hence referred to as Zero Emissions Vehicles (ZEVs). Instead, production of electricity becomes more important to lower GHG emissions making the sustainability of BEVs dependent on the source of electricity. In Europe the GHG-emissions from electricity production vary greatly between the countries hence the usage of BEVs could result in higher emissions compared to conventional vehicles using a combustion engine running on fossil fuels [90]. Nevertheless, a TMS in a BEV increases the vehicle efficiency and hence reduces energy consumption and in turn nonlocal emissions.

Another source of emissions is the manufacturing process. The raw materials for components need to be processed or mined from the ground, and in some cases these processes are related to lack of human rights [3]. The minerals are typically for the battery and include cobalt and lithium where most are found in concentrated areas in the world. Most cobalt is mined from the Democratic Republic of Congo [57]. Lithium reserves are situated in South America where 70% are located in the "lithium triangle" consisting of Argentina, Bolivia and Chile. Lithium mining requires large volumes of water and the big mining industries affect local communities where water shortages are becoming more common and the environment is damaged [12]. Some manufacturers are looking into alternative materials for batteries, but an increase in BEVs can require more of these materials and risk escalating the conflict. One solution besides using other materials is battery downsizing, which would result in smaller amounts of materials used, less weight and lower cost of BEVs. It would also decrease the driving range, a crucial parameter for BEVs. Therefore looking into ways of gaining efficiency becomes important and one of the important methods is a well-designed TMS with optimized energy usage.

In summary, there are challenges with building BEVs. Mainly during mining, manufacturing and electricity production where issues occur. BEVs have the potential of contributing to more sustainable transport but in some cases customers might be deceived into thinking they are using sustainable solutions, while the environment is affected by emissions somewhere else. This thesis does not aim toward solving all these ethical issues, but instead investigating one of the major uncertainties concerning BEVs that could assist in reducing their impact. An optimized TMS can increase the efficiency, lower the total impact and improve the overall performance across multiple areas of a BEV.

In 2015 world leaders agreed on 17 global goals to fulfill by 2030, concerning sustainable development in areas such as society and the environment [86]. For electric vehicles goals 11 "Sustainable cities and communities", 12 "Responsible consumption and production" and 13 "Climate action" are particularly interesting. By researching within the field of electric vehicles and their efficiencies, small steps could be taken into fulfilling these goals hence contributing to sustainable way of living.

2 General background

In this chapter a general background for the subject is briefly explained in order to provide a more extensive background and comprehensive explanation of the situation. The environmental aspect including the role of electric vehicles will be explained for a broader understanding of why electric vehicles are relevant for the future. A short background on the uncertainties surrounding BEVs today and a short projection of how the future looks like according to today's research. Besides the environment, other factors that drives the development of electric vehicles along with essential demands to fulfill for customers to purchase a BEV is included.

2.1 The environmental background

Since the industrial revolution in the 19th-century, high amounts of GHG-emissions have been emitted into the atmosphere, causing the temperature to rise by 1.1°C [32]. The rise in temperature has resulted in environmental changes which affects an increasing amount of people, as well as other species negatively [52]. Without any changes in the current rate of emissions emitted to the atmosphere, it is expected that the temperature will rise by up to 4.8°C until 2100. The Paris-agreement was signed in 2015 with the ambition to "limit global warming to well below 2°C , preferably to 1.5°C , compared to pre-industrial levels" [54]. By involving countries all across the globe to unite behind policies it took a step in the right direction to tackle the increasing temperature. However, with the current policies adopted the temperature in 2100 is expected to be $2.8\text{--}3.2^{\circ}\text{C}$, adding all policies from the Paris agreement it will be $2.5\text{--}2.8^{\circ}\text{C}$, which is above the target and can be seen in figure 1.

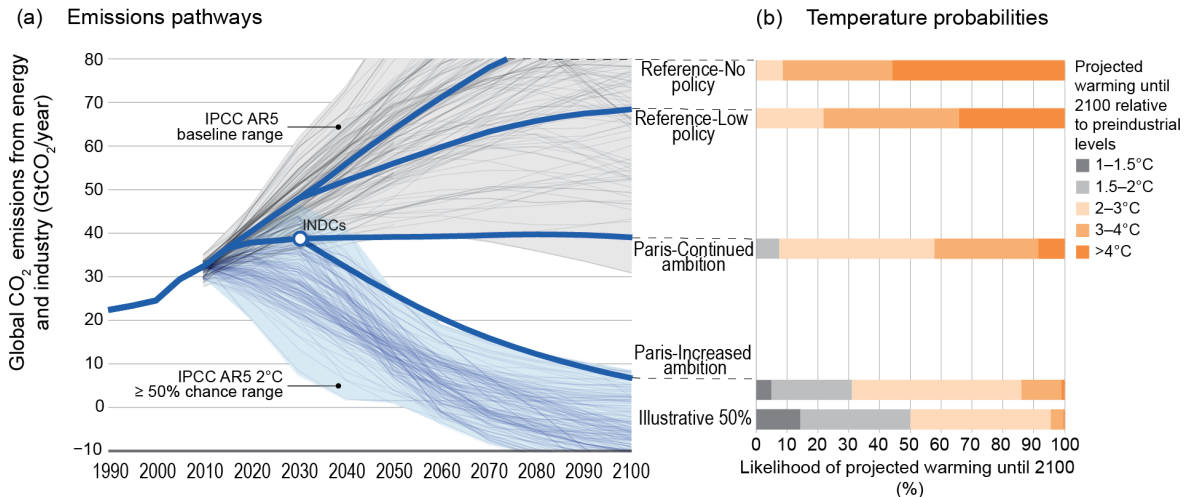


Figure 1: Scenarios for different increases in earth's temperature [85]

In figure 1 potential scenarios of the consequences of several ranges of increased temperatures are presented. Without any policies the expected scenario at 4.8°C is severe, but even with the adopted policies and Paris agreement, the consequences are very dangerous for our planet and its inhabitants. Besides the direct consequences, there are "tipping points" where higher temperatures triggers mechanisms with positive feedback loops, leaving us without control of the environmental changes. Previously it was thought to occur between $4\text{--}5^{\circ}\text{C}$ (i.e. avoidable without policies) but lately scientist claims 2°C are enough, it shows the importance of keeping the temperature below that to remain in control [30].

The increase in temperature is a result of the increased amount of GHG-emissions emitted by humans

since the industrial revolution [25]. Two-thirds of the effects from GHG-emissions are due to carbon dioxide (CO₂). The levels of CO₂ in the atmosphere are well above 400 ppm (parts per million) and has never before exceeded 300 ppm [25].

According to the *Intergovernmental Panel on Climate Change's* (IPCC) special report on global warming of 1.5°C, there was 580Gton of CO₂ left to emit to have a 50% change of staying below 1.5°C increase in temperature [6]. In figures 2 and 3 the scenarios and CO₂-budget are visualized.

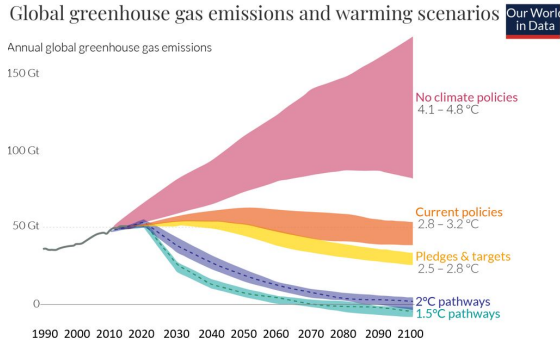


Figure 2: Global greenhouse gas emissions and warming scenarios [29]

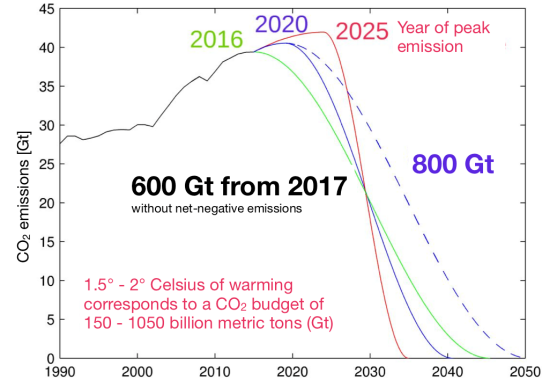


Figure 3: Carbon dioxide budget [103]

To increase the chance from 50% to 66% of staying below 1.5°C the budget instead becomes 420Gton. One of the previously mentioned "positive feedback loops" with melting permafrost releasing methane into the atmosphere has potential of deducting 100Gton from that budget. Since the report was released in 2018, more than three years have passed and by subtracting our emissions since then and using the higher-probability 420Gton budget, there are about 300Gton of CO₂ left to emit [74]. To achieve the target, a massive reduction of carbon dioxide emissions are necessary. According to UN's environment programmes emissions gap report, emissions has to reduce by more than half of today's levels by 2030, a 7.6% reduction every year [110].

Carbon dioxide is not the only emission to reduce, particulate matter (PM) and black carbon are affecting peoples health and contributes to global warming. The particles are in some cases smaller than 2.5 micrometer in diameter (PM_{2.5}) and accesses the lungs causing toxic compounds to enter the bloodstream. On a global level, PM_{2.5} are estimated to lead to 7 million premature deaths [79]. Carbon dioxide is a global affecting pollution, while PM is a local pollution, ICE vehicles driving in the city close to peoples homes and jobs emits PM, leading to worse effects. Black carbon is a type of particulate matter below 2.5micrometer that lasts only a few days in the atmosphere but can absorb a lot of heat energy, leading to near-term warming. Besides being more than 1000 times stronger than CO₂, it can dim sunlight for ecosystems and raise temperature in icy environments by increasing the albedo. Transport accounts for 26% of these emissions and have reduced them by 44% since 2000, but more work is necessary [9].

2.1.1 Emissions from battery electric vehicles

Global emissions the last few years has been 30-35 Gton CO₂ and above 50 Gton CO₂-equivalent emissions [48] [28]. Transportation was responsible for 24% of the total CO₂ emissions, out of which road(passenger)transport including cars accounted for 45%, resulting in 11% of all emissions globally [27]. In figure 4 the global GHG-emissions by sector are shown, 12.1% are due to road transport and shows that a substantial part can be reduced by improving in this sector.

Global GHG Emissions by Sector

2016 global emissions of greenhouse gases
(fuel combustion emissions attributed to energy consumers)

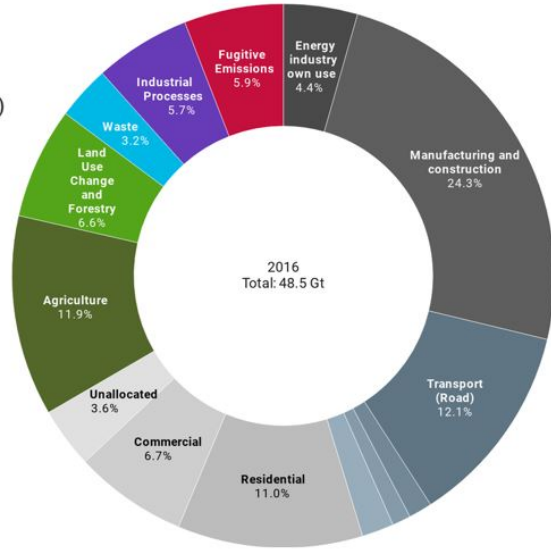
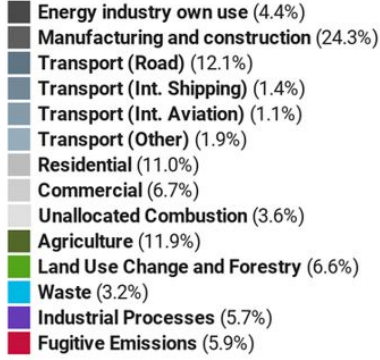


Figure 4: Global GHG emissions by sector [81]

In Europe the situation is similar to the global situation with transport being accountable for 27% of total emissions and passenger cars for 44% out of these [15]. A non-optimal actuality of the transport industry is that it is the only main economic sector that have increased its emissions since 1990 [2]. Additionally, passenger-kilometers traveled are expected to double and car-ownership increase by 60% the next 50 years [27]. With this in mind, a focus on the transport industry and to a large extent passenger vehicles will be important, with increasing travelling each vehicle will have to be even more efficient compared to today.

2.1.2 Life cycle of electric vehicles

Emissions created while using a vehicle are not the only ones to be considered. Manufacturing and end-of-life has become increasingly important with battery electric vehicles on the market. A common dispute regarding BEVs are that while driving creates next to none GHG-emissions, manufacturing of certain components requires much energy and emits a large part. Emissions created during manufacturing, driving and recycling are included in a life cycle analysis (LCA) where the whole process are accounted for and can be used for comparison. Besides manufacturing, there are two terms to know, the well-to-tank (WTT) emissions and tank-to-wheel (TTW) emissions. By only including TTW for BEVs they appear to be zero-emission vehicles, but the WTT emission which includes energy-production often alters the result. Driving a BEV in countries with low CO₂ emissions from renewable energy sources decreases the overall environmental impact, but using fossil fuel for energy-production will drastically increase BEVs environmental impact [109]. Certain life-cycle analyses claims that electric vehicles always will emit less CO₂ even if coal power is used, the benefit is somewhere between 22-81% depending on the case [108]. In figure 5 a comparison of various vehicles including BEV running on a global-mix of electricity of 518g CO₂/kWh, PHEV and fossil fuel cars in their well-to-wheel emissions. If the vehicle range of 200 km is doubled to 400 km a BEV will emit more than a plug-in hybrid vehicle (PHEV).

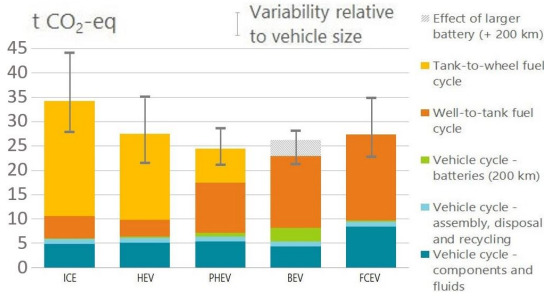


Figure 5: LCA of BEV from IEA [10]

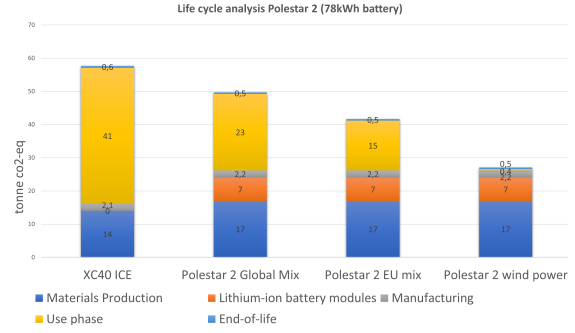


Figure 6: Polestar 2 LCA [24]

In figure 6 a life-cycle analysis conducted by Polestar for their model Polestar 2 is presented. It contains a Volvo xc40 equipped with an ICE as reference along with three different sources of electricity: global, EU and wind. The total emissions using a global mix is close to the ICE vehicle but rapidly drops for the cleaner EU-mix and even more for electricity produced using wind power. The *Polestar 2* is a large vehicle with long range and hence has a big battery, which contributes to higher overall emissions than figure 5. Besides electricity production, the battery production is a substantial part where both its size and origin plays a vital role in the end result.

The global mix at 518g CO₂/kWh is high compared to countries with more renewable energy sources in its electricity production. In table 1 a range of gCO₂/kWh per region is presented with WTT and total emissions compared to figure 5 [109]. From the table it can be seen that source of electricity is a very large factor behind the overall life cycle emissions created by a BEV.

Table 1: Total life cycle emissions in different countries [109]

Electricity Origin	g CO ₂ per kWh	t CO ₂ -eq. WTT emissions	Total life-cycle CO ₂ -eq. emissions
Global	518	14.5	22.8
EU	300	8.4	16.7
Germany	410	11.5	19.8
Poland	650	18.2	26.5
Sweden	20	0.6	8.9

In general, a LCA analysis is highly dependent on its input parameters which are many and difficult to calculate. The battery and electricity production are major factors, but for the vehicle its total driving distance and efficiency also contributes extensively. This will affect the outcome heavily and results in different sources claiming different results.

2.2 Policies, legislation and market

The situation with environmental change and electric vehicles in the transport sector hasn't gone without notice for citizens and policymakers. Besides the Paris agreement in 2015, movements for environmental awareness and legislation to decrease emissions have grown traction. EU adopted a target in April 2021 stating that net zero emissions in 2050 with a 55% decrease in 2030 compared to 1990's levels is the ambition [45]. This is part of the *European Green Deal* and transport has a target of 90% reduced emissions by 2050, with 30 million zero emission vehicles on the roads in 2030 [46]. Zero-to low emission vehicles (ZLEV) are vehicles emitting 0-50 g CO₂ per km and therefore includes BEV. They are part of a complex credit system from EU which allows manufacturers to get extra

economic benefits by producing more of them until 2030, creating incentives for development [44]. Besides this credit system, targets of 95 gCO₂ per km in 2024, a 15% reduction in 2025 and 37.5% reduction in 2030 compared to 2021 are present with additional legislation approaching in 2021 [44]. By developing and selling more BEVs manufacturers both benefits from lower overall CO₂-emissions and the credits system.

2.2.1 Electric vehicles post 2030

In 2021 a number of vehicle manufacturers have announced grand plans for electrification. Besides Tesla and Polestar with focus on electric vehicles today, traditional manufacturers such as Volvo announced they will only sell electric vehicles from 2030 [53]. Governments and other companies are also involved with demands on banning fossil-fuel cars in favor for BEVs [26]. The international council on clean transportation (ICCT) has made reports concerning levels of electrification and a case called *Vision 2050*. The level of electrification is investigated in the report *The role of the European Union's vehicle CO₂ standards in achieving the European Green Deal*, a baseline scenario is compared to 100% ZEV sales in 2030, 2035 and 2040 [77]. These scenarios are named after their ambition where 2040 is lower ambition, 2035 is moderate ambition and 2030 is higher ambition, it is assumed that more than 2 billion ICE vehicles will be manufactured and their efficiency to increase. The conclusion is that "in the lower ambition scenario, tailpipe emissions from road transport alone would exceed the total transport sector 2050 target" of 90% less emissions compared to 1990 levels. Moderate and higher ambitions plus the other transport emissions will also exceed the limit, showcasing the degree of difficulty.

In the report *Vision 2050: A strategy to decarbonize the global transport sector by mid-century* ICCT shows the baseline scenario for 2050 where GHG-emissions are expected to increase from 12 Gton in 2020 to 21 Gton in 2050. With "vision 2050" an ambitious but feasible target would end up at 4 Gton instead, close to the required 1.6 Gton needed for 1.5°C [78]. According to the report, energy production needs to be close to completely renewable and states that: "Electric vehicles are the single most important technology for decarbonizing the transport sector".

In conclusion, 2030 is less than ten years away and to tackle problems with the environment, a rapid increase of battery electric vehicles are necessary to reach the targets. While the transport sector aren't responsible for all emissions, it is for a substantial part and expected to grow in the future, additionally passenger vehicles are its biggest part.

2.2.2 Demands on electric vehicles

Battery electric vehicles could contribute towards lower emissions given that customers decide to purchase them. In 2020 the global stock of BEVs was 6.85 million vehicles, an increase of 44% since 2019 [49]. 2020 wasn't an exception, in 2019 the increase was 46%, 69% in 2018 and 78% in 2017 with an expected 70% increase in 2021 globally [19]. Although the increases are substantial, the global market share are low compared to the 70 million vehicles sold annually [35]. Different markets have very different sales, in 2020 a majority of all sold vehicles in Norway (cold climate), were BEVs while in Germany (moderate climate) they were below 2% [56].

According to the *International electric-vehicle consumer survey* from 2019, different markets have different concerns [59]. In Norway the cost is less important than driving range, while in Germany and US the cost is more important. In most regions a vast majority would consider purchase a BEV if the price was in parity to ICE vehicles and only about 20% would pay a 25% premium. The cost is a big drawback for BEVs. It is in most cases cheaper to use for its owners but most people aren't even close to afford one. Adding a lack of infrastructure where a report from the European union shows a big difference between countries in terms of charging stations, resulting in even deeper differences in prerequisites for owning a BEV [112].

The concerns about restrained range and higher costs are the most common, along with lacking infrastructures for charging. Even though average driving is noticeably lesser than the range of most BEVs, people want the extra comfort a longer range provides [55]. The cost of a BEV is largely due to the powertrain with 51% of total cost, which includes the battery [31]. The battery also provides the driving range, which creates a problem where cost and range are weighed against each other. A possible solution is lower cost per kWh capacity, which has fallen with 89% the last decade to 137\$/kWh and are expected to reduce even further [18]. Even if cost is expected to decrease, it might take several years until a sufficient level is reached. Depending on capacity it seems to be cheaper to manufacture a BEV compared to an ICE in 2026, at 80\$/kWh a 60kWh-equipped BEV will be cheaper while also providing adequate range [34]. There are exceptions, on Tesla's battery day in late 2020 announcements claiming 56% reduction in cost per kWh and 54% more capacity per kg within three years [20]. Such a decrease would result in a price well below the often mentioned break-even limit of 80\$/kWh will be achieved before 2026, making BEVs available for more customers.

2.3 The importance of thermal management for performance

Increasing the overall efficiency in all driving conditions and temperatures is one possible path, which a thermal management system can provide. In a study performed by American Automobile Association (AAA) from 2019, they investigated the effect air-conditioning and various ambient condition has on the range of five electric vehicles [8]. In the study it was noticed that overall range in a combined driving cycle using air-condition decreased by 30-50% in the cold and 10-20% in hot climate compared to optimal conditions (see figure 7). The variations in range between different models are affected by how efficient the thermal management system is for cooling and heating the components. There are more sources claiming a substantial decrease in range for unusual temperatures. *Ev-database* collects data from real tests, manufacturers and by using a model to estimate real world range, while comparing cold climate with optimal conditions a 25-30% range-reduction is reached [38].

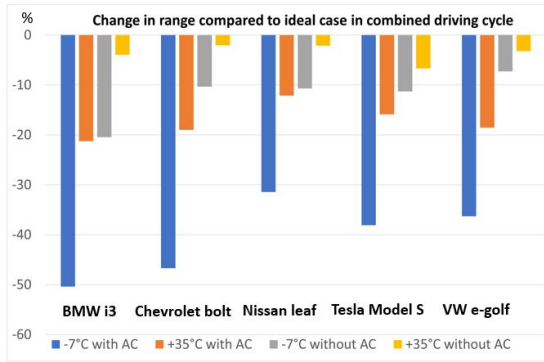


Figure 7: AAA range losses [8]

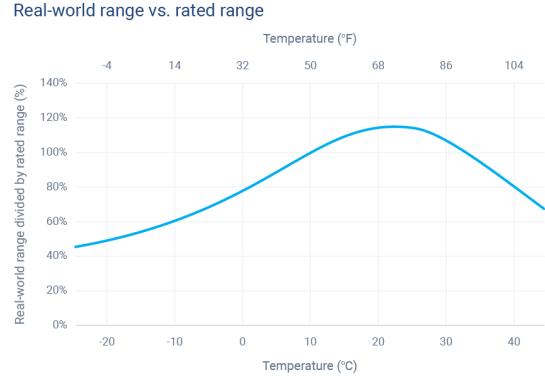


Figure 8: Temperature effects on range[58]

In figure 8 range in different temperatures, normalized based on official data are shown. The data are based on 4200 vehicles and 5.2 million trips and over 100 vehicle modes [58]. In colder climates range is reduced by 20-50% and in warmer climates up to 35%. From previous reports and studies it is evident how temperature affects the overall range of a BEV. Compared to the official figures the range can alter by 50% in worst case and this increases the range anxiety and therefore the reluctance for people interested in buying a BEV as their next vehicle. In order to make people more positive towards BEVs, the uncertainty in range as well as a decrease in cost is a leap in the right direction. While many factors creates range-losses a TMS has the potential of reduce this impact. The theoretical background to this phenomena will be further explained in the next chapter, theoretical background.

3 Theoretical background

In this section the theoretical background behind thermal management of a battery electric vehicle will be explained. In the chapter the *General background* the phenomena, trends and reasoning behind the subject were explained. In this chapter basics about electric vehicles along with a more detailed overview of the three main vehicle subsystems that need to be thermally managed: the battery, electric motor and passengers compartment. First, the traction battery which is addressed since it is known to be very sensitive to changes in temperature, resulting in changes in range, longevity and performance. Secondly, the electric motor is analyzed with focus on its thermal behaviour and requirements. Thirdly, the passengers compartment with demands set by passengers in the vehicle using air-conditioning are discussed. Finally, different methodologies of thermal management and the holistic perspective are explained in relation to optimizing the energy-flow in a BEV.

3.1 Basics of a battery electric vehicle

BEVs are usually fully-electric, rechargeable vehicles with a battery as internal energy source. The chemical energy inside the traction battery is converted into electrical energy and sent through an inverter to the electric motors. The motors convert electrical energy to mechanical energy which is transferred to the wheels through a gearbox and drives the vehicle forward. While the process might seem straightforward, there are many steps with energy transfer and conversion resulting in losses and limitations in vehicle performance. The battery do not only provide energy to the driven wheels, but also to all the auxiliary equipment. In figure 9 the energy flow in a battery electric vehicle in a simplified form is presented.

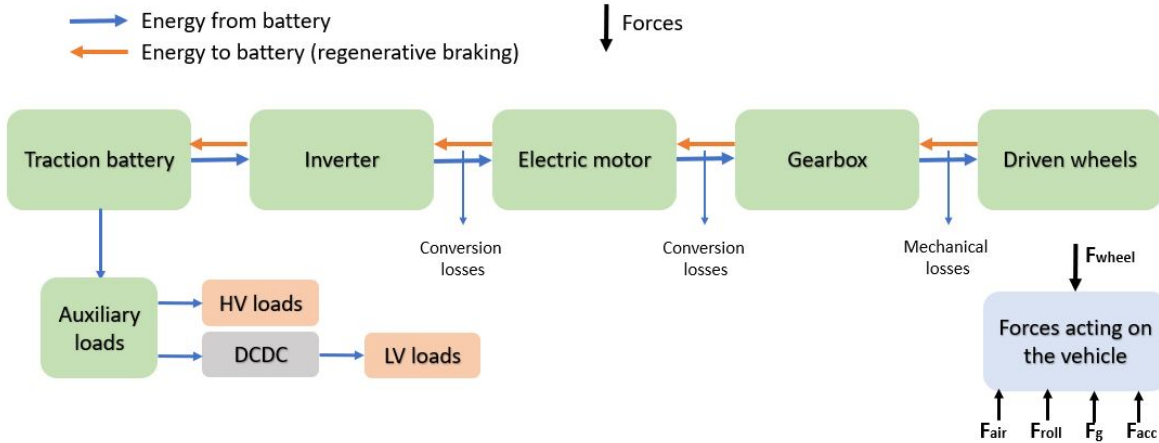


Figure 9: Energy flow within a battery electric vehicle

The energy in a battery is in chemical form and extracted as electrical energy and as direct current (DC). Electric motors typically operate using alternating current (AC), hence an inverter is necessary to transform the current thus creating losses. Similar to an ICE, the electric motor delivers power to the wheels and requires cooling to work properly, compared to the ICE it has less moving parts and is simpler. A combustion engine operates at a range of different speeds and loads, creating a need for a gearbox with multiple gear ratios for optimal use. An electric motor has a different torque-curve which decreases the need of a multiple-speed gearbox and often only uses one speed reduction [114]. From the gearbox to driven wheel the procedure is similar to other vehicles, driven wheels could be in the front, rear or both for a all-wheel drive version.

Auxiliary loads are energy-consumers not linked to traction, some examples are lights, pumps, air-conditioning and heaters [111]. The auxiliary loads consume less energy during normal driving but a large part in cold or warm ambient conditions for the purpose of thermal management. The big consumers are compressor for air-conditioning and heater for cabin or battery, as they run on high voltage. Smaller energy-consumers such as pumps and fans often run on low voltage and power from the battery can be extracted through a DCDC-converter to provide power. Vehicles using an ICE often has lower efficiencies at around 25%, resulting in high heat losses. These losses can be used to heat the passengers compartment in cold climates, resulting in more uniform efficiency in colder ambient conditions compared to BEVs.

3.1.1 Regenerative braking

Regenerative braking is a method used by vehicles equipped with a battery and electric motor to recuperate kinetic energy to electrical energy and charge the battery while driving instead of utilizing mechanical brakes to decelerate the vehicle, which only results in losses. The mechanical power generated is calculated using the following equation:

$$P_{regen} = T_{wheel} * \omega_{wheel} \quad (1)$$

Where:

- P_{regen} is the mechanical power generated [W]
- T_{wheel} is the torque at the wheel [Nm]
- ω_{wheel} is the angular velocity of the wheel [rad/s]

The energy transferred to the battery is going through the same path as the energy used for traction, only in reversed direction, see figure 9. For rear-wheel driven vehicles the maximum power available can be lower compared to front-wheel driven cars due to the load transfer effect. Too high torque on the rear wheels might cause a loss of traction leading to slip, however during normal driving the regenerative braking forces are manageable for most situations [1].

When the requested braking torque is higher than permitted, mechanical brakes assists and slow the vehicle down. The threshold for maximum regenerative power is commonly below 100kW and not utilized for deceleration above 2.9 m/s² [101]. In figure 10 the power required in the UDDS (urban dynamometer driving schedule) is shown, the top graph is with regenerative braking activated and the bottom one is without. In a city-cycle regenerative braking is very favorable, in some cases the regenerated energy corresponding to 27% of the total average energy supplied at the wheels especially in low-velocity aggressive city cycles [73].



Figure 10: Regenerative braking in UDDS driving cycle compared to mechanical braking

3.2 Vehicle dynamics and external forces

Vehicle dynamics determines how a vehicle behaves on the road during driving, typically different focus on stiffness and comfort are applied on different vehicles. The vehicle dynamics will determine how safe the vehicle is to drive, how predictable its behaviour are in various situations and in general determines its limitations. Battery electric vehicles are different in terms of the powertrain, but in terms of external forces acting on the vehicle while driving they remain the same type. One big difference compared to ICE vehicles is the placement of heavy components. The engine is positioned in the front of the car with a transmission towards the middle and a fuel tank in the rear. In a battery electric vehicle the traction battery is positioned in the middle floor and lowers the center of gravity (CoG) due to its high mass.

For studies concerning the thermal management, efficiency and energy optimization a detailed model using advanced dynamics is not prioritized. For the subject a simple rigid body could be used to model the vehicle with a powertrain providing traction and external forces resisting it. The simulations are performed using drive cycles with longitudinal movement rather than lateral from turns, also simplifying the process. Additionally, a drive cycle only works with a steady state model of the vehicle, as opposed to a complete dynamic model [71]. Although some physical events need to be considered externally, including load transfer for a realistic result. In figure 11 a longitudinal dynamics model of a vehicle is presented with the external forces. The center of gravity is located in the middle of the vehicle h_{CoG} meters above the ground. Considering only 2-D, rear left and rear right wheels are considered to be one rear axle, likewise for the front.

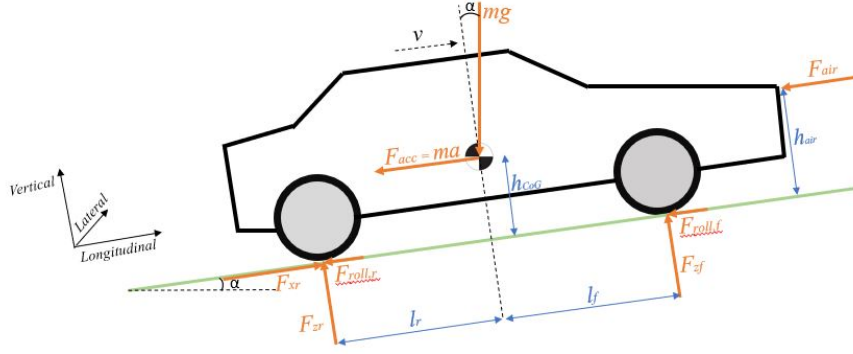


Figure 11: Longitudinal vehicle model with external forces

The air resistance F_{air} acting at a distance of h_{air} above ground. $F_{roll,f}$ and $F_{roll,r}$ is the rolling resistance in front and rear, F_{zf} and F_{zr} is the vertical forces from the ground acting on the wheels and F_{xr} is the traction force from the electric motor. mg is the vehicle mass and gravity acting at center of gravity along with inertia force F_{acc} located with a distance of h_{CoG} above ground. l_f and l_r are the distances from front- and rear axle to center of gravity while α is the road gradient. The traction force and external force are defined in following equations.

$$F_{traction} = \frac{T_{wheel}}{r_{wheel}} \quad (2)$$

$$F_{external} = F_{acc} + F_{air} + F_{grade} + F_{roll} \quad (3)$$

Where:

- $F_{traction}$ is the force provided by the electric motor [N]
- T_{wheel} is the wheel torque [Nm]
- r_{wheel} is the wheel radius [m]
- $F_{external}$ is the sum of air resistance, inertia, grade resistance and rolling resistance [N]

According to Newton's 2nd law of motion, the force on a vehicle depends on its mass and acceleration. The force acting to propel the vehicle from the battery and electric motor are counteracted by the external forces according to equation:

$$F_{traction} - F_{external} = m_{vehicle} * a_{vehicle} \quad (4)$$

Where:

- $m_{vehicle}$ is the total mass of the vehicle [kg]
- $a_{vehicle}$ is the longitudinal acceleration of the vehicle [m/s²]

If $F_{traction}$ is greater than $F_{external}$ acceleration will be positive and the vehicle will accelerate forward. The vehicle will decelerate if $F_{traction}$ is smaller than $F_{external}$, for example during regenerative braking.

3.2.1 Inertia forces

The inertia forces are due to a shift in velocity during a certain amount of time and are zero at constant speed. Acceleration occurs when a vehicle increases or decreases its velocity according to:

$$a_{vehicle} = \frac{dv}{dt} \quad (5)$$

The resulting forces are formulated by Newton's second law of motion where mass times acceleration equals the force. A more rapid shift in velocity causes a greater acceleration, resulting in a higher force taken from the electric motor and traction battery. The velocity is defined as positive when it travels forward in longitudinal direction, likewise for its acceleration. The acceleration forces defined as opposite to the vehicles acceleration since it opposes the event:

- $v_{start} < v_{final}$ results in $a_{vehicle} > 0$ and $F_{acc} < 0$
- $v_{start} > v_{final}$ results in $a_{vehicle} < 0$ and $F_{acc} > 0$

The equation used to calculating the inertia force F_{acc} is essentially Newton's second law:

$$F_{acc} = m_{vehicle} * (-a_{vehicle}) \quad (6)$$

Where:

- F_{acc} is the vehicles acceleration force [N]
- $m_{vehicle}$ is the vehicle's mass [kg]
- $a_{vehicle}$ is the vehicle's acceleration [m/s²]

3.2.2 Air resistance

When a body, in this case a vehicle, moves through a fluid, in this case air, it causes resistive forces often named air resistance. The air resistance is largely depending on a number of factors, this includes air density, vehicle speed, frontal area and drag coefficient. Typically the air resistance is divided into *pressure drag* and *skin friction*. Pressure drag appears due to a difference in pressure around the body caused by its shape and are for passenger vehicles often are greater than skin friction that is a result of wall shear stresses between body and fluid [106]. The aerodynamic force is calculated using:

$$F_{air} = C_d * A_{vehicle} * \rho_{air} * 0.5 * V_{rel}^2 \quad (7)$$

Where:

- C_d is the drag coefficient
- $A_{vehicle}$ is the frontal area of the vehicle [m²] ρ_{air} is the air density [kg/m³]
- V_{rel} is the velocity of the car relative to the surrounding air [m/s]

The drag coefficient is a dimensionless value depending on the vehicle's shape, a more sleek design will result in a lower coefficient, thus reducing the overall force. In table 2 a range of drag coefficients from electric vehicles are shown along with percentage reduction compared to their average drag coefficient 0.252.

Table 2: Drag coefficients for battery electric vehicles [47]

Vehicle model	drag coefficient	percentage difference to 0.252
Tesla Model S	0.240	-4.8%
Polestar 2	0.278	+10.2%
VW ID 3	0.267	+5.9%
Mercedes EQS	0.208	-17.5%
Tesla Model 3	0.230	-8.8%
Renault Zoe	0.290	+15.0%

From the table and equation 7 it is evident that low drag coefficient leads to a lower air resistance, thus increasing efficiency. The equation simplifies the situation since equipment and wheels alter on the vehicles, also the wind is assumed to be 1-D. A study found that a change in yaw angle increased the drag coefficient since it approaches in more directions [116]. For electric vehicles, aerodynamics is more important for two reasons. First, it increases exponentially with velocity and affects the crucial range. Secondly it also creates noise when turbulence occurs, an electric vehicle is quieter due to it lacking an ICE, emphasizing other sources of noise [87]. The A-pillar and mirrors are two vital areas where noise occurs, and by reducing the drag both noise and drag force reduces. While C_d is not depending on a vehicle's size, the **frontal area** is, a smaller vehicle will have a smaller area to slice through the fluid. The frontal area can be measured by having light in parallel with the longitudinal axis and calculate its projected area. While manufacturers in some cases provide drag coefficient, frontal area are not always available but can be estimated by multiplying its width by its height and a factor of 81% [88]. **The air density** is depending on ambient temperature, pressure and humidity and while comparing electric vehicles in ambient conditions it is vital. By assuming constant pressure and humidity, a function of air density depending on temperature can be created [83].

$$\rho_{air} = -0.0045174 * T_{amb} + 1.193 \quad (8)$$

From equation 8, a difference of 12.3% between -10°C and 20°C can be extracted, where a higher temperature results in lower density which lowers the total air resistance.

3.2.3 Road grade resistance

Grade resistance is due to a difference in altitude on the road, typically an uphill or downhill. An uphill will require a higher power output due to gravity opposes it. As for most things, there is usually a downhill after an uphill, this works the opposite way and gravity instead contributes with force and relieves the electric motor's work. In equation 9 the force from road grade is presented:

$$F_{grade} = m_{vehicle} * g * \sin(\alpha) \quad (9)$$

Where:

- $m_{vehicle}$ is the vehicles total mass [kg]
- g is the gravitational constant at 9.81 [m/s²] α is the road angle between the road and horizontal plane

In figure 11 the road grade can be seen, with an increasing road angle α the force-vector consisting of mass and gravity will also increase its angle compared to the vertical plane with α degrees. As the angle increases, the longitudinal vector component grows and the vertical vector component decreases, creating a larger resistance resulting in a higher demand of power. Most driving cycles are performed at level ground where the presence of road gradient resistance is essentially zero. However in reality, depending on where the vehicle is driven, this force is to reckon with.

3.2.4 Rolling resistance

Rolling resistance is essentially a torque loss occurring at the wheels when a vehicle is driving [71]. A number of different phenomena causes rolling resistance and the total force depends on what one chooses to include. These phenomena are for example friction in gear meshes and drag from brake discs and wheels, but the main factor is material hysteresis at 90% of the total losses [84]. In equation 10 the rolling resistance force can be calculated.

$$F_{roll} = m_{vehicle} * g * C_r \quad (10)$$

Where:

- $m_{vehicle}$ is the vehicle's total mass [kg]
- g is the gravitational constant [m/s^2]
- C_r is the rolling coefficient

In some cases the force is multiplied by $\cos(\alpha)$ where α is the road grade, but since the values are so small it can often be neglected for road angles within a reasonable spectra. The rolling coefficient is what can be different due to conditions such as temperature, pressure and road surface. Some studies have found an exponential dependency on velocity for the rolling coefficient, but for most part velocities found in driving cycles results in a linear behaviour and C_r can be approximated to about 0.01 [71].

3.2.5 Limiting vehicle dynamics

The top speed of a vehicle is either limited through software by the manufacturer or by the electric motor through max rpm or lack of power. When the external forces are too high, for instance due to acceleration, velocity or road grade the vehicle will not accelerate further. In addition to top speed there are more limiting factors which includes *slip* and *load transfer*. **Slip** occurs due to lack of traction which largely is due to friction coefficient μ , longitudinal force and vertical force using following equations

$$S_x = \frac{(\omega_{wheel} * r_{wheel}) - v_x}{|v_x|} \quad (11)$$

when angular velocity times radius equals the vehicle's speed, there is no longitudinal slip.

$$F_x = \mu * F_z \quad (12)$$

The maximum traction force F_x is depending on friction coefficient and the vertical force, if it exceeds the limit the wheel starts rotating faster than the vehicle's speed, resulting in slip and an uncontrolled driving situation.

Load transfer occurs during acceleration and deceleration and is a central phenomena in vehicle dynamics. It appears both longitudinally and laterally, considering a driving cycle with only longitudinal

driving the lateral load transfer is neglected here. Longitudinal load transfer means that compared to static case (constant speed) the load on the axles shifts during shift in velocities. The center of gravity (see figure 11) is located above the wheel-axes and produces a momentum around the rear axle during acceleration and front axle during deceleration. The momentum shift results in lower vertical forces on one axle, which may result in slip. In the following equations the static forces are presented:

$$\sum F_{vertical} = F_{zr} + F_{zf} - m * g * \cos(\alpha) = 0 \quad (13)$$

$$\sum F_{longitudinal} = F_x - F_{roll} - F_{air} - m * g * \sin(\alpha) = 0 \quad (14)$$

Where F_{zr} , F_{zf} and F_x are longitudinal and vertical forces. Knowing maximum regenerative braking capacity is important in electric vehicles, it is a balance between vehicle dynamics and maximum regenerated power. The dynamic forces with load transfer can be derived from equations 13 and 14 to form:

$$F_{zr} = \frac{(m * g * (\sin(\alpha) * h_{cog} - \cos(\alpha) * l_r) + m_{vehicle} * a_{vehicle} * h_{cog} + F_{air} * h_{air})}{l_r + l_f} \quad (15)$$

where vertical rear axle force and weight distribution can be calculated. By combining equation 15, 1 and 2, the maximum regenerative power can be calculated:

$$P_{rmax} = \frac{r_{wheel} * \omega_{wheel}}{\mu * (l_r + l_f)} * ((m * g * (\sin(\alpha) * h_{cog} - \cos(\alpha) * l_r) + m_{vehicle} * a_{vehicle} * h_{cog} + F_{air} * h_{air})) \quad (16)$$

In figure 12 the maximum allowed regenerative power without slip is presented. Two different friction coefficients are used to represent wet asphalt (0.4) and dry asphalt (0.7). The center of gravity height for a saloon car (0.45m) and a SUV (0.65m) are also represented to showcase the difference in terms of allowed power. In figure 13 the maximum regenerated power limited by vehicle dynamics is presented with vehicle parameters. In figure 13 a comparison of the external forces in different velocities shows that at 90 km/h roll and air resistance are equal, but grade and acceleration resistance are substantially larger, with same vehicle parameters as in figure 12. Thus driving including more acceleration or uphill, will have a higher energy consumption per driven distance than cycles with low acceleration.

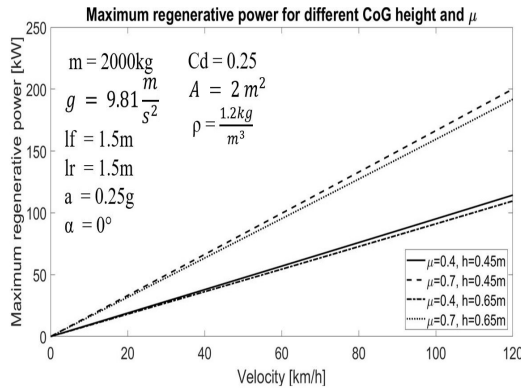


Figure 12: Max regen power from veh. dyn.

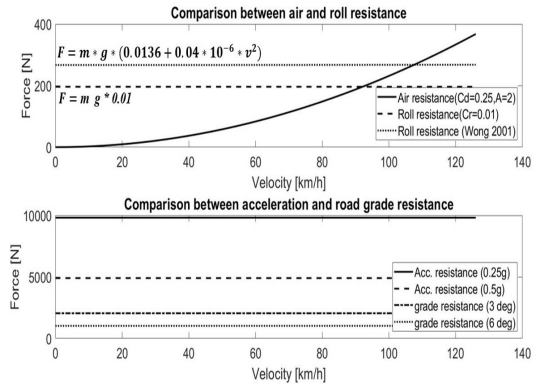


Figure 13: Comparison between external forces

3.3 Lithium-ion battery

In this section the basics of a battery will be explained as well as how thermal management affects the performance, capacity and longevity in a BEV.

The traction battery inside a battery electric vehicle is the main source of energy for all electrical components such as electric motor, DCDC-converter and HVAC. There are several variations in terms of cell technology, dimensions, placement, energy densities and thermal management methods by manufacturers. While there are variations, the basic principle behind the battery remains the same. A lithium-ion battery consists of an anode, cathode, separator, electrolyte, separators and has two terminals, one positive and one negative with a potential difference between 3-4V [99].

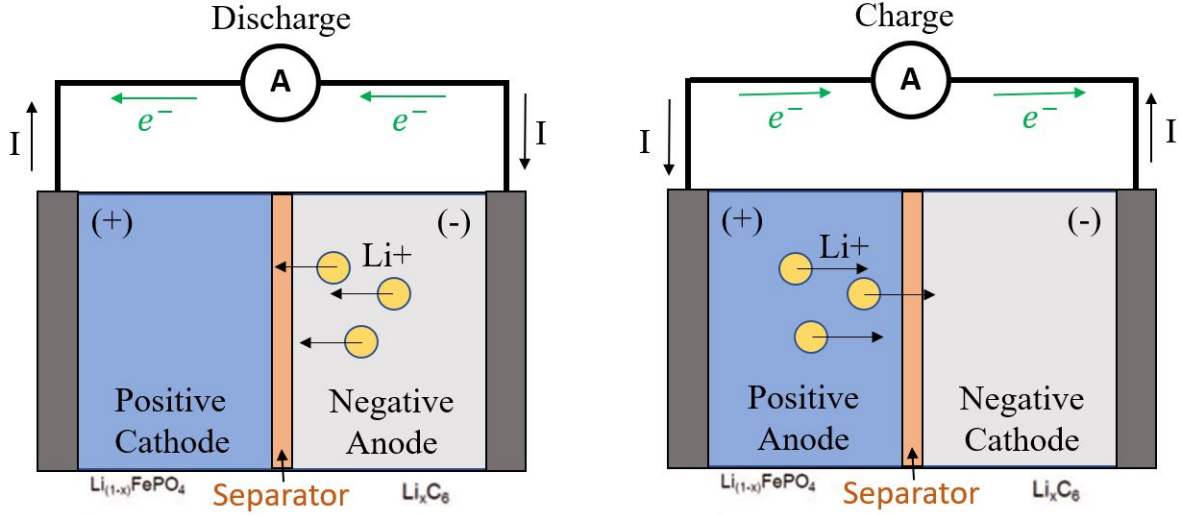


Figure 14: Battery during discharging and charging

In figure 14 the basics of a battery is presented in both charging and discharging. Chemical reactions occur in the anode and cathode, which results in a flow of ions, creating a current and electrical energy that discharges the battery. Discharging occurs when power is drawn from the battery and current flows from positive to negative while lithium-ions and electrons flow in opposite direction. As the battery discharges, the lithium-ions is released from the anode in a oxidation-process and flows to the cathode through the separator and electrolyte. A fully charged battery has a state of charge (SOC) of 100% and reaches its maximum voltage. During discharge both the SOC and voltage decrease and the energy is depleted. To increase the energy it has to be charged, this process reverses the discharge process and lithium-ions flows back into the negative terminal, thus increasing the voltage and SOC [82]. During charging and discharging heat losses occur according to equation:

$$P_{losses} = P_{irreversible} + P_{reversible} = I_{battery}^2 * R_{internal} + I_{battery} T_{battery} \frac{\partial U}{\partial T} \quad (17)$$

The reversible losses can, as the namne states, be reversed in the process. The irreversible losses are also called ohmic resistance losses, exponentially depending on the current and linearly on the ohmic/ionic resistance. Ohmic losses also cause a voltage drop inside the battery that limits the power as SOC and voltage drop. The total power drawn from the battery can be calculated:

$$P_{battery} = (U_{battery} - I_{battery} * R_{internal}) * I_{battery} \quad (18)$$

In equation 18 the losses due to internal resistance is taken into account, the same resistance present in ohmic losses. This resistance is not constant in a battery and is heavily affected by the state of charge and the temperature. In a study of internal resistance in different temperatures, a lithium ion phosphate battery decreased the resistance by 60% from 0°C to 25°C and about 65% for a lithium-ion battery [92]. In another study with similar results created an equation to describe internal resistance depending on temperature $R(T) = 90.196e^{-0.08T} + 25.166$ (where R is in mΩ) resulting in 68% difference from 0 to 25°C [94]. With a very cold battery in sub-zero temperatures, the internal resistance is substantially higher and results in higher irreversible losses. The state of charge affect internal resistance and when SOC is low, the resistance increases [76]. In figure 15 the internal resistance of a lithium nickel-cobalt-aluminium (NCA) battery in various temperatures and SOC are shown.

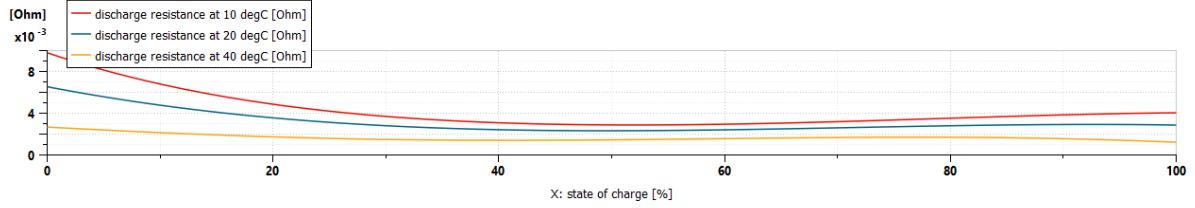


Figure 15: Internal resistance in various temperatures and SOC from Amesim

The discharge rate of a battery is referred to as *C-rate* and it describes how fast a battery is fully discharged. 1C means that the battery has 0% SOC after 1 hour, 2C is twice the discharge rate and thus only need 0.5 hour to discharge. A higher discharge rate will result in higher temperatures due to more heat generation and losses [97]. For a cylindrical 18650 li-ion cell in 22°C ambient, 2C resulted in a 23°C increase in temperature after a full discharge at 0.5C increased temperature by 4°C [97].

3.3.1 Battery thermal management

A battery is very sensitive to which temperature it operates in. Very much like humans, around room temperature is optimal but commonly a range of 15-35°C is considered best [104]. In some cases this range can expand to be between 0°C and 45°C but this is more a reasonable range than an optimal one. There is a difference in charging and discharging, charging below 0°C is not recommended for li-ion batteries since diffusion in the anode is too slow [67].

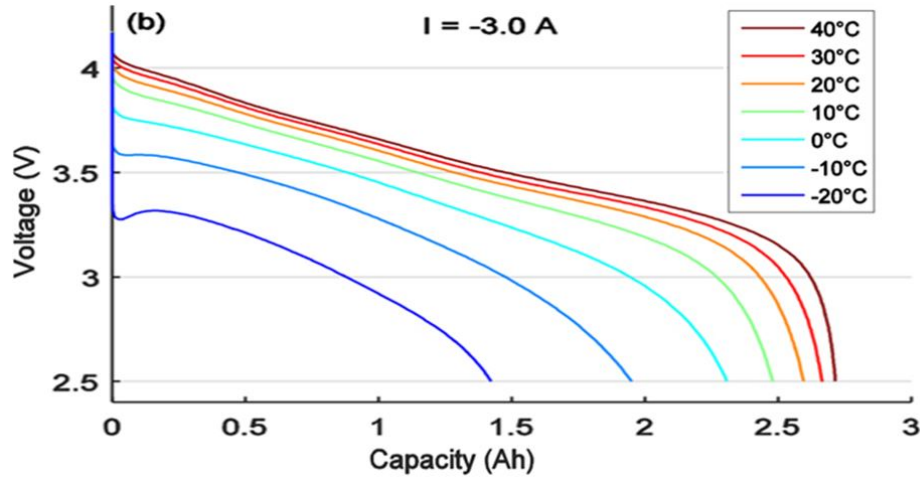


Figure 16: Battery capacity in different temperatures [68]

In colder climates the battery performs worse since it has higher internal resistance, discharging is possible in sub-zero temperatures but at the cost of a lower efficiency and capacity [67]. In a discharge test of a panasonic li-ion cell at 1.07C and rated capacity of 2.8Ah, the capacity was 2.5Ah in 10°C, 2Ah at -10°C and below 1.5Ah at -20°C, almost half the capacity is lost (see figure 16) [68]. Another study discharged a li-ion cell in temperatures ranging from -15°C to 25°C and received 23% lower capacity in the coldest temperature compared to optimum [98]. In general the battery becomes "slower" or more "sluggish" in colder temperatures due to a range of phenomena [66]. In addition to performing worse, it also damages the cell through "lithium plating". Lithium plating appears at sub-zero temperatures at the negative electrode and can cause permanent damage on the cell, resulting to loss in capacity och short-circuit [107]. In essence it occurs due to lithium ions forms a lithium metal at the electrode, which makes it unavailable in the process of charging or discharging and decreases capacity, a higher c-rate will speed up this phenomena. The fact that a battery is far from operating at its peak in colder temperatures has to be considered when designing a thermal management system of for BEVs to increase capacity and thus range, but also longevity and safety.

In warmer climates the battery has a low internal resistance and works relatively well with high capacity. At temperatures above 50°C it can start to expand and vent, but also affects the longevity of the cell [68]. Therefore charging at too high temperatures are not recommended either. Temperatures above 30°C are considered as elevated temperatures which affects ageing of the cell [68]. At 30°C cycle life reduces by 20%, at 40°C by 40% and around 50% at 45°C. There are multiple ways temperature can affect the longevity of the cell, both cycling time and shelf time are important. A cell left unused in storage for a year at 40% SOC will have different capacity left, at 25°C 96% is preserved while only 75% is left at 40°C [69]. A common phenomena at higher temperatures are the increased forming of solid electrolyte interface (SEI) layer on the anode (see figure 18. SEI layer obstructs the interaction inside the cell and thus increases resistance [70]. In figure 17 a study performed at a lithium-ion battery with charge and discharge at 2C between 0-90% SOC for different temperatures. The difference between the lower and higher temperatures was that cycle life reduced considerably. Resistance went up as a consequence of more SEI reactions and resulted in a more rapid decay of the cell's capacity [115].

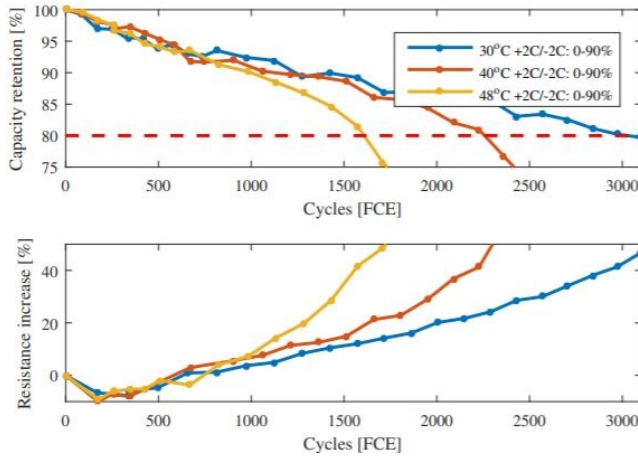


Figure 17: Battery aging for 30, 40, 48°C [115]

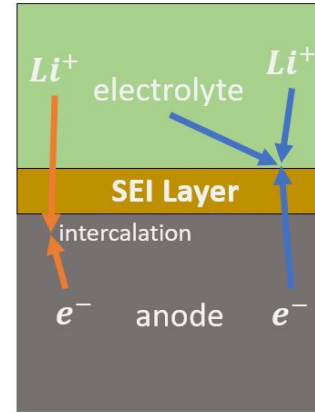


Figure 18: SEI layer

At higher temperatures than normal the battery might overheat leading to thermal runaway, a highly hazardous phenomena a thermal management system has to prevent. In temperatures above 60°C the risk appears and at 100°C it is critical and can initiate a three-step chain-reaction difficult to stop. The steps begins with an increasing internal temperature, then heat accumulation, gas release and exothermic reactions leading to combustion of the flammable electrolyte and explosion [96].

3.3.2 Thermal management methods

A lithium-ion battery cell has a nominal potential of about 3.7V depending on cell chemistry, to acquire a higher voltage the cells are connected in series and to increase the capacity they are connected in parallel to form battery modules. The modules are then arranged in a battery pack which includes the battery management system (BMS), mechanical protection and thermal management system. There are many different methods for cooling or heating a battery in a BEV, this includes air cooling, liquid(direct/indirect) cooling, fin-cooling and use of PCM which are illustrated in figure 19 [75]. In terms of heating in colder climate positive temperature coefficient (PTC) heaters and waste-heat recovery from electric motors are often utilized.

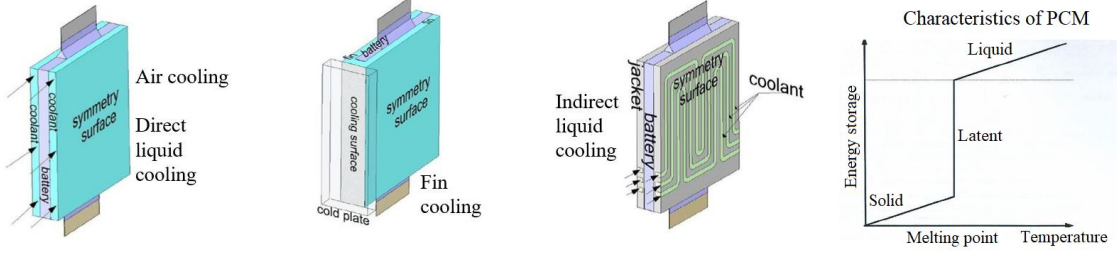


Figure 19: Illustration of different cooling methods [105]

Air cooling is the most simple method where air is used to cool the cells inside the battery pack. The air can be retrieved directly from ambient air in a passive system by convection or blow air directly alternatively through an evaporator or heater in active systems [93]. **PCM cooling** uses phase-change materials (PCMs) for cooling and are considered to be passive. By absorbing heat it changes phase from solid to liquid or liquid to gas, when the phase shift is complete the cooling capacity is minimal and hence needs a complementary cooling method [95]. **Fin cooling** utilizes convection and conduction to cool the battery, typically the fins are made from a metal and adds weight [75]. **Liquid cooling** can be both direct and indirect. Direct liquid cooling cools cells by submerging them in a liquid without separation. Indirect cooling instead separates the liquid from the cell and cools through a cooling plate or a cooling pipe using conduction. This is one of the most common methods used by manufacturers today, the liquid inside flows through the plate or pipe which is in contact with the cells and minimizes temperature gradients. Conduction and convection commonly used for cooling of batteries are presented in the following equations:

$$q_{cond} = -k * A * (T_{cell} - T_{amb}) \quad (19)$$

Here k is thermal conductivity [$\frac{W}{m \cdot K}$], A is the area [m^2], T_{cell} and T_{amb} are the cell and ambient temperature, respectively [K].

$$q_{conv} = h * A * (T_{cell} - T_{amb}) \quad (20)$$

Here h is heat transfer coefficient [$\frac{W}{m^2 \cdot K}$]. Cooling capacity required can be calculated using Bernardi's equation, see equation 21.

$$E = m * C_p * \Delta T = P_{losses} - h * A(T_{cell} - T_{amb}) - e * \delta * A(T_{cell}^4 - T_{amb}^4) - Q_{ext,cond} \quad (21)$$

The equation includes the rate of temperature change, rate of heat generation (losses), convection heat rate, radiation heat rate and conduction heat rate [105]. In order to keep the temperature within the optimal limits in all ambient temperatures it is crucial to heat it up or cool it down using an efficient thermal management system.

3.4 Electric motor

Electric motors use electric energy and convert it to mechanical energy with high efficiency. The efficiency can reach above 95% at specific operating points and transfers the power through a gearbox to the driven wheels, providing propulsion driving the electric vehicle forward. Commonly there are three different types of electric motors in BEVs: AC induction motor, externally excited synchronous motor (EESM) and the permanent magnet synchronous motor (PMSM) which is used in tTesla model 3. The PMSM has many advantages well suited for BEVs including high power density and efficiency, low mass and moment of inertia and at the same time a robust and compact component [80]. One drawback is that some material used, for instance Neodymium Iron Boron and some steel alloys may include ethical and environmental issues. The PMSM is commonly utilized by many different manufacturers, making it relevant for additional investigation.

The PMSM consists of two main components, its rotor and its stator and they are not mechanically connected to each other besides the bearings that can cause mechanical losses and they are both often made from ferromagnetic steel and are isolated. In the stator, there are several coils made out of copper wires where the strands are coated with an isolating material to avoid short circuits within the coils. The stator is stationary while the rotor is rotating depending on the frequency of the magnetic field created by the current. The magnetic field is produced by the three phase windings and based on its input current magnitude, it creates a torque transferred by the rotor to mechanical power. The output power from the electric motor can be expressed as:

$$P_{em} = T_{em} * \omega_{em} \quad (22)$$

Here T_{em} is the torque [Nm] and ω_{em} is the angular velocity [rad/s]. The torque is produced by the PMSM is commonly expressed using a rotating coordinate system known as dq-coordinates. In the dq-frame, the PMSM torque equation is expressed in terms of currents, flux linkages and inductances as:

$$T_{em} = \frac{3p}{2} * (\Psi_d i_q - \Psi_q i_d) = \frac{3p}{2} * (\Psi_{PM} i_q + ((L_d - L_q) i_q i_d)) \quad (23)$$

Where Ψ_d and Ψ_q is the d and q-axis flux linkages [Wb], i_q and i_d are the d and q-axis currents [A], Ψ_{PM} is the magnet flux linkages [Wb], L_d and L_q are the d- and q-axis inductance [H]. The power output from the electric motor is transferred to the gearbox which reduces speed and increases torque at the wheel. After considering the power-loss related to gearbox efficiency, the output power is calculated:

$$P_{wheel} = \eta_{gearbox} * P_{em} = \eta_{gearbox} * T_{wheel} * \omega_{wheel} = \eta_{gearbox} * (gearratio * T_{em}) * \left(\frac{\omega_{em}}{gearratio}\right) \quad (24)$$

3.4.1 Losses in electric motors

The temperature window for electric motors where they can operate are wider compared to li-ion batteries. Temperatures above 100°C are possible but cooling is necessary to avoid isolation melting at around 180°C [91]. Cooling is also required to maintain high performance and longevity of components inside a PMSM and for automotive purposes the loads can be high for a long period of time, thus increasing the importance. The rise in temperature is due to the heat produced by losses inside an electric motor. Losses include copper losses, iron losses, stray losses and mechanical losses [89].

Typically the losses increase with the load, one of the reasons is that with increased torque, the current increases due to their relation. In figure 20 different types of losses as a function of load are

presented for the losses present. Stray losses are not accurately determinable but vary with the load and can be approximated as 1% of total power [62]. The mechanical losses include both frictional from bearings and windage from air resistance during rotation, they can be neglected at lower speeds [89]. Two main types of losses in electric motors are copper losses and iron losses out of which copper losses are the greater one [63]. The iron losses increases exponentially with speed while copper losses remain constant, not depending on the speed and instead increase with increased current.

Copper losses, also known as resistive losses, are the result of electric resistance from the copper wires (coils) inside the stator. The copper losses can be calculated as:

$$P_{cu} = n * R_{winding} * I_{em}^2 \quad (25)$$

Here n is the amount of phases (typically 3), $R_{winding}$ is the stator winding phase resistance and I_{em} is the current. There is also a phenomena called the *skin effect* due to the alternating current, this leads to higher current density in the outside of wires but is not included in this equation. With a higher torque request due to higher loads, the current increases and results in higher losses in the windings. The resistance is not constant, but instead varies with temperature according to:

$$R_{winding}(T) = R_0 * (1 + \alpha_0 * (T_{wire} - T_{ref})) \quad (26)$$

Where R_0 [Ω] is the reference resistance at the reference temperature T_{ref} [K] which is commonly around 25°C. T_{wire} [K] is the actual copper temperature and α_0 is the temperature coefficient of resistance which is 0.00393 for copper. From equations 25 and 26 it is evident that copper losses are highly depending on the temperatures, by limiting the copper's temperature a higher efficiency can be achieved. As an example, the difference between 25°C and 75°C is around 20%. Overall efficiency can be decreased with as much as 5% if temperature is kept at 25°C instead of 100°C [89].

Iron losses is under normal circumstances the second largest source of losses at 20-25% of the power losses, which consists of magnetic hysteresis losses and induces eddy current losses where hysteresis is the main source [89], [91]. The overall iron losses can be calculated as:

$$P_{fe} = P_h + P_e = K_h * B^n * f + K_e * B^2 * f^2 \quad (27)$$

Here K_h and K_e are hysteresis and eddy current parameters, f is the supply voltage frequency, B is peak flux density and n is depending on material, B and f . Modeling of these losses are more difficult compared to copper losses with a high error rate. The temperature of the stator and rotor where iron losses occur affects the losses where a higher temperature gives slightly lower losses in comparison to copper losses [117].

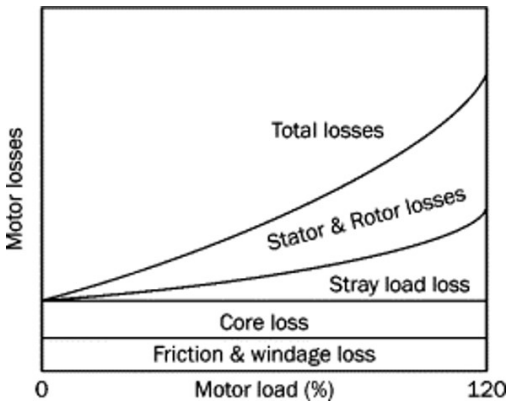


Figure 20: PMSM losses [118]

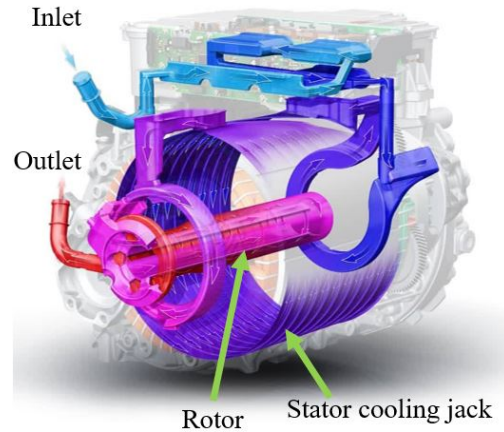


Figure 21: Electric motor cooling [60]

3.4.2 Electric motor thermal management

There are multiple methods to keep an electric motor within its operating range. For electric machines with lower loads and thus lower currents, "open" and "self ventilated" machines can be used. They provide a cheap and simple cooling effect suitable for lower loads but are not suitable for automotive use. Liquid cooling suits higher power density machines and are effective due to the water or oil flowing to cool it. A water cooling jacket surrounding the stator or channels flowing through it is commonly used, see figure 21 where a liquid cooling system is presented. The liquid enters at the top and flows through the power electronics cooling plate, to copper winding ends, through the cooling jacket and inside the rotor before exiting. Thermal conduction inside the motor is problematic, the copper is positioned inside the stator where they are isolated from the stator iron using slot liner commonly in mylar or nomex based materials. The copper strands are commonly coated with several layers of insulated coating, which reduces the heat transfer even further, however to mitigate this issue the windings are potted or impregnated with epoxy which improves the heat transfer and thus cooling.

3.5 Passenger compartment

Maintaining appropriate temperature levels for battery and electric motors is crucial for their longevity and overall safety. The passenger compartment should be kept between 20-25°C for passengers comfort. Air-conditioning in vehicles are used to control the temperature and depending on ambient conditions it can consume high amounts of energy. A study performed by American automobile association (AAA) with five BEVs in cold and warm climate with and without air-condition (AC) was performed too see how driving range is affected. While decrease in driving range in colder climates without AC is around 10-20% it becomes 30-50% with AC turned on. For warmer climates driving range decreases by less than 7% while AC turned on decreases range by up to 20% [8].

BEVs have less heat losses compared to conventional powertrains where efficiency is lower, resulting in BEVs efficiency being more sensitive to colder climates. In addition to controlling the temperature of passenger compartment, the AC system is commonly used to cool other components, thus consuming more energy [64]. In a study where various compressor concepts for electric vehicles were investigated, a middle-sized BEV was tested in WLTP driving cycle for summer, spring and winter conditions [64]. Solar radiation in the summer was the highest, in spring rather low and at zero during the winter. Results showed that the heater and AC consumed most energy in winter conditions while being close to zero in spring conditions at 20°C, which is illustrated in figure 22.

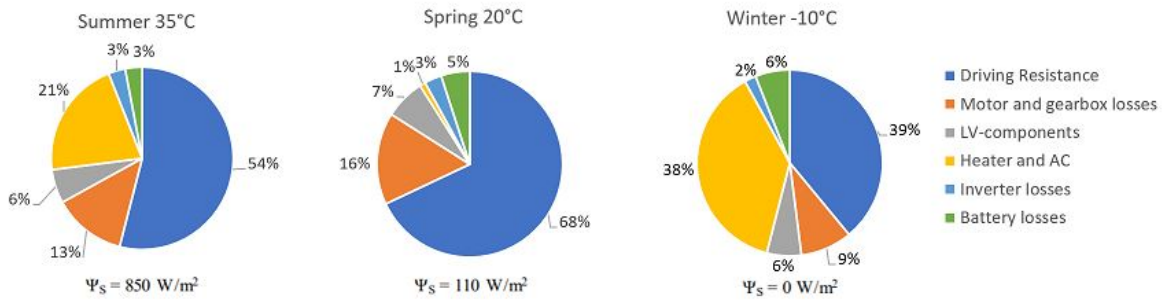


Figure 22: Energy consumption of different system in a BEV in summer, spring and winter [64]

3.5.1 Cooling passengers compartment

Cooling of the passengers compartment is performed by the AC by utilizing a reversible Carnot cycle. A Carnot cycle is a thermodynamic cycle that can transport heat energy from one place to another

using refrigerant, a compressor, condenser, evaporator and expansion valve. Air is transported to the condenser where refrigerant deposits energy and flows through the expansion valve and absorbs heat energy through the evaporator and back to the compressor for a new cycle. At warm ambient conditions the condenser deposits energy to the atmosphere and absorbs heat from the passengers compartment. In figure 23 a pressure-enthalpy (PH) diagram with the four stages in a carnot cycle is illustrated. The diagram is for R134a-refrigerant and horizontal lines inside the curve marks its temperature. In figure 24 the reversible carnot cycle flow can be found including its two modes. The first mode is during cold ambient climate and warming of passengers compartment, the second is for warm ambient conditions. The energy flow remains the same, however depending on ambient conditions the source and final space are shifted.

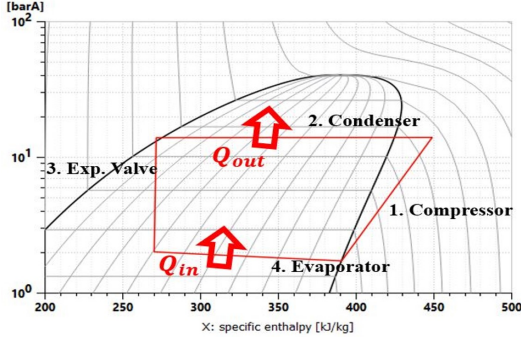


Figure 23: PH-diagram R134a Carnot cycle

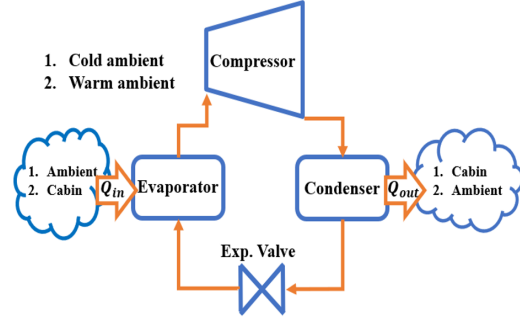


Figure 24: Flow scheme for a Carnot cycle

3.5.2 Heating of passengers compartment

Heating of the passengers compartment can be done in two different ways. A positive temperature coefficient (PTC) heater that transforms high voltage electric energy from the battery to heat the cabin using resistance. The efficiency is close to 100% since heat is the wanted energy type, the advantages are its simplicity, quick heating time and the fact that it works in any ambient temperature [100].

The other method for heating the passengers compartment is by a heat pump. Heat pumps are commonly used by some manufacturers today, including Tesla and Kia/Hyundai. Kia/Hyundai claims only a 10% range reduction in colder climates compared to optimal conditions, while other BEV ranges decreases more [22]. Tesla introduced a heat pump in their model y and the same concept is currently used in their new model 3, since in real world winter tests heats pumps have proven to be way more efficient resulting in the increased range [21].

Heat pumps simply operate on a reverse Carnot cycle where the condenser deposits energy to the passengers compartment and the evaporator absorbs energy from the cold ambient air. Since warmer air contains more energy than cold, a heat pump is more efficient in slightly cold temperatures than freezing temperatures around -20°C . The efficiency is commonly called coefficient of performance (COP) and can exceed 1. The COP value is determined by input compressor power and output heating/cooling power according to:

$$COP = \frac{Q_{out}}{Q_{in}} = \frac{Q_{evap,cond}}{Q_{compressor}} \quad (28)$$

COP values can be compared to the efficiency of a PTC that reaches a theoretical maximum of 1, while for heat pumps COP sometimes reaches 3-4 [5]. Therefore a heat pump might seem to have an efficiency above 100% which isn't correct, a heat pump moves the energy rather than creating it, thus reaching values above 1. By incorporating heat pumps to heat up passengers compartments efficiency and overall range are improved, especially for colder climates.

3.6 Holistic thermal management system

The traction battery, electric motor with power electronics and the passengers compartment are the three areas where thermal management are necessary in a BEV. The battery are highly sensitive for high temperatures in terms of safety and longevity while cold temperatures reduces both efficiency and capacity. The electric motor with power electronics have a wider operating range where colder temperatures are more acceptable and below 100°C is sustainable for longevity while copper losses reduces efficiency in high temperatures. Passenger compartment's temperature window is to ensure comfort and important to control for an optimal driving range and performance.

There are multiple situations and conditions where a thermal management system is required, likewise there are numerous different thermal management systems used in BEVs. The three areas in need of thermal management are simplified and illustrated in figure 25.

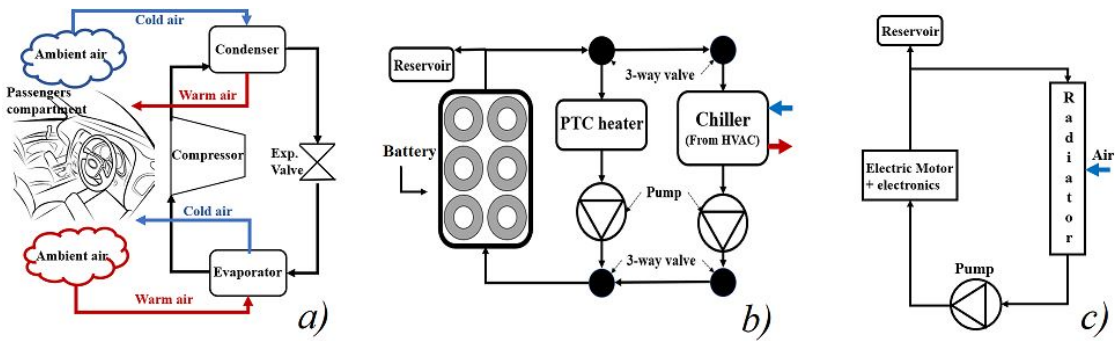


Figure 25: Thermal management layouts. a) Passengers compartment, b) Battery, c) Electric motor

In the thermal management loops refrigerant flows through hoses and is driven by low-voltage pumps. A reservoir is used to maintain performance in the systems and three-way valves control the flow inside the loops. In figure 25 a) the HVAC-loop for the passengers compartment shows how heat is transported from ambient air to inside the vehicle or the other way around. In 25 b) the battery has two different paths depending on its temperature, either it flows through a PTC-heater or a chiller that uses the HVAC to remove heat. The HVAC therefore has a vital role to cool both the cabin and the battery. In 25 c) a simple circuit used for cooling the electric motor is used, since heating is not included it requires less components. A radiator with fan cools the refrigerant by utilizing a high temperature difference between electric motor and ambient air.

The three loops in figure 25 operate individually and each control system only considers one loop each time. In certain conditions loop a) might heat the cabin, loop b) heat the battery and loop c) cool the electric motor and consumes energy to transport waste heat. The three loops can also cooperate and recover waste heat using a holistic approach. The holistic approach for thermal management is a method to optimize the energyflow inside a BEV and are implemented in various ways. Waste heat from components inside the BEV are transported to other components in need of heating and reduces the auxiliary load from pumps, heaters and fans. Holistic thermal management systems can become more complex compared to individual solutions, but can also reduce price by reducing the amount of components, which affects overall price. Two manufacturers using a holistic approach are tesla and kia/hyundai. Kia/hyundai's system scavenges heat from both the electric motor, inverters and chargers but also the traction battery to use for the cabin, thus minimizing battery energy consumption and maximizing driving range [17]. Tesla uses a component called the "super bottle" in model 3 since 2018. The super bottle is a package combining two pumps, a heat exchanger, a bottle (reservoir) and a valve to control the refrigerant flow [7]. There are two different modes the valve can choose from, either connect the loops of battery and electric motor in series or in parallel. By connecting in parallel

cooling can take place through the chiller from HVAC according to figure 26.

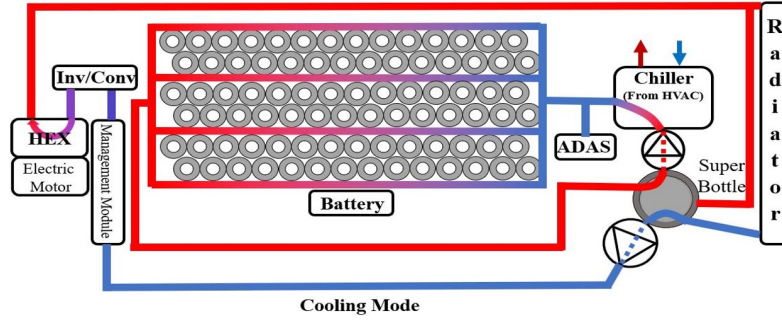


Figure 26: Cooling mode with super bottle tesla model 3 (based on [7])

The super bottle valve is in cooling mode connecting the entry and exit of the battery and chills the refrigerant using the chiller. The electric motor and electronics are separated from the other loop and are being cooled by the radiator. The passenger compartment system is separated from the chiller. In figure 27 the other mode where the super bottle connects them in series for heating the battery. While stationary, the phases of the electric motor can be set in such a way that losses and no wheel-rotation is achieved to heat up the battery. Approximately 3-3.5 kW of losses can be produced per motor and eliminates the need of a PTC heater to heat the battery.

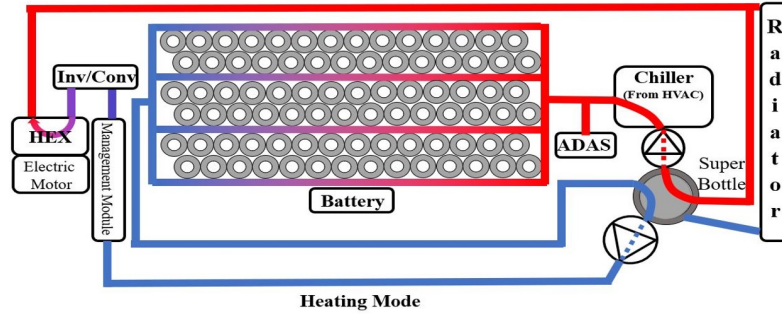


Figure 27: Heating mode with super bottle tesla model 3 (based on [7])

The super bottle is not the only solution to take advantage of holistic effects, in Tesla model Y a more complex solution called the octovalve was introduced. The octovalve is the evolution of super bottle and contains a plastic and aluminum refrigerant manifold, a nylon 8-way valve with electric step motor, a chiller and 2 pumps [13]. It is capable of providing 15 different thermal management modes where 12 are heating modes and 3 are cooling modes which enables multiple cases in a complex control system. In heating mode the octovalve makes it possible to extract heat from not only the battery, electronics and ambient air, but also the cabin. In sunny winter days the cabin is heated up through solar radiation, the heat can be transferred through the octovalve to heat up the battery while stationary [13]. The Tesla model y equipped with a thermal management system utilizing this method increased driving range by 10% [16]. Additional manufacturers developing a holistic TMS is Bosch who claims longer range and longevity from their TMS [36]. Mahle is another company with focus on holistic approaches in their TMS and claims a 20% increase in driving range at 0°C [51]. Although some manufacturers such as Chevrolet with parallel loops are still reluctant towards the strategy, it can increase range and longevity, while also limiting components and therefore overall costs [113].

4 Modeling and simulation methodology

In this chapter the methodology used for building the Amesim model and running simulations is being described. The model was built in an iterative process with smaller steps, later on verified with official vehicle data. Additionally the driving cycles used for simulating and evaluating the concepts of TMS strategies are being described.

4.1 Methodology

A model of a BEV with a TMS was gradually built in Amesim using a step-by-step methodology. The model is constructed in six main steps with substeps in between with the following approach:

- **v1:** A simple model with the powertrain, vehicle and driver without any thermal management or control systems. Parameters from the components initial values are used to a large extent while some are adapted to BEVs. A PMSM electric motor drives the rear wheels through a one-speed transmission. A li-ion battery delivers the power directly to the electric motor with a build-in converter for the current.
- **v2:** Adding two parallel and simple cooling circuits for the electric motor and traction battery. Circuits includes pumps, radiators, valves and hoses with properly dimensioned components.
- **v3:** Including a PTC-heater for traction battery, control systems added for thermal management loops to work more efficiently and keep components within its temperature range.
- **v4:** Adding low-voltage power consumers with a DCDC 12V component, also adding high-voltage consumers including heater and compressor.
- **v5:** Including the third thermal loop for the cabin (HVAC). The HVAC cools and heats the cabin and cools the battery through a chiller. The v5 was used for validation and is the base-model for the TM concepts.
- **v6:** The final version includes all concepts for thermal management strategies. Peak-I, heating for re-generative braking, connected battery and electric motor and others are sub-models of v6.

The created BEV model with the TMS for the battery, electric motor and passengers compartment was used to perform simulations of different scenarios, conditions and strategies possible. Based on data provided by the literature and official sources such as the EPA, the model could be validated, further simulations and models of the concepts of TMS strategies could be developed, simulated and evaluated. In figure 28 and 29 the fifth and first version of the model is illustrated to show the development.

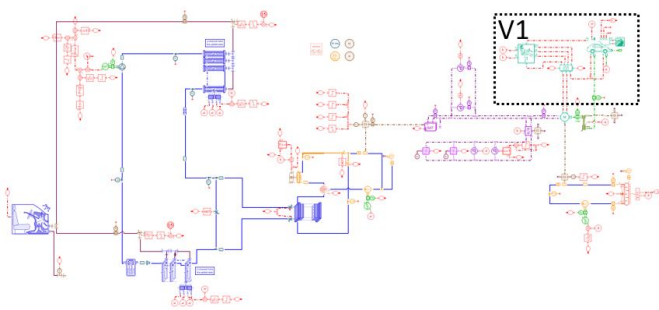


Figure 28: V5-model showing the V1-part

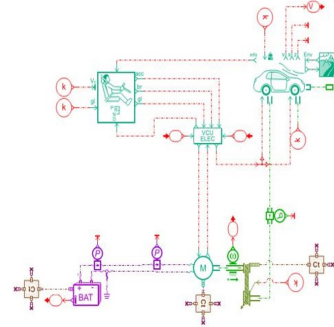


Figure 29: V1-model

4.2 The Amesim model of a BEV

The BEV model consists of several subsystems which include the driver, vehicle, battery loop, electric motor circuit, HVAC with control system and the auxiliary components. In the following chapters these subsystems are explained, together with the parameters specified for different components.

4.2.1 Driver and vehicle

The driver and vehicle submodels contain the information about the vehicle parameters, driving cycle and how much regenerative braking is allowed. These are illustrated in figure 30 where components are represented with illustrative images and connections between them with lines. The driver receives inputs from vehicle and vehicle control unit (VCU) including power, forces, speed and vehicle data and sends acceleration commands to the VCU. Commands on acceleration or deceleration are illustrated in figure 31 where the signals are depending on the driving cycle requests. The VCU then interpreters the information along with the parameters such as SOC and rotary speed and sends signals to the electric motor which actuates the commands.

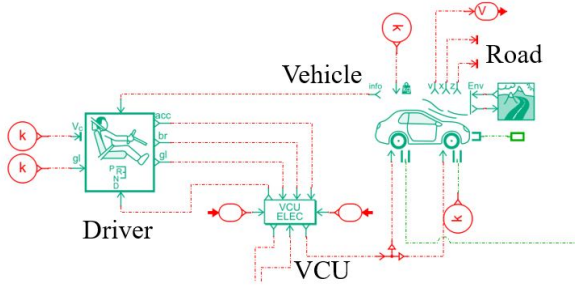


Figure 30: Driver submodel in Amesim

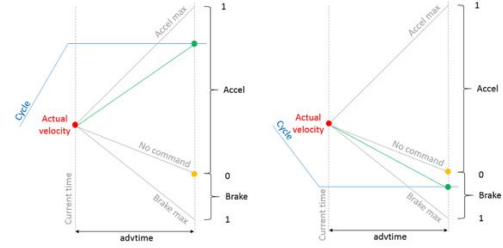


Figure 31: Driver control from Amesim

The driver model calculated the required force using equation 3 and the power required using equation 29 where $F_{external}$ represents the forces acting on the vehicle and V_v is the vehicle's velocity.

$$P = F_{external} * V_v \quad (29)$$

A standard passenger vehicle based on current electric vehicles are used for testing the concepts, based on the parameters which represents the market of BEVs. In Europe the best selling BEVs are the Tesla model 3 and Y, Renault zoe, Hyundai kona, Nissan leaf and VW ID 3 [50]. They belong in the compact vehicle class with curb weights ranging between 1.5-2 tonnes, battery capacity between 40-75 kWh and power between 100-200 kW. To create a standard vehicle that represents the market today, the specifications are based on these models. In table 3 the vehicle's parameters are provided.

Table 3: Driver and vehicle parameters for the standard vehicle

Model	Standard vehicle
Curb weight	1800 kg
Tire dimensions [W/H-R]	215/45-R18
Drag coefficient Cd	0.27
Frontal area	2.3m ²
Roll coefficient	0.01
Driven wheels	RWD

4.2.2 Battery loop

The battery loop includes a battery model with a thermal mass that is being heated or cooled by the TMS. Optimal temperature range for battery operation is between 15-35°C with the acceptable range between 0-45°C, hence the TMS is designed to keep temperatures between 0-35°C. There are two thermal loops used for controlling the battery temperature and the refrigerants path is decided by a thermostat and circulated by a single pump. The battery loop and thermal management strategy are illustrated in figure 32 and 33 respectively.

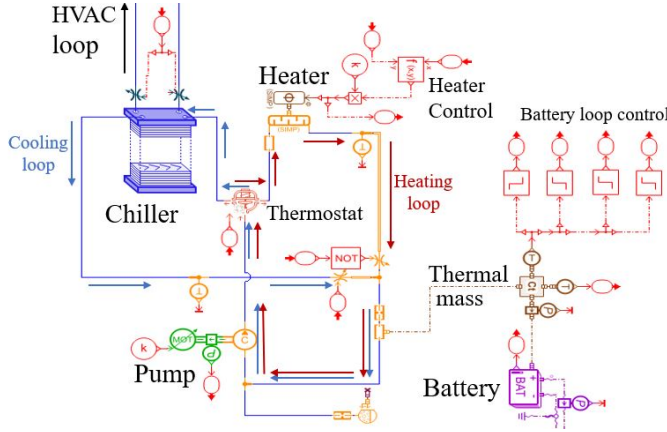


Figure 32: Battery loop in the model

Battery Temp [°C]	Path	Heater/ HVAC
$T < 0^{\circ}\text{C}$	Heat-loop	On/Off
$0^{\circ}\text{C} < T < 35^{\circ}\text{C}$	Heat-loop	Off/Off
$T > 35^{\circ}\text{C}$	Cool-loop	Off/On

Figure 33: Battery TM strategy

During heating the coolant flows through the thermostat to the heater where it is being heated up at the maximum power 7 kW. The heat energy depends on the battery temperature and decreases linearly to zero while battery temperature increases to 0°C. The coolant then flows to the thermal mass that acts as an indirect liquid cooling system and exchanges heat energy before it returns to the pump. At normal temperatures where neither cooling nor heating is required the coolant flows through the heater without receiving any heat energy.

In cooling mode the coolant flows through the thermostat and the chiller. The chiller is connected to the HVAC loop and acts as a heat pump where energy from the ambient air is extracted and exchanged to the battery loop. The chilled coolant flows to the battery and thermal mass, absorbing heat before returning to the pump. All components are parametrized using the data from the literature or publicly available for the corresponding vehicle models. These data include pumps, masses and efficiencies. Power for the components are either withdrawn through the DCDC low voltage system or directly through the battery using high voltage to realistically account for energy consumption. Battery characteristics is based on the actual electric vehicles in terms of capacity, weight and voltage (see table 4).

Table 4: Battery model specifications

Cell chemistry	Nickel-Cobalt-Aluminum (NCA)
Total battery pack energy Q_{pack}	65 kWh
Available battery pack energy $Q_{available}$	60 kWh
Nominal battery pack voltage	360 V
Battery pack capacity	180 Ah
Layout	99 in series, 3 in parallel (99S3P)
Total mass of cells	260 kg

4.2.3 Electric motor loop

The electric motor loop includes the cooling circuit with pump and radiator, the gearbox and electric motor itself. In Amesim the maximum torque, speed and power can be set by using the efficiency maps with speed and torque to consider the losses. The heat generated due to losses is transferred to a thermal mass which represents the cooled surface where heat is transported away by the liquid cooling system. The ambient air is then utilized to cool the coolant that is pumped through the circuit. In figures 34 and 35 the electric motor loop and power output are shown.

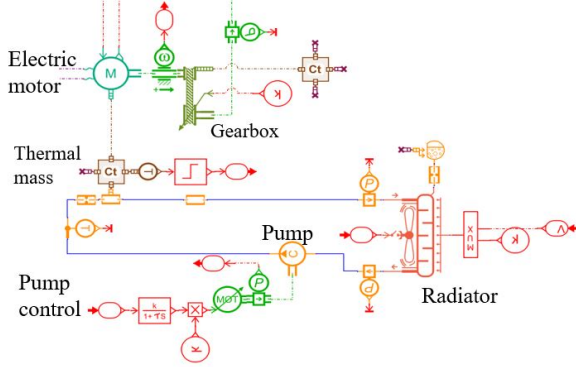


Figure 34: Electric motor loop from model

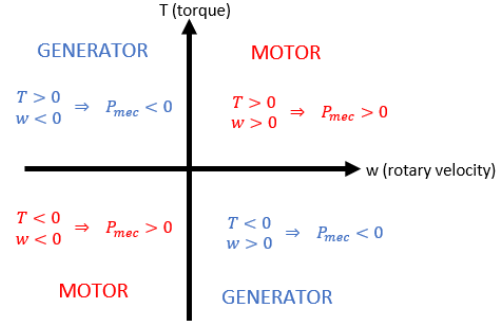


Figure 35: Motor control from Amesim

The top speed is set to 180 km/h and used to obtain the gear ratio in the gearbox that transfers power from electric motor to the rear wheels. In the standard vehicle model the electric motor loop is only cooled by the radiator, it is programmed to start once temperature exceeds 80°C. Power consumed by the radiator and pump are withdrawn from the low voltage circuit through the DCDC. In table 5 the specifications of the electric motor and gearbox are presented.

Table 5: Electric motor characteristics from the model

Motor type	Permanent Magnet Synchronous Machine (PMSM)
Max motor power	150 kW
Max motor torque	350 Nm
Max motor speed	12000 rpm
Gear ratio & efficiency	8.0 & 0.98
Activation temperature	80°C

4.2.4 HVAC and control system

The HVAC includes all parts for the air-conditioner/heat pump, cabin and the whole control system to keep both battery and cabin within their preferred operating temperature ranges. There are several control strategies that can be implemented with more efficient and rapid simulations but manufacturers are seldom transparent with their own strategy. The strategy is based on the target temperatures with PID-controllers that requests varying rotational speed the HVAC-compressor and there are three objectives to fulfill: cooling the cabin, heating the cabin and cooling the battery. In addition to controlling the compressor, fans and switches linked to the evaporator and condenser are considered as well in order to operate more efficiently and thus optimize energy-usage. In figure 38 and 37 the control system and full HVAC are illustrated.

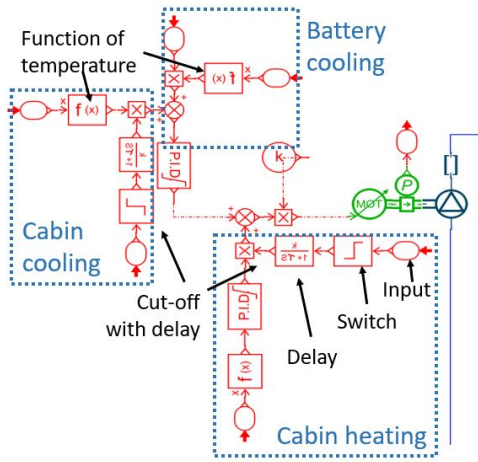


Figure 36: Compressor control from model

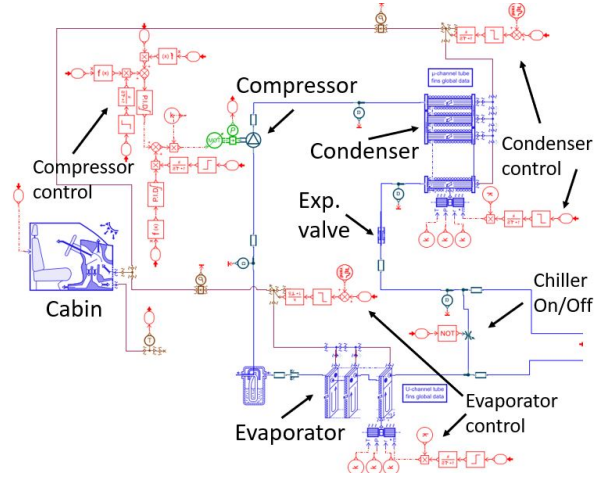


Figure 37: HVAC loop from model

The battery cooling receives input from the battery circuit control, both the actual temperature and switch-input to cut off the signal, thus avoiding disturbing the cabin cooling. A target of 35°C is set in the function, lower values activates the cut-off with a delay for increased numerical stability. The cabin cooling receives input from the cabin in a similar way as the battery temperature. 25°C is set as requested value with a cut off at 23.75°C to avoid high fluctuations from the control system. To extract heat the condenser valve opens and air flow to the cabin. In addition the airflow is limited at the condenser and increased at the evaporator to capture more energy. The cabin heating receives the same input as cabin cooling control, but uses different temperatures. Here 20°C is set as requested temperature and cut-off at 23.25°C to ensure stability. A valve opens at the evaporator to provide cool air for the cabin. Airflow in the condenser is increased while it is decreased at the evaporator, thus improving performance and saving energy from the low voltage system. Specifications on the components are from other vehicle models and from literature and parameters, see table 6.

Table 6: HVAC characteristics from the model

Compressor max. speed	3500 rpm
Compressor displacement	80 cc
Compressor efficiency (vol./isen./mech.)	0.6/0.75/0.9
Target/cut off temp. battery cooling	35/35 $^{\circ}\text{C}$
Target/cut off temp. cabin cooling	25/23.25 $^{\circ}\text{C}$
Target/cut off temp. cabin heating	20/23.75 $^{\circ}\text{C}$
Refrigerant	R134a

4.2.5 High and low voltage auxiliary

The high and low voltage auxiliaries include all the fans, pumps, heaters and compressors used in the vehicle. BEVs range is extra sensitive at hot and cold temperatures largely due to auxiliary loads. Instead of using the low voltage battery, energy from the traction battery is used and converted to suit low voltage components. For parts that requires high power (e.g. the compressor and heater) high voltage is needed to limit the currents. In figure 38 the model's auxiliary subsystem is illustrated where different loads are represented by different components with predefined parameters.

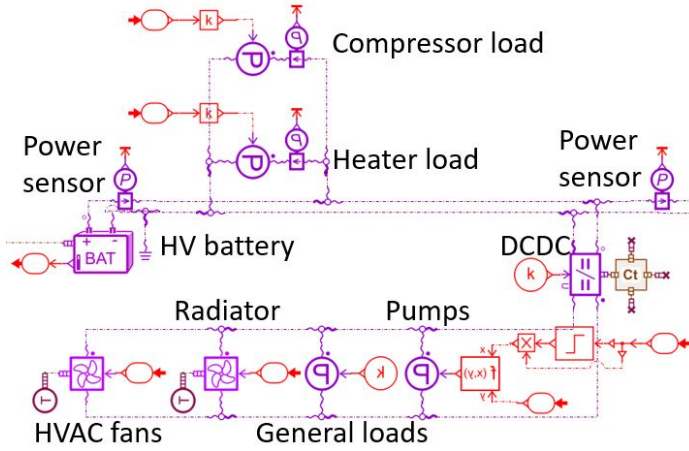


Figure 38: HV and LV auxiliary load system

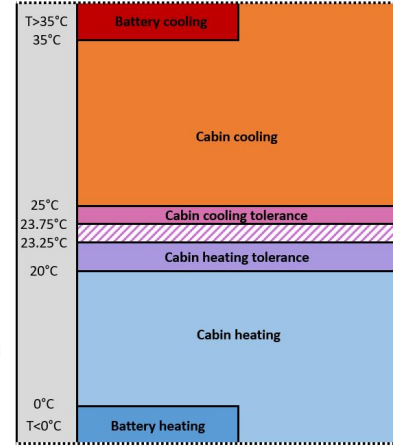


Figure 39: TM strategy used in the model

During driving the high voltage consumers send out signals through a power sensor, which is received by a generic load connected to the traction battery. Low voltage consumers work in a similar way where an input signal initiates the withdrawal of power, depending on how much the TMS requires. In more extreme temperature conditions auxiliary loads are significantly higher, in figure 39 the TM strategy is illustrated for various temperatures (assuming ambient temperature is the same as components). At cabin-temperatures above 25°C it is being cooled, and above 35°C battery cooling is required as well, resulting in high auxiliary loads. At optimal conditions between 20-25°C the loads will be lower due to lower requirements.

Table 7: Auxiliary loads characteristics from the model

Compressor max. power	3000W
Battery heater max. power	7000W
Pumps max. power	50W
General loads max. power	50W (continuous)
Radiator power nominal/max	140/180W
HVAC fan power	60W
DCDC voltage	12V

4.3 Driving cycles and ambient conditions

A BEV is exposed to a wide range of driving conditions where temperatures range from far below the freezing point up to hot temperatures during summer. In addition, driving varies in different situations with city, rural, and highway driving. The vehicle has to perform well in all conditions with sufficient range and comfort and this can be tested using driving cycles in various conditions. A driving cycle is a set of data-points containing both speed and time and are used by authorities today to test vehicle's performance before they enter the market. The most common variants are transient driving cycle where speed varies substantially to represent real-life conditions, resulting in more acceleration and deceleration. A common parameter used to visualise how much acceleration force a driving cycle causes is the Relative Positive Acceleration (RPA) which is defined as:

$$RPA = \frac{\int v(t) * a_{positive}(t) dt}{\int v(t) dt} \quad (30)$$

4.3.1 WLTP and NYCC driving cycles

Worldwide Harmonized light vehicle Test Procedure (WLTP) is a driving cycle used in Europe since 2017 when it replaced New European Driving Cycle (NEDC). Unlike NEDC it is based on real driving and data, it is both longer, faster and more demanding thus resulting in higher consumption. WLTP includes different stages of driving such as city, urban, rural and highway within 30 minutes and range estimations based on WLTP are commonly considerably closer to actual range than NEDC [14]. The WLTP varies depending on vehicle type, class 1 and 2 are for lower power-to-weight vehicles, at a ratio above 34 W/kg class 3 is used with low, medium, high and extra high-speed cycles [42].

New York City Cycle (NYCC) is a low speed drive cycle representing city driving with multiple starts and stops. NYCC is significantly shorter, less than 2 km driven distance and average speed of 11.4 km/h [41]. Due to its start-and-stop characteristics there are lots of accelerations and decelerations within a short distance, resulting in high energy consumption per kilometer and therefore lower range. Air and roll resistance are low compared to higher speed driving cycles and energy from accelerations and auxiliary loads increases in importance. This is where regenerative braking and efficient thermal management becomes vital. In figures 40 and 41 the WLTP and NYCC driving cycles are illustrated.

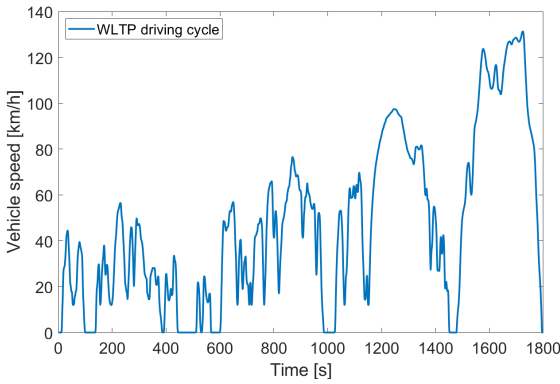


Figure 40: WLTP driving cycle profile

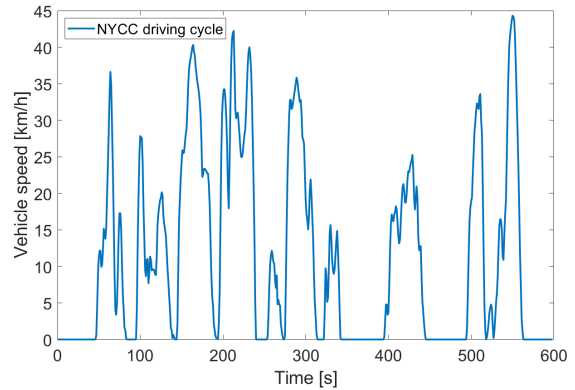


Figure 41: NYCC driving cycle profile

4.3.2 UDDS and HWFET driving cycles

Urban dynamometer driving schedule (UDDS) is known as Federal Test Procedure (FTP-75, see figure 42) is a driving cycle used mainly in North America. It is based on its predecessor FTP-72, but accounts for hot start and a ten minute long "soaking part" where the vehicle is stationary. In total the cycle lasts 40 minutes (with the ten minute stationary period), maximum speed is 91km/h and distance shorter than 18 kilometers. Similarly to WLTP is a combination of multiple driving scenarios including urban and city driving. It is one of the main testing cycles used by the Environment Protection Agency (EPA) whom tests vehicles in North America [39].

Highway Fuel Economy Driving Schedule (HWFET, see figure 43) is another test cycle used by EPA with focus on highway driving. The total driving distance is 16.5 kilometers during 13 minutes due to its high average speed of 78km/h [40].

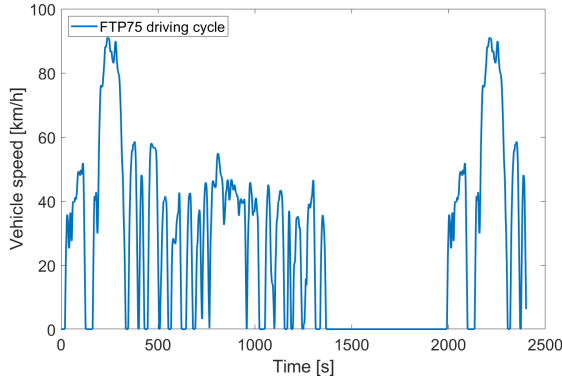


Figure 42: FTP75 driving cycle profile

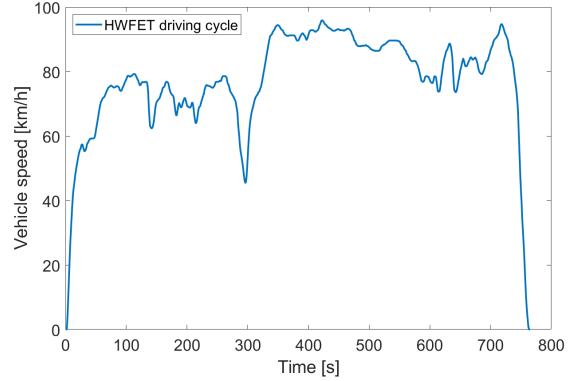


Figure 43: HWFET driving cycle profile

UDDS and HWFET are combined when EPA tests the range and consumption of new BEVs. EPA has developed a formula to calculate range based on city and highway driving where city is weighted to 55% and highway to 45% according to following equation: [43]:

$$Range_{combined} = CF * (Range_{city} * 0.55 + Range_{highway} * 0.45) \quad (31)$$

Where CF is a correction factor set to 0.7 by EPA based on actual testing [33]. EPA allows for different tests of EVs where manufacturers can either choose a two-cycle test with UDDS and HWFET and use 0.7 as correction factor or a five-cycle test that includes three additional tests [4]. These are the high-speed US06 driving cycle, the SC03 with high temperatures and air-conditioning on and finally a cold test at cold temperatures using UDDS, putting the thermal management at test. By running the five-cycle test procedure manufacturers can use a different correction factor, for example Tesla proposed the correction factor 0.765 for their model Y and 0.705 for model 3, resulting in longer rated driving range [33].

4.3.3 Real world based driving cycles

Driving cycles are fundamentally limited by the way they were developed, as approximations on driving patterns suitable for lab-environments. Real world driving is difficult to reproduce in a driving cycle, hence the official range estimations differ from real world range experienced by the drivers. The European commission started the ARTEMIS project to develop driving cycles based on actual data and different conditions for more accurate results [61]. Artemis includes three different driving cycles: urban, rural and highway based on data collected from vehicles driving in Germany, Greece, France and UK and the project as a whole involves multiple European research laboratories. The highway cycle has an average velocity of 100 km/h and a peak at 150 km/h and lasts for almost 30 km. Several highways have top speeds above 120 km/h, compared to HWFET and WLTP that either too slow or reach high velocities for short time instances.. In figure 44 the Artemis highway cycle are illustrated where higher speeds are more common. In figure 45 Artemis urban driving cycle is illustrated where accelerations and decelerations are more common than in the highway cycle, but at lower speeds.

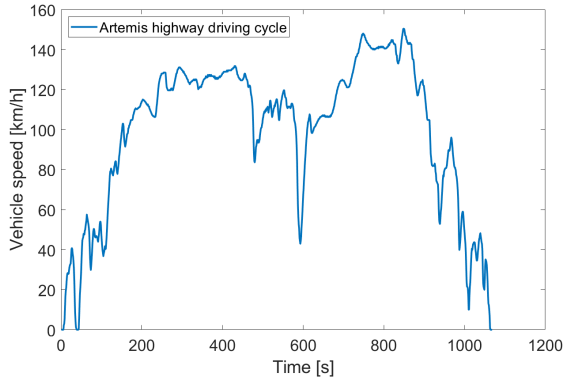


Figure 44: Artemis highway drive cycle profile

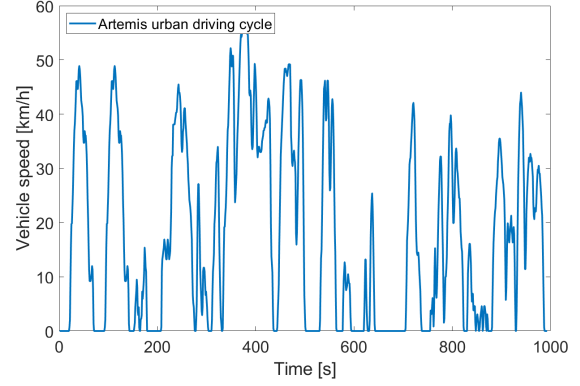


Figure 45: Artemis urban drive cycle profile

In table 8 the characteristics for each driving cycle are presented including type, distance, velocity and accelerations. To represent different driving scenarios, time and distances. NYCC has the lowest average and top speeds, but instead has high accelerations and RPA. WLTP and Artemis highway have the highest top speed and longest distance but low accelerations and RPA, resulting in higher air resistance compared to acceleration forces. HWFET has the lowest acceleration and RPA while Artemis urban is the opposite. The standard vehicle and the concepts for TM strategies are tested for all driving cycles for diversified conditions to cover a wide range of driving scenarios.

Table 8: Driving cycles parameters

Cycle	Type	Time [s]	Distance [km]	Avg. speed [km/h]	Top speed [km/h]	max pos. acc. [m/s^2]	max neg. acc. [m/s^2]	RPA	Temp [$^{\circ}C$]
WLTP	City, Urban, rural, highway	1800	23.3	46.5	131.3	1.58	1.49	0.15	23
NYCC	City	598	1.9	12	45	2.7	2.3	0.29	23
UDDS	City, Urban	1874 (2401)	17.3	33 (26)	91	1.5	1.5	0.16	23
HWFET	Highway	765	16.5	78	96	1.4	1.5	0.07	23
Artemis Highway	Highway	1068	29.5	100	150	1.7	2.9	0.12	23
Artemis urban	Urban	993	4.9	58	18	2.4	2.8	0.30	23

4.4 Driving conditions

In Europe temperatures during summer can on average go above $30^{\circ}C$ and reaching over $40^{\circ}C$ during very hot days [37]. In winter months the temperature decreases to well below $0^{\circ}C$, commonly $-10^{\circ}C$ on average in some cities and down to $-20^{\circ}C$ depending on location [37]. In the United States the temperatures are similar, ranging from $-20^{\circ}C$ during winter and above $30^{\circ}C$ in summer months. A BEV has to handle all conditions while delivering acceptable performance and therefore the TMS has to be tested in both normal temperatures as well as extreme temperatures.

Driving in demanding conditions such as -15°C and 40°C has previously been proven to limit the performance. In colder climates the battery is affected with lower capacity and higher inner resistance, the air-density is higher resulting in higher air-resistance (especially at high velocities) and to keep components within their operating range auxiliary loads increase. The extra energy consumption from these phenomena decrease driving range, in some cases reduced by half the optimal range. In driving with a lot of deceleration, regenerative braking allows the vehicle to recuperate a portion of energy otherwise wasted in the mechanical brakes; at cold temperatures regenerative braking is heavily limited and thus leads to more losses. At warmer temperatures the battery is performing more efficiently but its longevity is affected and after a certain point every increased degree results in a shorter life. Also high auxiliary loads for the battery, electric motors and cabin result in a shorter driving range than in optimal conditions.

In between the extreme cold and hot temperatures there are also reductions in range, though not as severe. At 0°C the temperature is cold enough to require auxiliary energy consumption, and is usually where regenerative braking becomes available, making it a relevant condition for testing. The battery, electric motor and passengers compartment have different optimal operating conditions, however all three subsystems perform well at 20°C . In addition, most driving cycles used for determining official range of BEVs are performed at 20°C , and can be regarded as an "optimal condition" for benchmarking.

4.5 Verification of Amesim model

A model is only as good as its input parameters for simulations, without real vehicle data results can vary significantly, though it can be verified by analyzing the output parameters from the model. The BEVs available on the market today have all been verified in different driving cycles and have been assigned their official driving range. In Europe the range is determined by WLTP and in US EPA is responsible for the official rated range using their testing cycles. By comparing results from simulations with official data, it is possible to verify the driving range for vehicles. The focus of this work is to identify trends and differences between different BEV models rather than actual values due to lack of detailed vehicle data and experimental testing. The vehicles chosen for comparison are divided into three different classes: small city car, medium sized car and large premium car based on their characteristics. It is worth mentioning that they all have different TMS with different strategies, but uses indirect liquid cooling.

The smaller city cars are a mix of the top selling BEVs with recently launched cars. They have a smaller battery, lower weight, power and range but are affordable. Most of these vehicles are only sold in Europe and thus lacks official rating from EPA. Examples include Europe's top selling BEV Renault zoe and Mazda mx30 designed with philosophy that a small battery and low price is a higher priority than long range. The larger premium vehicles are representing the most expensive types of BEVs, often with long official ranges. Tesla model X, Mercedes EQS and Audi e-tron are used based on their market share and long range. In table 9 the city and premium vehicles included in the validation of the Amesim model are presented together with their official range in WLTP and EPA tests.

Table 9: Small city and large premium BEV range parameters

Model	Range WLTP [km]	Range EPA [km]
Renault Zoe	385	Not Tested
Honda e	222	Not Tested
Volkswagen ID3	420	Not Tested
Peugeot 208-e	339	Not Tested
Mazda mx30	200	Not Tested
Mercedes EQS 450	770	Not Tested
Audi e-tron	436	355
Tesla Model X	507	413

The medium sized car is similar to the standard vehicle used for analyzing different TMS concepts (see table 3) and is a mix of longer range Tesla models such as model 3 and y with high performance and cars with smaller cost and lower performance including the Volkswagen ID4 and Hyundai kona. This particular segment of vehicles has plenty of different strategies for cooling where Tesla and Hyundai have newly developed TMS which have proven to be highly efficient. There are also Polestar 2 and Volvo xc40 recharge with less information about the TMS, similar to Volkswgaen ID4. In table 10 the vehicle range parameters are presented.

Table 10: Mid-size BEV range parameters

Model	Range WLTP [km]	Range EPA [km]
Polestar 2 Dual Motor	470	373
Volvo XC40 recharge	418	333
Tesla Model 3 SR	448	421
Tesla Model Y LR	505	521
Volkswagen ID4	496	400
Hyundai Kona	484	413

In the simulations each BEV model is assigned parameters such as weight, power, capacity and drag coefficient, an example using polestar 2 is presented in table 11.

Table 11: Polestar 2 dual motor parameters

Model	Polestar 2 dual motor (AWD)
Curb weight	2198 kg
Battery (cell) mass	312 kg
Battery capacity (usable)	78 (75) kWh
Battery voltage, architecture	400V, 108s3p
Power, torque and speed	150+150 kW, 330+330 Nm, 12500 RPM
Tire dimensions [W/H-R]	245/40-R20
Cd, A	0.278, $2.3 m^2$
Gear ratio	8.57

The vehicle model is then tested in WLTP, UDDS and HWFET at 23°C initial temperature for the vehicle subsystems and ambient temperatures. Air-conditioning is turned off in the test to imitate the official tests and the simulation is run once with a half-empty battery in the start. The corresponding EPA range is in EPA are calculated using equation 31 with 0.7 as correction factor and a higher weightage towards the city cycle. The total energy consumed in the driving cycle is measured using sensors and retrieved from the post-processing in Amesim. By including total energy consumption, driven range, time and available energy in the battery the total range can be calculated using the following equations:

$$Q_{consumed} = \int_0^{t_{cycle}} E_{consumed} dt \quad (32)$$

$$Range = \frac{Q_{available}}{Q_{consumed}} * distance_{cycle} \quad (33)$$

Here $Q_{available}$ is the available capacity in the battery [Wh], $distance_{cycle}$ is the driven distance [km], $E_{consumed}$ is the average energy used in the driving cycle [W] and t_{cycle} is the time spent driving [h].

4.5.1 Verification of TMS

The WLTP, UDDS and HWFET driving cycles are conducted in optimal temperatures, leading to uncertainties in the performance of the TMS. Testing the model in those driving cycles at the same temperature is the first step in verifying the model, a comparison between actual testing and simulation results in multiple driving conditions is therefore performed as a second step.

American Automobile Association (AAA) performed tests in 2019 where the results for the driving range in cold and hot ambient conditions with the HVAC on and off were compared to those in optimal conditions. The difference in range was up to 50% for one of the five BEVs (see figure 7). In these tests AAA used a driving cycle consisting of UDDS, HWFET and US06 with a high speed run until capacity was too low to sustain a sufficient velocity [8]. The vehicles were charged and had the same testing temperature before the tests. BMW i3, Chevrolet bolt, Tesla model S P75D, Nissan leaf and Volkswagen e-golf were tested and apart from Nissan leaf they all utilize liquid cooling and PTC heaters.

Simulation of the tests can be made simpler by choosing starting parameters without waiting for hours to reach correct temperature. Likewise the energy consumption can easier be measured and the driving cycle can be performed individually without significantly increasing testing time. The vehicles using liquid cooling were simulated the UDDS, HWFET and US06 for five different scenarios: -7°C with and without HVAC, 23°C without HVAC and 35°C with and without HVAC and then compared to results from the AAA study. In figure 46 the ranges achieved by the AAA study for BMW i3, Chevrolet bolt, Tesla model S P75D and Volkswagen e-golf during the various conditions are presented.

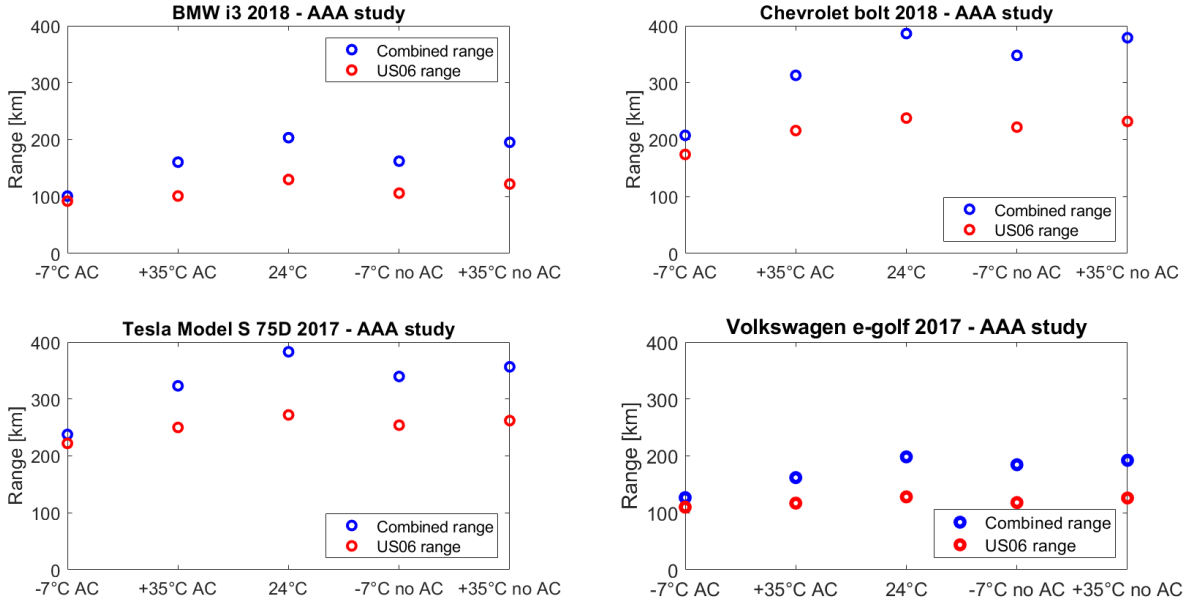


Figure 46: AAA range for different vehicles and operating scenarios

5 Thermal management simulations and concepts

In this chapter the impact of how driving cycles and conditions that affect performance of a BEV is presented and in what ways is investigated. A few concepts for thermal management strategies are presented with theoretical background and explanations in how they have the potential to improve performance of BEVs. The first concept is the most straightforward with preconditioning while the other have a more technical profile based on the literature and theory. Additionally the concepts are combined to form even further optimized strategy for thermal management.

5.1 Driving cycles and conditions in simulations

There are many variables to investigate, optimize and connect to different physical phenomena that varies in all types of situations in a BEV. If they are scaled down to a few minor areas where energy is consumed, the problem becomes more understandable. In a BEV there are mainly four areas where energy are consumed: battery to wheel with losses from both conversion and friction, battery losses, high voltage auxiliary systems and low voltage auxiliary systems. Depending on driving, such as different driving cycles, energy is consumed at different rates and proportions which in the end affects driving range for most types of vehicles. Driving conditions and especially ambient temperature affects BEVs to a higher extent where one of the four areas, the high voltage auxiliaries, accounts for a large part. In shorter driving cycles auxiliary energy consumption becomes a big part of the overall consumption and traction energy is a smaller part in demanding conditions. Regenerative braking is a unique feature for BEVs and allows energy to be regained, but only during certain conditions, if temperature is too cold it cannot work and energy consumption increases. Simulations for the standard vehicle model in WLTP, HWFET, FTP-75, NYCC, Artemis highway and Artemis urban in -15, 0, 20 and 40°C for a standard version of the BEV is performed. The target is to investigate how various conditions affect the efficiency and how different driving cycles affects range.

5.2 Preconditioning - the effect of initial temperatures

The three components with thermal management circuits are the traction battery, the electric motor and the passengers compartment. In demanding conditions with the vehicle exposed to ambient temperatures for a longer period of time, for instance during the night, these components will have the same temperature as ambient air. In hot summer days solar radiation can heat up the cabin to temperatures well above ambient and higher than 50°C, resulting in higher demands on the cooling system. There are also higher requirements to cool the electric motors and at certain temperatures to cool the battery. In the colder temperatures battery performance is significantly reduced and energy has to be spent on heating the battery. If the starting temperatures can be within the optimal operating range before driving, less energy has to be withdrawn out of the battery to control the temperatures. For this concept, the main objective is to identify how much energy can be saved and in what components during different types of driving. Parking the vehicle in a garage or temperature controlled space allows it to keep temperatures within optimal range. The temperature can also be controlled through energy taken from the power grid during charging, then used to power the air condition and heat pump.

Preconditioning is known by manufacturers to improve performance and is recommended in demanding conditions [11]. Previous studies have investigated the subject for BEVs, in one study the authors test an EV in -7°C and 35°C for a 52.8 km commute with and without preconditioning. The heater reduced range by 34.7% and air conditioning by 32.7%, using preconditioning 1.7% and 3.9% higher range was achieved [65]. In the same study they concluded that battery longevity was affected by preconditioning, between 2.1 to 7.1% less capacity fade and in warm temperatures 3 to 13.8% reduction in resistance growth. In addition to studies, there are several tests performed by vehicle owners in actual driving

situations. A Tesla model y with a heat pump is tested in a series of videos where temperature with and without preconditioning was -1°C and -9°C . The overall driving was 51km with a combination of rural and highway and conditions are similar besides initial temperature. Regenerative braking was not available with a cold battery and in -1°C preconditioning was found to reduce energy consumption by 5.1% and by 11.1% in -9°C [23].

The simulations in Amesim will use the 6 different driving cycles from chapter 4.3 with cold temperatures -15, -10, -5 and 0°C ambient, and 10, 20, 30, 40°C for warmer temperatures. In each cycle the battery and electric motor is set to 25°C , and cabin to 22°C with TM activated throughout the cycle. The standard vehicle is used with 50% initial SOC in all tests with regenerative braking available for battery temperatures above 0°C . In table 12 the testing conditions in each cycle are presented.

Table 12: Parameters in preconditioning concept

Ambient temperature $^{\circ}\text{C}$	-15	-10	-5	0	10	20	30	40
Battery+motor temperature $^{\circ}\text{C}$	-15/25	-10/25	-5/25	0/25	10/25	20/25	30/25	40/25
Cabin temperature $^{\circ}\text{C}$	-15/22	-10/22	-5/22	0/22	10/22	20/22	30/22	40/22
Solar radiation $[\text{W}/\text{m}^2]$	0	0	0	0	150	300	450	600

5.3 Peak I - minimizing the peak currents

In a BEV all the power to different subsystems including electric motor power, low voltage auxiliaries and high voltage auxiliaries. In certain driving situations the traction force is high, for instance at higher speeds, high acceleration or uphill high load driving, resulting in a high power withdrawal from the traction battery. During these situations the power to auxiliary systems could momentarily be limited to even out power output from the battery by at a later stage use a bit more energy. Power from the battery comes from current multiplied by voltage and the losses inside the battery, also known as irreversible losses are calculated according to the following equation:

$$P_{irreversible} = R_{internal} * I_{battery}^2 \quad (34)$$

Here $R_{internal}$ is the internal resistance and $I_{battery}$ is the output current from the battery. By increasing the total power output and thus the current, losses increases exponentially. The internal resistance is commonly not large and the irreversible losses are not much more than a small fraction relative to output power. From the theoretical background it is evident that a higher discharge rate with higher current results in lower capacity, the temperatures are higher and need to be controlled by the TMS. Since the TMS accounts for a substantial part of the auxiliary loads, the strategy of when to use it at a micro scale could lead to lower overall losses at macro scale.

In the study *An Optimal Energy Management System for Battery Electric Vehicles* the authors have a similar approach where they limit the 4kW cabin heater at certain loads [102]. Three variables are aimed to be minimized, the difference between cabin temperature and desired temperature, difference in mean power and difference in overall power. The test is performed in EPA driving cycle FTP-75 without the ten-minute soaking phase. Ambient temperature was -10°C , starting cabin temperature 0°C with a target of 22°C . The strategy is called EMS, and in the end of the driving cycle it reduces battery losses by 13% by controlling the heater resulting in a decrease of the current peaks. Without EMS cabin temperature stabilizes at 22.5°C and heating power remains constant, but both parameters fluctuates significantly with EMS. Battery losses do not account for a large part of overall losses and efficiency-effect is low. A recommendation from the study is to include more components in the strategy, which is the purpose of the concept in this case. The other components includes air conditioning for the cabin and cooling for the battery, other smaller loads from the DCDC consume such low power

that increased complexity is not worth it. The control system used in the model is based on PID-controllers with input on difference between actual and target temperature, similar to the report. A large difference results in higher input signals for the battery heater and compressor which controls cabin and battery temperature. By monitoring the power used for traction, an equation can be created and used as a factor FP, multiplied to the input signal from PIDs:

$$FP = \left(\frac{P_{max} - P_{traction}}{P_{max}} \right)^2 \quad (35)$$

Here P_{max} is maximum output from the electric motor [W], $P_{traction}$ is the power output for the moment [W]. In order to affect consumption more at the higher loads the difference in power is exponential and makes FP affect auxiliary power less during lower loads. During decelerations regenerative braking results in negative traction power and thus puts the input signal above 1, leading to an increased output. For the compressor an absolute value of the traction power was used to avoid disturbing the control system. The principle remains the same with limiting the current peaks. When the battery is being charged a higher power request from auxiliaries limits the current peaks and thus the losses. In figures 47 and 48 the implementation of the strategy in Amesim together with the schematic diagram is presented.

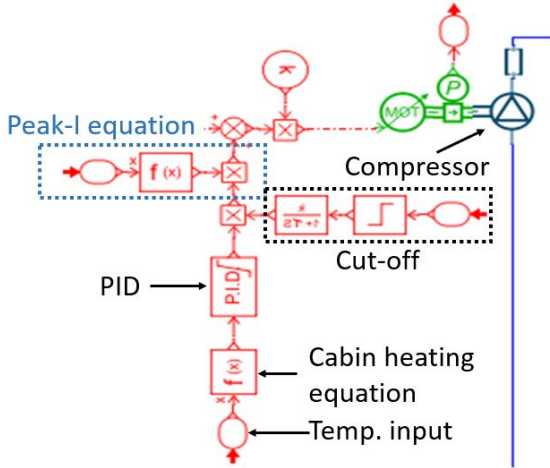


Figure 47: Amesim Peak-I model

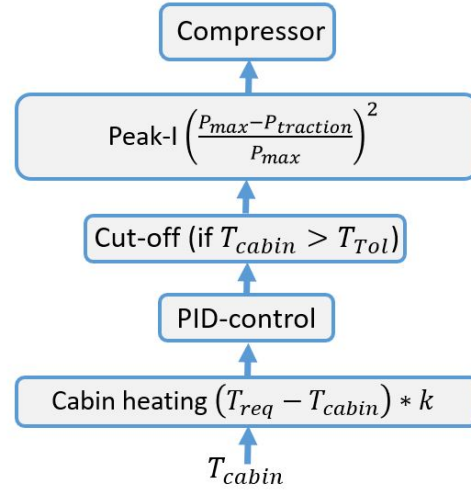


Figure 48: Cabin cooling - block diagram

The *Peak-I* strategy was implemented in the model and simulated for the six driving cycles as well as -15°C, 0°C, 20°C and 40°C. The standard vehicle was used, starting SOC was 50% and regenerative braking was activated for temperatures above 0°C.

5.4 Re-gen - heating up battery for regenerative braking

Regenerative braking offers a major difference compared to vehicles with a combustion engine. The feature allows for kinetic energy to be harvested to chemical energy in the battery instead of heat energy in the friction brakes. The maximum allowed regenerated energy depends on two main areas: the mechanical and the electrical. The mechanical aspect is due to the electric motors maximum power and vehicle dynamics where a too high torque can result in wheel slip and unsafe vehicle behaviour. BEV manufacturers in some instances limit regenerative braking to 80-100 kW and a deceleration of around 2.7 m/s² depending on vehicle model. The electrical aspects include maximum charge current (c-rate) but also SOC and temperature the battery currently possesses. In case of a fully charged battery, regenerative braking cannot

A well-established and experienced electric vehicle tester conducted a range of tests of multiple electric vehicles and regularly publishes data and information about their performance, noticing the regenerative power of a Tesla model 3 varied with SOC and temperature [72]. In the tests it was concluded that a low SOC and high battery temperature provided optimal conditions for regenerative braking while a high SOC or low temperature instead limited it. Additionally it was noticed that maximum regenerative braking capacity was varying between 0 and 85 kW, instead of being either on or off. In the Amesim model SOC and temperature limits are incorporated with a binary system of either maximum or zero power and no available regenerative braking below 0°C and above 90% SOC. In order to provide a realistic scenario, a function depending on SOC and battery temperature is necessary instead of switching between zero and maximum according to:

$$\begin{array}{l|l} \text{SOC} < 90\% \text{ and } T_{\text{battery}} > 0^{\circ}\text{C} & \text{Maximum regenerative braking available} \\ \text{SOC} > 90\% \text{ or } T_{\text{battery}} < 0^{\circ}\text{C} & \text{No regenerative braking available} \end{array}$$

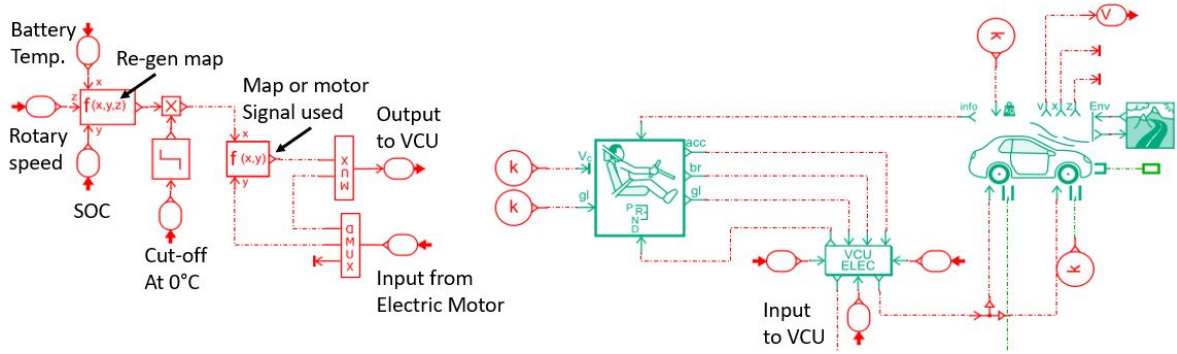


Figure 49: Regenerative braking control module in Amesim

In figure 49 the modification in the Amesim model to incorporate a new regenerative braking map is illustrated. The torque and power signal from the electric motor is passed through the new control system where it decides on what to request from the VCU. The VCU receives the signals and actuates the task. In a range of various experiments using a Tesla model 3 where the tester connects to the CAN-system and visualizes data while driving, these includes battery temperature, SOC and maximum permitted charging. This data is collected and used for creating a dual-variable function of SOC and temperature. In figures 50 and 51 the data map and approximated 3D-plane are presented.

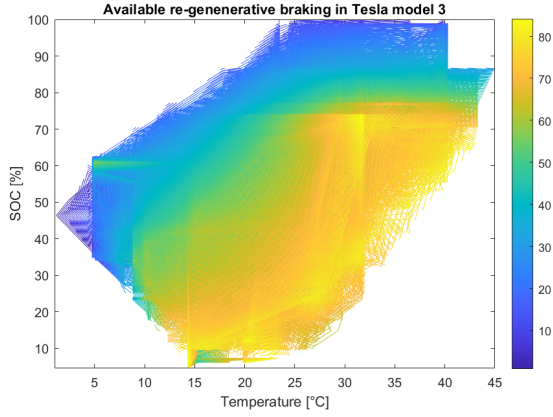


Figure 50: Regen-map from Tesla Model 3 [72]

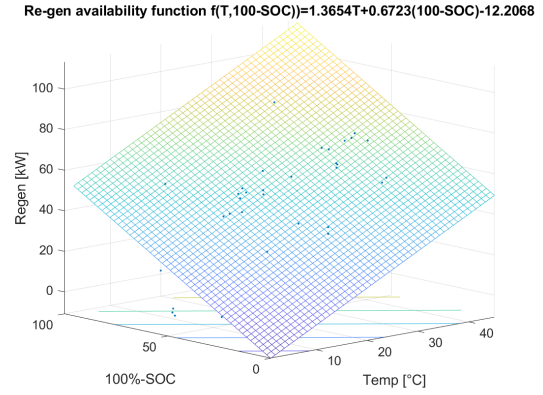


Figure 51: 3D-plane from data points

From the map it is clear that not all data points were available, for instance low SOC at very low and high temperatures, but also in the higher SOC for a cold battery. The low SOC-high temperature can be assumed to have high regenerative braking available in contrast to high SOC-low temperature. Low SOC-low temperature are more complex to approximate, but from the map assumptions of about 50% regenerative braking power is available which is the case for the approximated function:

$$f(T_{battery}, SOC_{used}) = 1.3654 \left[\frac{kJ}{s \cdot ^\circ C} \right] * T_{battery} + 0.6723 \left[\frac{kJ}{s} \right] * SOC_{used} - 12.2068 \left[\frac{kJ}{s} \right] \quad (36)$$

Here $T_{battery}$ is the battery temperature and SOC_{used} is the used capacity, if for instance 25% SOC remains, SOC_{used} becomes 75% and simplifies the function where both inputs being zero equals no regenerative braking available. Additionally, the factor for temperature is twice as high compared to the SOC factor, implying that temperature affects maximum regenerative power the most. Equation 36 allows for optimization in terms of consumed energy heating up the battery to make regenerative braking available to a larger extent. Unlike preconditioning where energy is taken from the grid to power the TMS, there are multiple cases where a BEV has to use energy from the battery. Under the assumption that all energy from the battery heater is transferred to the battery and that heating due to internal resistance is low, energy required to heat up the battery to zero becomes:

$$E = m_{battery} * C_{cells} * \Delta T = 260 * 2 * T_{initial} \quad (37)$$

Here the standard vehicle battery has a cell mass of 260 kg, a specific heat capacity of $2 \text{ kJ}/(\text{kg} * \text{K})$, thus the initial battery temperature becomes important. Assuming that SOC is within the range and that full regenerative power is available above 0°C , different driving cycles have different conditions according to table 13.

Table 13: Regenerative braking various driving cycles

Driving Cycle	Total re-gen. energy [kJ]	Break-even temp. [$^\circ\text{C}$]
WLTP	3960	-7.6
FTP75	3241	-6.2
HWFET	803	-1.5
NYCC	748	-1.4
Artemis Highway	2884	-5.5
Artemis Urban	2135	-4.1

The longer driving cycles can generate more energy and city oriented cycles have more energy per travelled distance. The data is gathered from simulations using the standard vehicle at optimal temperature and SOC. Simulations to test actual performance utilized the re-gen map from tesla model 3. The first step is to perform a pre-heating cycle where the battery is heated up with constant power of 7kW from the initial temperatures -1, -3, -5 and -10°C. The power consumed during the pre-heating is then saved for a range of new battery temperatures used while starting the driving cycle. For example, starting temperature of -5°C and heating up to +1°C is an increase of 6°C and results in a certain energy consumption. Since SOC affects total regenerative power, two different levels of battery charge are used: 30% and 70% to find differences between the cases. From table 13 WLTP is one of the driving cycles with high energy regeneration and the shorter highway cycle HWFET one of the lower, both are tested with the purpose of investigating if pre-heating the battery by using its own energy becomes more efficient.

5.5 BEM - connecting components in a holistic approach

The Battery and Electric Motor (BEM) are two of the main areas in a BEV which requires thermal management. They work optimal in different temperature ranges where the battery is more sensitive and performs best between 15-35°C and the electric motor can be very cold and above 100°C. The electric motors efficiency are largely depending on iron losses and the copper losses, which is high temperature dependent and likes it cold. The thermal mass inside the electric motor is significantly lower than the thermal mass of the battery, thus can energy be transferred between the components to cool the motors without noticeably affecting the battery temperature. A mass of 260 kg of battery cells compared to 5 kg of copper in the electric motor are used in the model, temperature increase in the battery can be calculated using:

$$\Delta T_{battery} = \frac{m_{EM} * c_{EM} * \Delta T_{EM}}{m_{cells} * c_{cells}} = \frac{5 * 0.377 * \Delta T_{EM}}{260 * 2} = 0.0026 * \Delta T_{EM} \quad (38)$$

Here c is the specific heat capacity of the cells and copper, if the electric motor is cooled from 100°C to 30°C, the battery temperature rises with 0.1°C assuming optimal conditions. According to the equation, battery mass is of great importance, a reduced mass will heat up quicker and thus may not absorb as much heat from the motors to cool them. In the Amesim model the electric motor component uses a complex system to model the iron losses and are hence excluded in this concept. During colder ambient conditions dissipated heat losses from the motor can be transferred to the battery to heat it up and result in synergy effects. By heating up the battery with the electric motor's losses, the need of a heater is eliminated which saves cost and reduces weight. By connecting the two components thermal management circuits using a valve they can work in both parallel and series depending on the condition, largely due to various temperatures. In the Amesim model a 4-way valve is incorporated to control the flow of coolant, by varying the valves position the components can be connected in series or in parallel depending on scenario. Additionally, the electric motor model is modified with a different component to increase control over the losses. The updated component also includes a separate inverter that can be seen in figure 53.

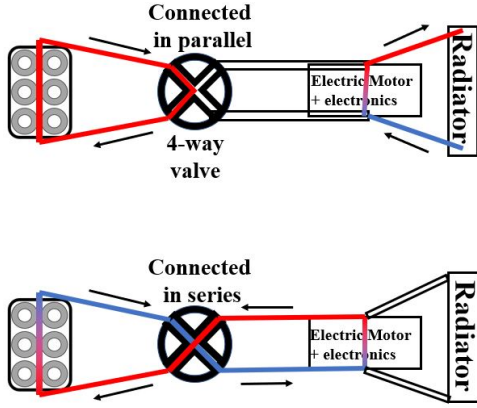


Figure 52: Series and parallel TM circuit

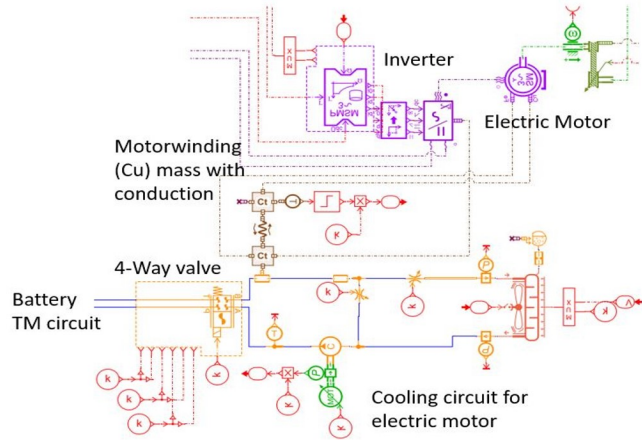


Figure 53: Amesim BEM model

In figure 52 the principle behind the 4-way valve is illustrated. When the battery is cold or within standard temperatures its TM circuit can be in series with the electric motor to cool it. During higher temperatures they are in parallel and the radiator is used to cool it. The heater is turned off even at very cold temperatures since the electric motor is being heated up quickly while the battery takes longer time and remains cold, thus eliminating the effects and consuming energy for the heater. The internal resistance inside the battery commonly decreases when temperature rises. Although this consumption is small part of the total energy consumed, it becomes even smaller by utilizing the concept. Internal resistance varies a lot depending on cell chemistry and other parameters. By using the expression previously mentioned: $R(T) = 90.196e^{-0.08T} + 25.166$ and the irreversible internal losses $P = R * I^2$ the difference can be approximated. An increase in temperature of 0.1°C from 20°C due to cooling the electric motor from 100°C to 30°C would result in resistance decreasing by 0.5% from 43.4 m Ω to 43.2 m Ω . The copper losses in an electric motor depends on the copper wire resistance, which is temperature dependent according to: $R(T) = R_0 * (1 + \alpha_0 * (R_{wire} - R_{ref}))$. Reducing temperature from 100°C to 30°C results in a 21% reduction in resistance, with copper losses accounting for a big part of total motor losses the efficiency can be increased noticeably. Simulation using the Amesim model with battery TM loop and electric motor TM loop connected are performed at -15°C , 0°C , 20°C and 40°C in the six different driving cycles. The standard vehicle with 50% SOC is used in this concept as well.

6 Results

In this chapter the results from model verification, different driving cycles and conditions as well as the concepts *Preconditioning*, *Peak-I*, *Re-gen* and *BEM*. In addition to range from the various models, the background with energy consumers and differences is provided for a full-scale picture of the results.

6.1 Amesim model verification results

The total of 14 different BEVs used for verification of the model were simulated in WLTP driving cycle along with FTP75 and HWFET forming the EPA testing procedure. Temperature during these tests is considered to be optimal with very low energy consumption by components other than what is used to provide traction force. The car models are divided into three different categories, the smaller city car, medium vehicle and large premium vehicle to observe and investigate possible differences or trends. For smaller city cars and one premium vehicle EPA does not provide any official range data to compare with. However, WLTP includes official data on all BEVs used for verification in this test.

In figure 54 the results of the simulations for all the 14 vehicles in both WLTP and EPA are presented together with the official range. The first five models are city vehicles, the middle ones are medium vehicles and the last three are large premium vehicles organized in order for the purpose of clear visualization. In WLTP the model is providing results which correlate well with the official range data. Both for city and medium vehicles the difference is low, for large vehicles only one shows a clear difference between the model result and the targeted official results. In EPA the results depend on which BEV is being considered. Polestar 2, Volvo xc40, Volkswagen ID4 and Audi e-tron shows very close results to data from the manufacturers. All Tesla models including model 3, model Y and model X are showing lower range from the model compared to official range while Hyundai kona is slightly underestimated by the model. An additional observation from the figure is that none of the simulation results in EPA are exceeding the range provided by EPA driving cycles. On average WLTP results in 22% higher estimated range than EPA based on simulation results. The difference between WLTP and EPA in terms of official data is a bit lower at 11%, largely due to Tesla models official range is similar in the two testing cycles.

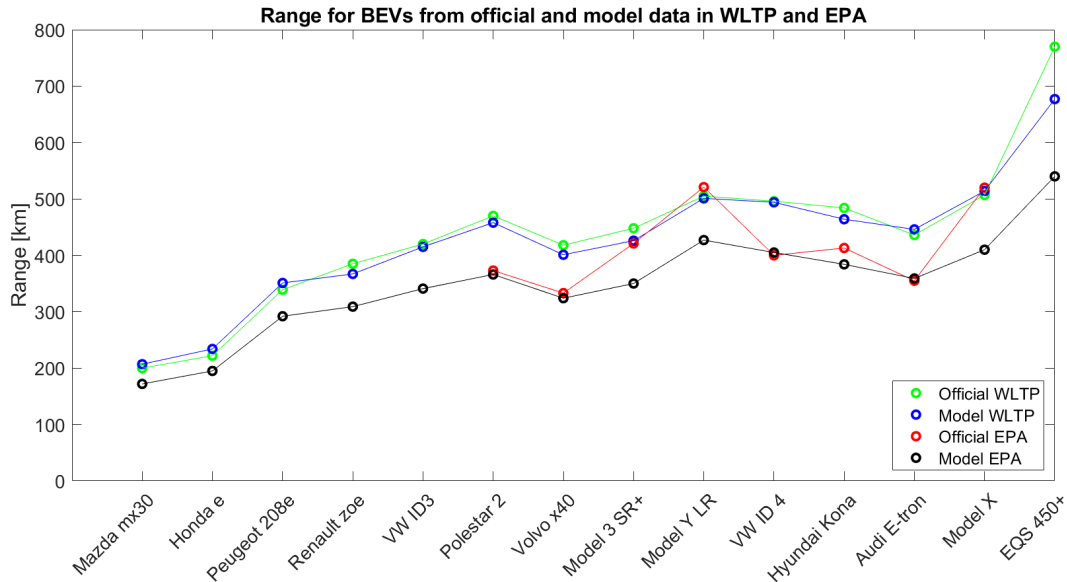


Figure 54: Model verification - range in WLTP and EPA from official data and simulation

In table 14 additional data from the simulation is presented. The difference between official range and simulation range and the standard deviation for WLTP and EPA for three vehicle segments. WLTP shows a small difference for all three types and for city and medium vehicles standard deviation are very low. Large vehicles show a slightly higher difference and standard deviation. Difference for EPA cycles are higher and the model seems to underestimate the ranges, but the result depends on which vehicle is considered.

Table 14: Model verification difference and standard deviation

	City vehicle WLTP	City vehicle EPA	Medium vehicle WLTP	Medium vehicle EPA	Large vehicle WLTP	Large vehicle EPA
Official range/Model range	0.995	-	1.028	1.091	1.046	1.138
Standard deviation	± 0.041	-	± 0.020	± 0.090	± 0.099	± 0.198

The driving cycles used for official range measurements are performed at ambient temperatures where the TMS has a low utilization rate. In this theses the TMS of a BEV is the central theme and the model is verified to a certain extent by testing four vehicles: BMW i3, Chevrolet Bolt, Tesla Model S75D and Volkswagen e-golf. They are tested in three driving cycles: UDDS, HWFET and US06 for both cold and hot ambient temperatures with and without the air-conditioner on according to the AAA-study [8]. In figure 55 the results from the simulations and the study are presented. The lowest range is achieved at -7°C with air-conditioner on and best range is at optimal or hot temperatures without the air-conditioning. The BMW i3 results shows that the model mimics the trends for different cases, overall the range is slightly lower but close to the AAA-study results. Chevrolet bolt and Tesla model S75D also shows very few differences between the study and the model, at -7°C without air-conditioning the model range is a bit lower but the overall trend remains similar. Volkswagen e-golf shows high correlation too in terms of driving range for different cases, the model provides the results close to what was reached by the AAA-study, indicating that the TMS of the model is trustworthy.

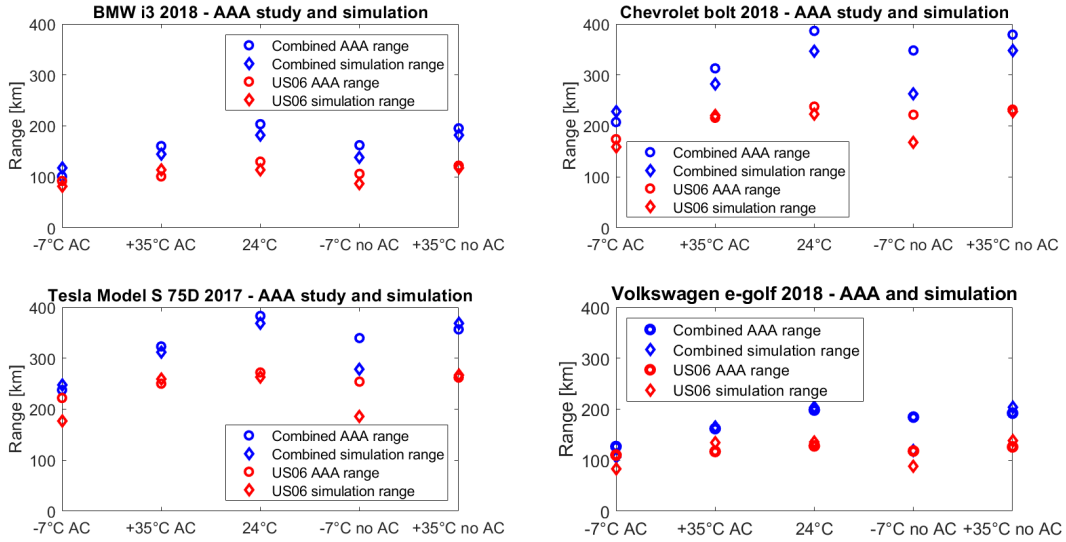


Figure 55: Model TMS verification - comparison of range with AAA study

6.2 Driving cycles and ambient temperatures results

The average power consumed by battery losses, low voltage auxiliaries, high voltage auxiliaries and the powertrain to provide traction varies depending on the case. In figure 56 the average power from the consumers are presented for five drive cycle tests and at four different temperatures. These are: WLTP, EPA, NYCC, Artemis highway and Artemis urban at -15, 0, 20 and 40°C.

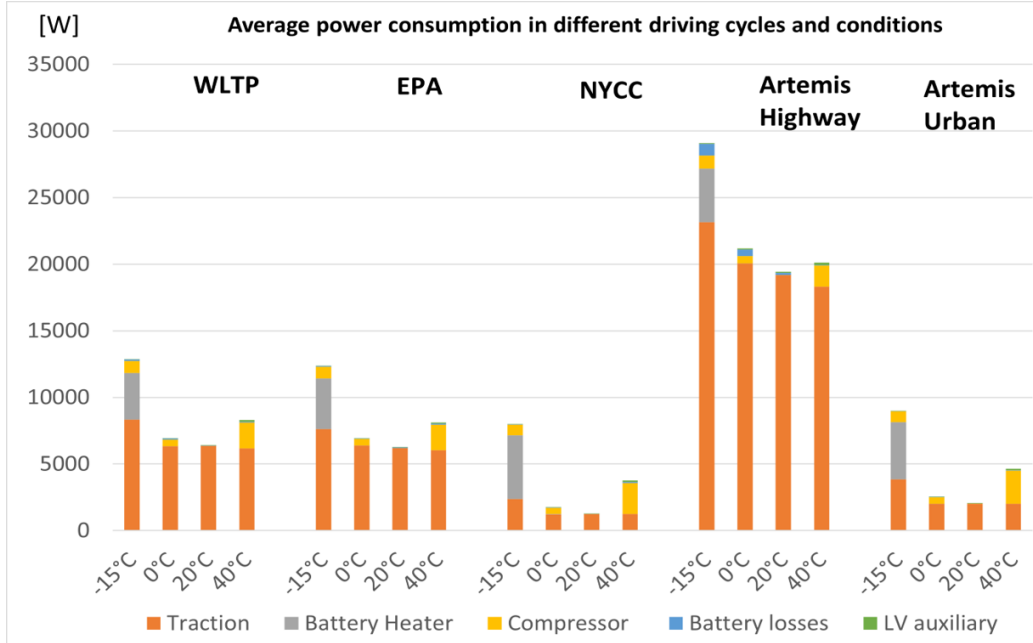


Figure 56: Average power in different driving cycles and conditions

A comparison of conditions and consumers shows a wide difference of findings relevant for expanding knowledge which concerns the performance of BEVs connected to its thermal management. In most scenarios the traction power is by far the highest consumer. At -15°C battery temperature does not overcome 0°C to allow for regenerative braking and colder ambient air results in higher air density and thus air resistance, which is extra noticeable at higher velocity cycles such as WLTP and Artemis highway. The lower air resistance is an important factor behind the lower traction power at higher temperatures.

The battery heater is set to be in use below 0°C, its linear power output in relation to battery temperature makes it appear larger in short cycles such as NYCC and medium cycles like Artemis urban. In those two scenarios the battery heater is the largest power consumer and decreases electric driving efficiency resulting in a shorter range.

The compressor used in the HVAC system to heat and cool the passengers compartment and to cool the battery at higher temperatures is more active during demanding conditions. At 0°C and 20°C average power consumed by the compressor is very limited due to lower demands. At -15°C it works harder to heat up the cabin and at 40°C the compressor consumes the most power. Cooling both the cabin and the battery. Comparing Artemis highway and urban shows a clear difference where the lesser demanding and short urban cycle uses most power on the compressor while it is a small part for the high demanding and longer highway cycle.

Battery losses and low voltage auxiliary are very small throughout all different scenarios, at some driving cycles in high temperature they become a bit more significant but no more than 3-4% of total power at most.

A comparison between the driving cycles shows that WLTP and EPA are similar in terms of characteristics. Total power is lowest for 20°C followed by 0°C, highest power is found in -20°C and 40°C mainly due to the heater and compressor increases their consumption. NYCC and Artemis urban both are very low consumers of power but at extreme conditions power usage increases threefold, making them more prone to consume energy on auxiliaries than traction power from rolling resistance, acceleration and air resistance. Artemis highway has a very high top speed and is a demanding driving cycle. It is evident from the figure that compared to other scenarios power consumption is very high, but at the same time a long distance is travelled. Traction power takes up most of the total energy where air resistance is crucial due to the high speeds. Auxiliary loads are not as large part of the total energy but the lack of regenerative braking at -15°C leads to the highest consumption out of all the different scenarios.

A common method to visualize differences and to compare driving cycles to each other is by measuring energy-per-distance, or kJ/km. In figure 57 the energy consumed per distance in all driving cycles and the four temperatures is presented. There are three different bars, the blue one representing total energy per distance, the orange representing traction-energy per distance, including regenerative braking, which is represented by the yellow bars.

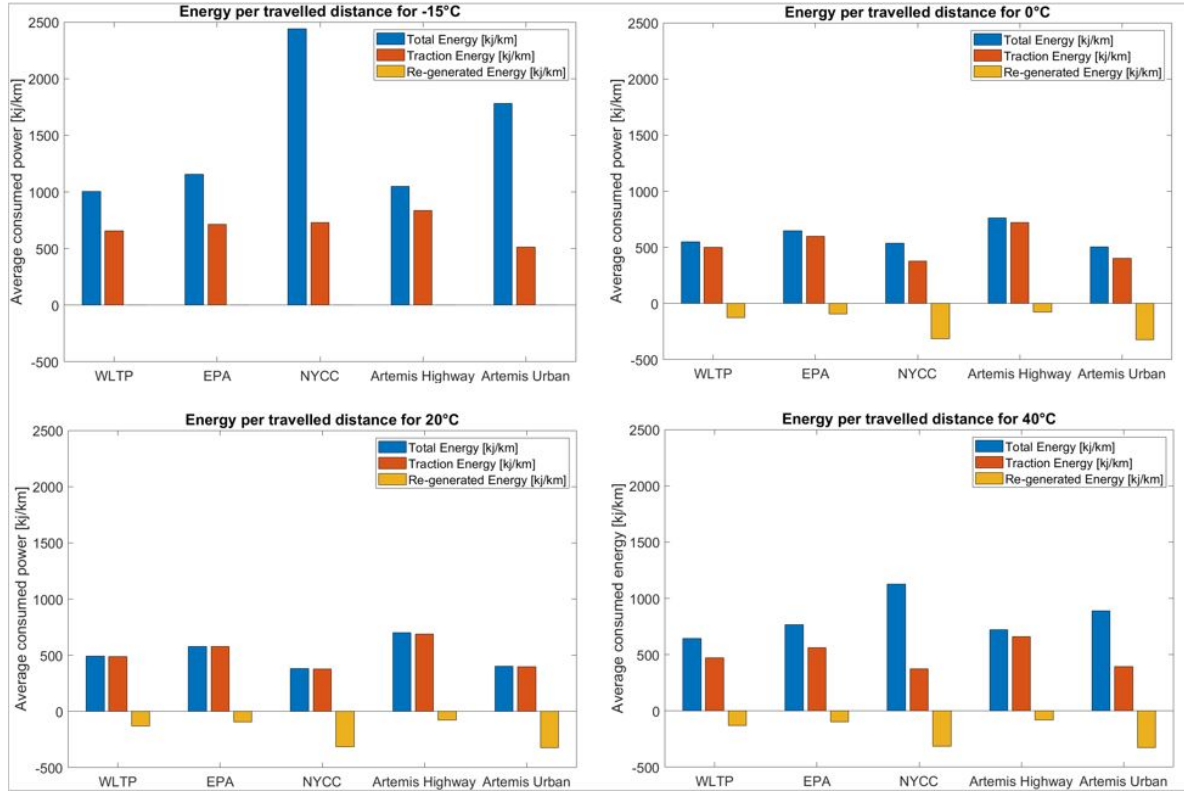


Figure 57: Energy per distance in different driving cycles and conditions

In the top left energy per distance for -15°C is seen and since regenerative braking is turned off at lower temperatures it has by far the highest values of all temperatures. In figure 56 the distance travelled wasn't taken into account, hence the distribution appears different. NYCC has below 2km travelled and a relatively large energy power consumption throughout the cycle, mainly due to that auxiliary loads are highest. At the other conditions the results are relatively similar with regenerative braking available and lower energy consumed per distance compared to the coldest scenario. NYCC

and Artemis urban has the most regenerated energy per distance, both are city/urban focused and thus more deceleration to take advantage of, which explains their drawbacks in the coldest scenario. Artemis highway has the least regenerated energy while WLTP and EPA are located towards the middle.

For the optimal conditions the total energy and traction energy are almost identical due to low consumption from auxiliaries, in the extreme conditions the bars are more differentiating since auxiliaries are used more frequently.

In figure 58 the range in WLTP and EPA for temperatures ranging between -15°C and 40°C with a temperature increment of 5°C . The driving range in WLTP is higher compared to EPA as seen in multiple other scenarios. Optimal temperature in terms of driving range is around 25°C where the energy is virtually only consumed by the electric motor to drive the vehicle forward. When temperature drops or increases auxiliary systems becomes more engaged and range is significantly affected. For this specific case, using the standard vehicle, range in WLTP is at most 440km during optimal conditions and drops to 350km at 40°C and 220km at -15°C .

A reduction of 50% in cold ambient conditions using air-condition is in line with previous test conducted by other actors, for instance AAA got similar results for their models. The study performed by geotab consisting of data from over five million real world trips using BEVs in various conditions is presented in figure 59. In addition the range in WLTP and EPA normalized to the highest range is illustrated in the same figure. The driving range at optimal conditions is one in all three cases and occurs at 25°C . A comparison at higher ambient conditions shows that simulation results are slightly higher compared to real-world data. At temperatures between 0°C and 20°C the situation is similar where the model seems to be overestimating the range and can be explained by the regenerative braking strategy. Similarly to Tesla, manufacturers do not permit maximum regenerative braking at colder temperatures unlike models based on a more binary approach resulting in more energy recuperated in simulations than in reality, hence a higher range. At the very low temperatures real world range in relation to maximum range is in line with simulation results where a drop of 50% is present for WLTP, EPA and real-world results.

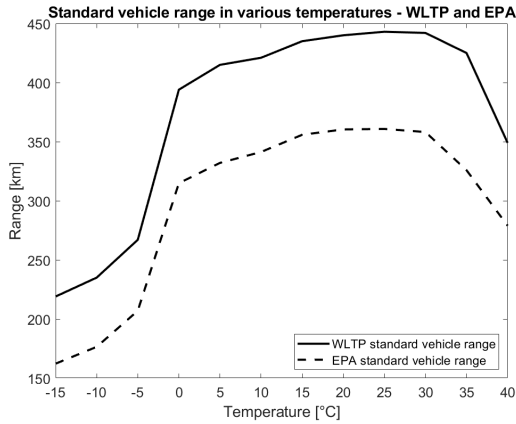


Figure 58: WLTP and EPA range

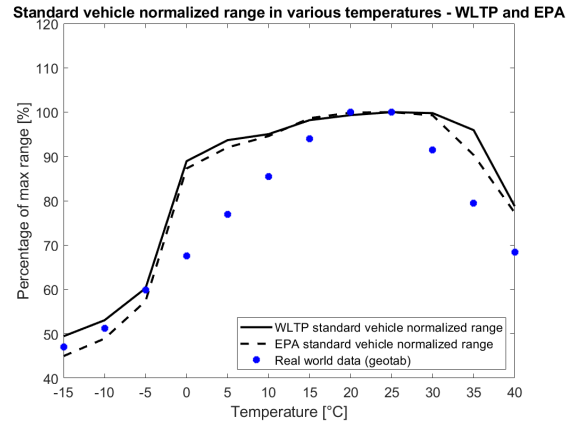


Figure 59: Normalized range with geotab

6.3 Preconditioning concept results

Preconditioning is different compared to the other concepts since it depends on the driver rather than intelligent thermal management strategies or connected components. The effect also depends on length of the driven distance, ambient conditions and type of driving as can be seen in figures 60 and 61. Where the range without preconditioning relative to using preconditioning is presented at both cold temperatures: -15, -10, -5 and 0°C as well as warm temperatures: 10, 20, 30 and 40°C for the driving cycles.

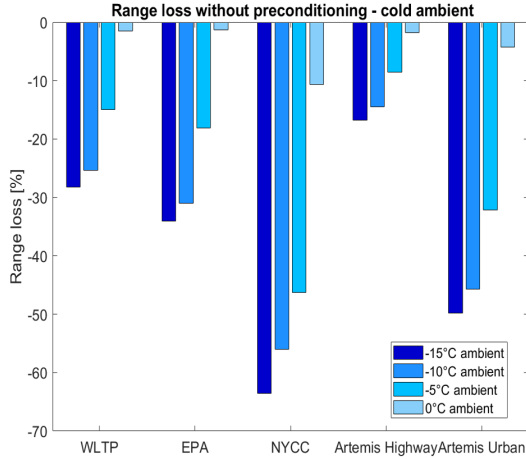


Figure 60: Reduced range in cold conditions

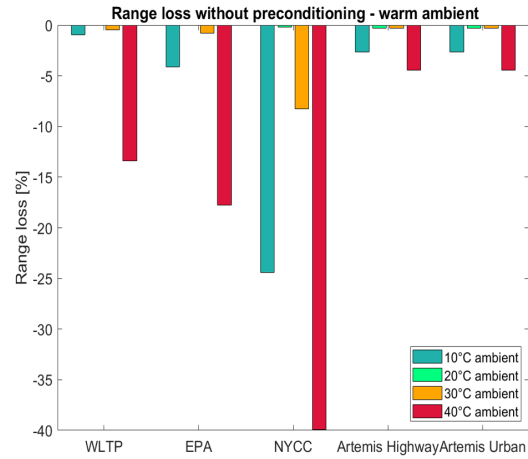


Figure 61: Reduced range in warm conditions

Preconditioning the battery and cabin in colder ambient temperatures has a massive impact on driving range. By heating them up to 22.5°C and 25°C driving range is more than doubled in some scenarios. In every scenario the range loss increases with dropping temperature and it is more pronounced for city/urban oriented driving cycles. Artemis urban loses between 5-50% and NYCC loses up to 65% due to the short distance driven and high energy consumption from the auxiliaries. Regeneration of energy by braking is not available without preconditioning for the three coldest cases and partly explains the high range loss. Higher velocity cycles such as Artemis highway and WLTP do not suffer as much loss with 15% and 30% respectively and the longer distance also contributes to limit preconditionings benefits.

Preconditioning at warm temperatures does not have such a significant impact as at colder conditions. 20 and 30°C receives barely any benefits due to optimal initial values, at these temperatures on-board TM strategies can serve a greater purpose. 10°C uses some air conditioning for the cabin and affects range in some scenarios. Driving at 40°C causes the compressor to consume energy cooling both the cabin and battery. In NYCC range is reduced by 40% and on average the other cycles obtains 4-18% range loss.

In figure 62 temperatures and power consumption from auxiliaries with and without preconditioning in WLTP for -15, 20 and 40°C are illustrated. Initial temperatures in the passengers compartment with precondition rapidly changes before the compressor starts and controls the temperature towards the requested one. Battery temperature is more stable due to higher thermal mass and requires no heating or cooling which saves energy. Without preconditioning both compressor and heater use higher power to control the temperature. At 40°C the compressor uses an average power of 2kW without and below 1kW with preconditioning. In -15°C battery heater consumes on average 3.5kW throughout the cycle

and compressor consumes a bit more average power without precondition. 20°C has a relatively stable temperature and very low power consumption, as noticed before auxiliaries withdraws low power and changes in initial temperatures do not make a noticeable difference.

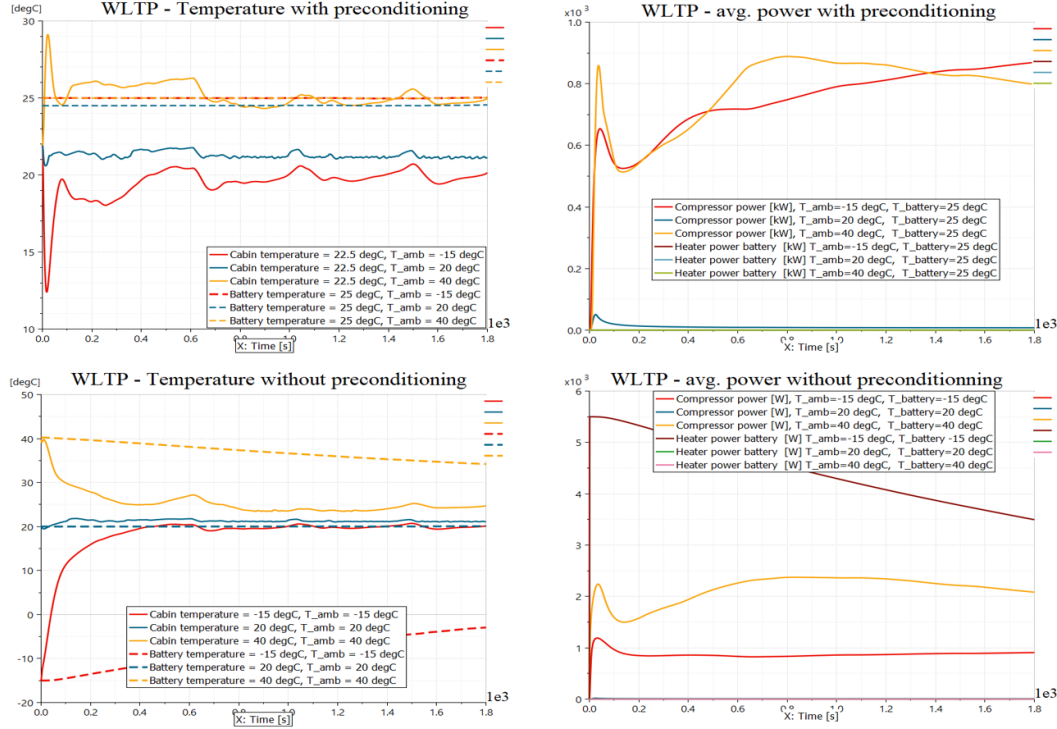


Figure 62: Temperature and power consumption with and without preconditioning

In summary preconditioning shows how sensitive BEVs are towards changes in conditions where the important driving range can drop to levels where performance is close to being unacceptable while energy consumption rises. Preconditioning can be made possible by plugging in the charger to the grid while it is parked at home, at work or at common parking spots. However Manufacturers and BEV developers are not the main responsible, but can make it easier. Solutions that facilitates preconditioning can be considered as part of thermal management strategies in a BEV and proves to have a great potential of improving the performance in demanding ambient conditions.

6.4 Peak-I concept results

The Peak-I concept is based on the theory that by limiting the current peaks and spreading out the power consumption of auxiliaries during higher motor load, losses can be decreased and longer range achieved. All driving cycles and the four ambient conditions are used for the simulations for the concept. In figure 63 the difference in range between the concept utilizing peak-I and the standard model is presented in percent. Range is affected in a randomized pattern where it increases for some cycles and conditions while decreasing in other. In 40°C the concept improves range by between 0.3-2%, mainly in Artemis cycles with high load. For 0°C and 20°C where auxiliary consumption typically remains low the Peak-I concept does not do much difference, neither positive or negative. In -15°C the result is varying, for WLTP and NYCC range is reduced by 2-3% but for EPA and Artemis cycles range is improved by up to 2-2.5% instead. The control strategy utilized in the auxiliary systems is interfering with the concept strategy and results in difficulties while trying to control the temperature.

In figure 64 the battery losses with the concept relative to without Peak-I are presented. In addition the average battery losses as a part of total energy consumed are provided and illustrates the low significance of battery losses for the overall energy usage. Overall battery losses range between 1-3% and thus reductions have a small impact on the total driving range. 0°C and 20°C are barely affected and warm conditions are only improved noticeably in Artemis highway. At colder temperatures the losses are reduced by up to 16% in NYCC while not being affected at all in Artemis urban. While battery losses experiences 16% reduction, driving range in NYCC at -15°C is not improved, on the contrary. Battery losses in Artemis urban are not affected, but still the driving range is improved by up to 2%, implying that more factors caused by the Peak-I concept affects driving range.

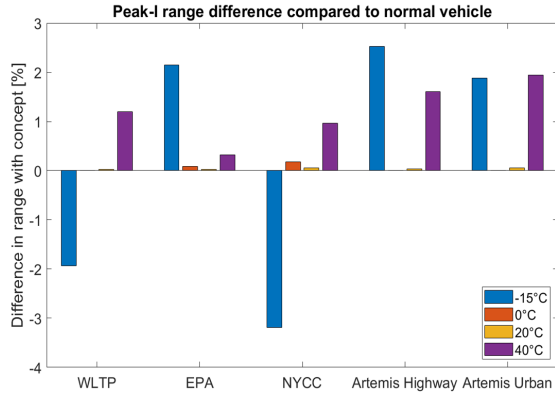


Figure 63: Range difference with Peak-I

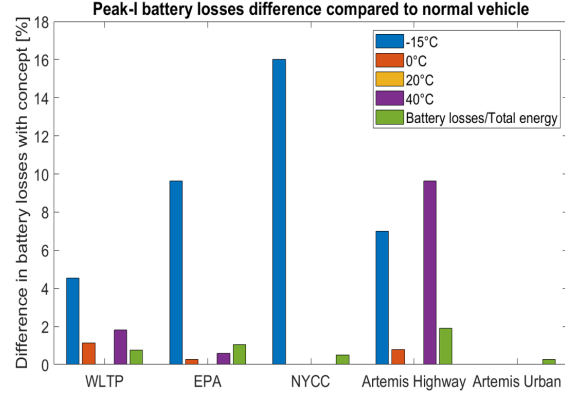


Figure 64: Battery losses difference with Peak-I

Decreasing power output from auxiliary systems at higher motor load can make the vehicle slower in reaching the requested temperature in passengers compartment and battery. In figure 65 temperature in these subsystems in WLTP drive cycle is presented. Fluctuations in temperature are present with Peak-I but are kept to a minimum level and are not affecting the performance or experience of either components or passengers compared to a standard BEV. In the demanding temperatures the curve takes a bit longer to reach certain levels but is quickly compensated for when demands on electric motor to provide traction drops. In higher loads the Peak-I concept limits the current taken from the battery and during regenerative braking it consumes more power with the same effect. Difference in current output are illustrated for a portion of Artemis highway cycle in 40°C in figure 66. In certain cases current peaks are reduced by up to 5%, depending on the scenario it could reduce momentary losses by 10%. Under standard loads the concept does not provide a significant difference in current output resulting in a lower overall reduction.

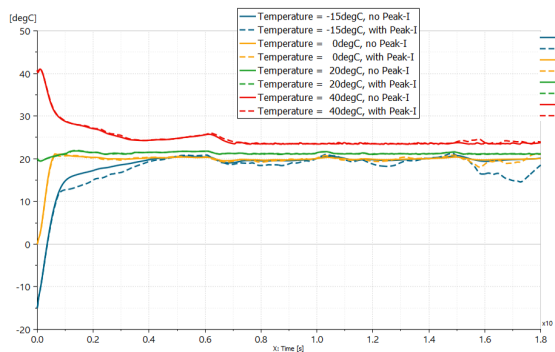


Figure 65: Cabin temperature with Peak-I

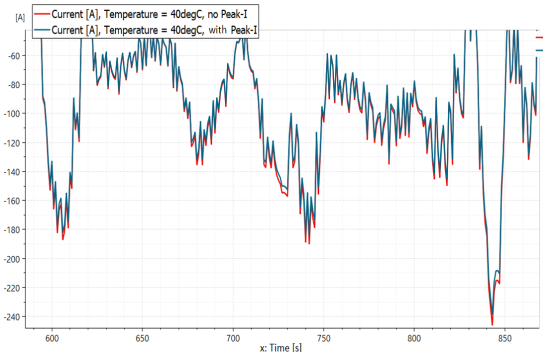


Figure 66: Current form battery with Peak-I

6.5 Heating for re-gen concept results

The heating for re-gen concept is different since it does not provide difference in range compared to other models but investigates under which scenarios investing energy to heat up the battery allows for more regenerative braking. In figure 67 the energy required to heat up the battery from a given temperature below zero to above zero. Initial battery temperatures were -1, -3, -5 and -10°C and target temperature 0, 1, 3 or 5°C. The lowest energy required is by heating from -1°C to 0°C while the highest is from -10°C up to 5°C. The heat energy was provided by the battery heater which in this test had 7kW continuous power. Energy is presented in kilojoule and ranges between 750 and 8700 KJ in different scenarios. The energy put into the heater is transferred with varying efficiency depending on scenario, which is illustrated in figure 68. From the figure it is evident that a large temperature difference results in a higher transfer-efficiency close to 1 while being below 0.7 for the lowest temperature difference between start and final value, ΔT .

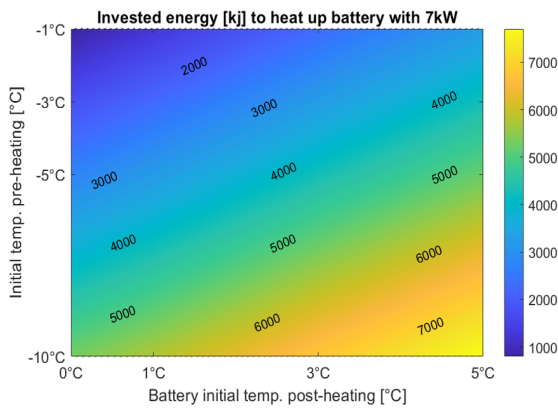


Figure 67: Invested energy with pre-heating

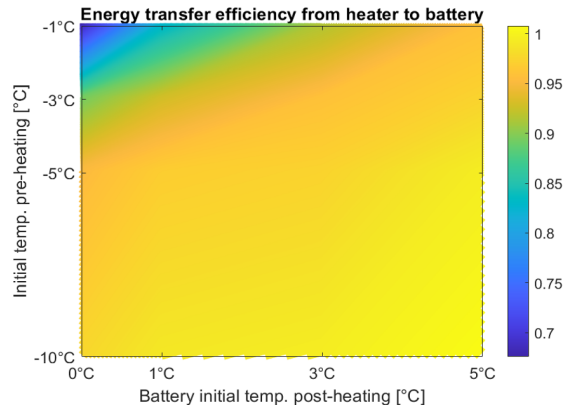


Figure 68: Transfer efficiency with pre-heating

Maximum permitted regenerative power is governed by SOC and battery temperature, simulation using 30% and 70% SOC at similar temperature and the same driving cycle thus delivers different results. By measuring the invested energy and regenerated energy throughout the full driving cycle a coefficient of performance (COP) can be calculated. A coefficient above 1 results in more energy returned compared to energy invested, making heating up the battery to provide regenerative braking efficient. The energy regenerated already accounted for the losses in the system and represents the energy used to charge the battery.

In figure 69 the COP for WLTP at 30% SOC is presented. In the scenario with least ΔT COP exceeds 3 and every other scenario starting at -1°C is above 1, although -1°C up to 0°C is most efficient. Heating from -3°C results in a COP between 0.7-1.7 where heating up to 3 and 5°C is below 1 in COP. At -5°C only one target temperatures provide a COP above 1, heating it up to 0°C is worth it while up to 1, 3 or 5°C fails to return the invested energy. At very cold temperatures such as -10°C COP stays between 0.4 and 0.55 and can not be considered as an efficient investment.

In figure 70 a similar case is simulated besides having more energy left in the battery at 70% instead of 30%. The area where COP are above 1 are smaller and the lower regions are darker compared to SOC at 30%, implying a lower efficiency. At -1°C up to zero COP is below 3 and out of the in total 16 cases, only five are above 1 in terms of COP. At initial battery temperatures of -5°C and -10°C COP is below 1 and for -3°C only target temperatures of 0°C and 1°C at 1.22 and 1.02 are efficient.

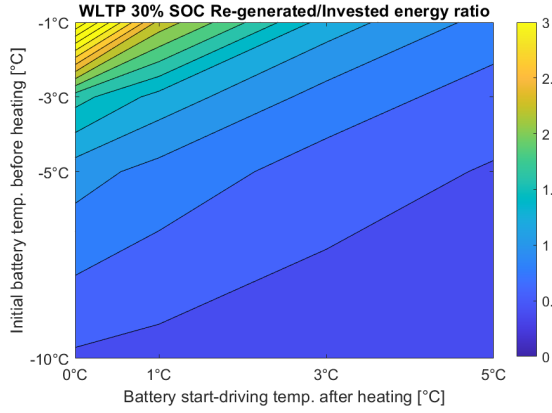


Figure 69: COP for WLTP and 30% SOC

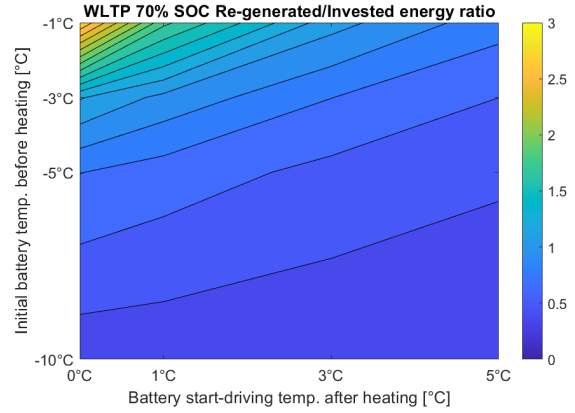


Figure 70: COP for WLTP and 70% SOC

In figure 71 the coefficient of performance for HWFET with 30% SOC with the same initial and target temperatures as for WLTP is presented. HWFET is a short driving cycle with less energy regenerated and thus fails to provide sufficient energy while driving to return the invested energy while heating up the battery. In -1°C and heating up to 0°C where WLTP delivered more than three times the invested energy, HWFET only achieves 0.7. The worst case scenario at -10°C heating up to 5°C is less than 0.1 making the invested energy more than 10 times larger than the regenerated energy and thus not worth it.

With higher SOC at 70% the COP for HWFET drive cycle was investigated and are presented in figure 72. Due to the lower efficiency seen in figure 68 in transfer efficiency between heater and battery the highest COP is found at initial temperature -1°C and a target of 1°C at 0.33 with worst scenario dropping to 0.065. None of the scenarios for HWFET proved to be an efficient investment, no matter the ΔT or SOC level while WLTP had seven and five out of sixteen per case with a COP above 1.

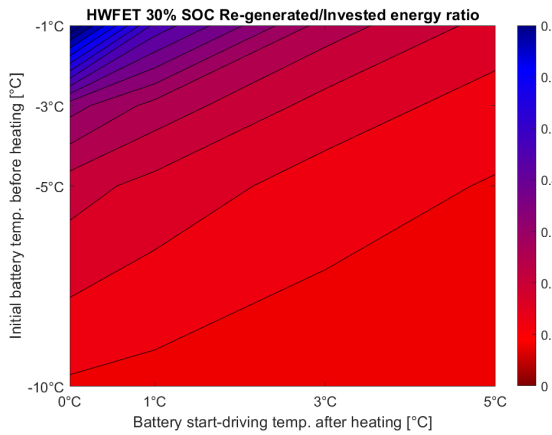


Figure 71: COP for HWFET and 30% SOC

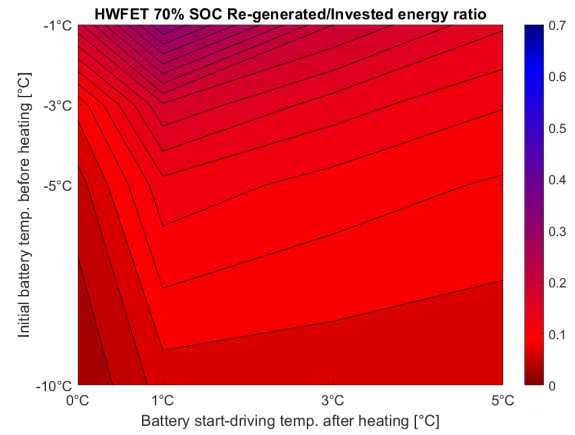


Figure 72: COP for HWFET and 70% SOC

6.6 BEM concept results

The BEM concept is similar to the Peak-I concept being a strategy implemented in the BEV to elongate driving range by reducing copper losses in the electric motor and internal resistance inside the battery. In figure 73 the difference in driving range with the concept divided by the range of a standard BEV is presented. In all five drive cycles range is decreased at 40°C and increased in -15, 0 and 20°C. At higher temperatures the battery is already warm and requires cooling from the chiller provided by the compressor which has to work harder to cool both the electric motor and the battery. By utilizing the radiator circuit and running the battery TM circuit and electric motor TM circuit in parallel instead of series it is possible to avoid a decrease in the driving by up to 1.5%. For the other temperature values, the driving range is increased with the largest effect seen in 20°C with almost 1.5% increased driving range. -15 and 0°C increases at most by about 1% due to the radiator working more efficiently at colder ambient conditions, thus keeping the electric motor cooler at lower energy consumption. WLTP, EPA and Artemis urban has a low top speed and lower loads compared to NYCC and Artemis highway. These parameters are driving factors behind increased copper losses and the benefits with the BEM concept are therefore lower.

In figure 74 the average power consumption for different components in Artemis highway is presented with and without the BEM concept. Without regenerative braking in -15°C the traction power is the highest, the heater is not turned on and therefore uses zero power. Battery losses are mostly present in cold temperatures and compressor power consumption at high temperature. Lowest average power consumption occurs at the optimal condition of 20°C with very low auxiliary power consumption.

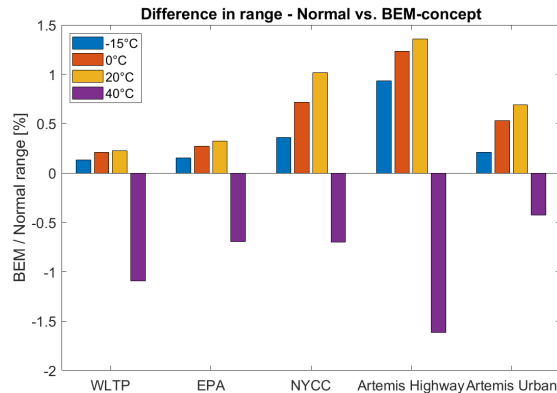


Figure 73: Range difference with BEM concept

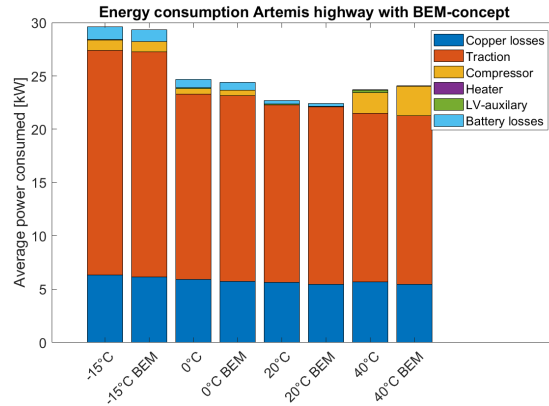


Figure 74: Artemis Highway average power with BEM

Connecting the battery TM circuit to the electric motor TM circuit will increase battery temperature slightly while reducing that of the electric motor significantly. In figure 75 temperature in both components for Artemis highway is illustrated with dashed lines representing the BEM concept and lines representing a standard BEV without the concept. The results are presented for ambient temperatures -15°C and 20°C, the battery has a temperature variation of approximately 10°C and electric motor reaches above 100°C. Cooling the electric motor with the battery's thermal mass compared to the radiator is more effective where in the end of the cycle it differs almost 20°C in battery temperature between the two cases.

The lower temperature results in lower copper losses in the motor as presented in figure 76. The decreased copper losses with the BEM concept compared to a normal BEV is presented along with the size of copper losses relative to total energy consumed. In EPA, NYCC and Artemis urban the

reduction in losses is very small due to low temperature difference. In WLTP the difference in losses is between 0.4-3.7%. On average, 11% of all energy consumed is due to copper losses. In Artemis highway the velocity and load are the highest, which leads to high copper losses at 25% of total energy. The reduction is 2.5% at -15°C , 3% at 0°C , 3.2% at 20°C and 4.4% at 40°C . Increased compressor energy consumption eliminates the gained efficiency for the high temperature scenario but contributes noticeably toward the increased range in the other temperatures.

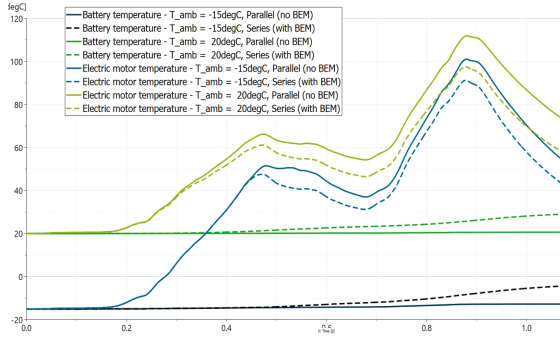


Figure 75: Artemis highway temp. with BEM

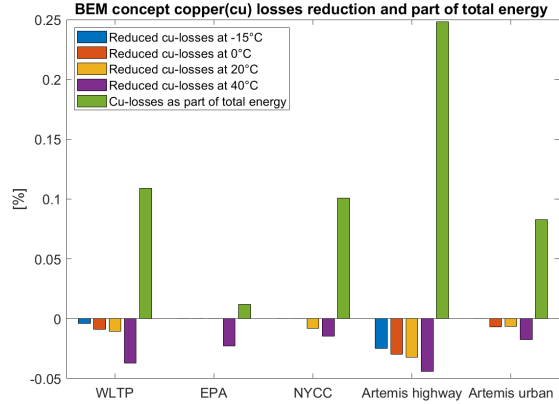


Figure 76: Copper-losses difference with BEM

The two concepts BEM and Peak-I are possible to combine to one common concept and can utilize synergy effects from them both. The energy used while driving a cycle with the concept is lower and thus range can be increased. The percentage difference in range are presented in figure 77. Besides EPA at hot temperatures, the driving range in a cycle is increased for every single scenario with up to 2.1% depending on temperature and cycle. Compared to range difference with only Peak-I the range-increase is more consistent throughout the cases but for a few cases the driving range is a bit reduced. Compared to only the BEM in terms of driving range difference, the increase is very similar. For the coldest cases where Peak-I assists and contributes with synergy effects the results is improved.

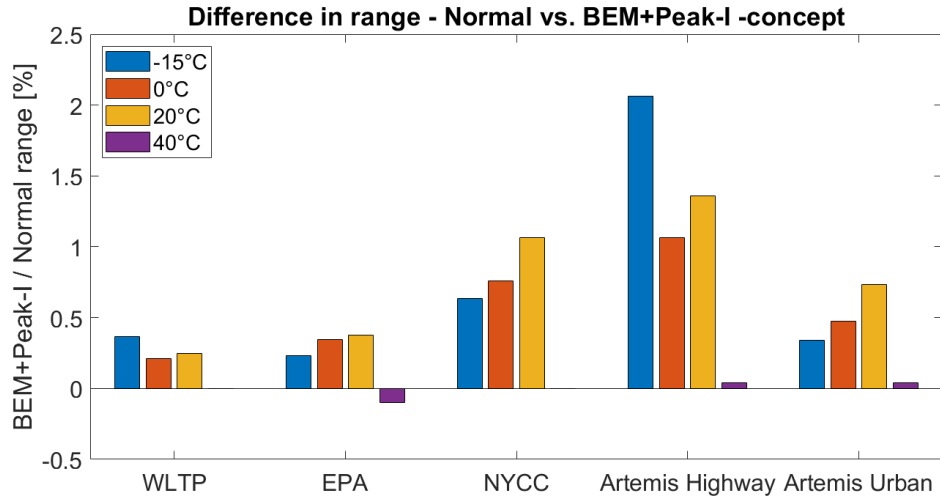


Figure 77: Range difference using a combination of Peak-I and BEM

7 Discussion

In this chapter the results and findings are discussed with the general and theoretical background and literature in mind. The overall background and the role of BEVs, the Amesim model validation and the results from simulations are included and investigated a bit further. In addition the aims of the thesis are addressed in relation to the results and findings.

7.1 Background and validation of the Amesim model

Thermal management of BEVs is a very broad subject with a lot of possible entries and methods that could be used. From real-world data it is evident that range is heavily affected by temperatures deviating from the optimal operating range. Many manufacturers are developing new systems designed to take advantage of holistic effects to deliver better and more consistent performance for their customers. It is also clear that the development is very rapid, more than most people could imagine a few years ago, largely driven by legislation, customer demands and changing climate. Investigating the role of the transport sector on a global scale quickly reveals its importance in achieving the targets on the limited global warming. The role that BEVs play in this matter is crucial and it makes this thesis very interesting and relevant with plenty of options and areas to investigate.

An approach with a real vehicle driving in demanding conditions is one way that would be interesting to investigate further, however, this would require complex testing equipment, more resources and also limit the scope to a certain vehicle. Amesim simulation models representing BEVs and their TMS are a more efficient way of working within the subject making it possible to perform virtual testing. A wide range of different BEVs can be simulated, parameters and conditions altered and different strategies on TMS can be constructed efficiently. While a real-world testing procedure might be more accurate than 1D-simulations using values based on approximations between different vehicle models it is also more resource-consuming. A full test in Amesim including preparations, simulation and post-processing can be made within 15 minutes while real world testing would require much more time, which shows the impact virtual testing can have. A model is only as good as the input parameters and can only produce results based on physical models, which might lack important aspects found in real tests. Therefore the first step after building the complete model is to test and verify it by using input data from a range of BEV on the market today.

In chapter 6.1 the validation results were presented for BEVs and their TMSs. A comparison between the official data and simulation results for WLTP and EPA showed that the model was fairly accurate in terms of delivering correct driving range results. Testing procedures are very complicated and clearly adapted for being performed in reality, not adapted or optimized for being replicated in virtual testing. Therefore there will always be some differences in how the tests are conducted which can affect the outcome. **However, in the validation process it is not always the absolute values that are interesting, it can often be the overall trends** and the simulations performed herein captured the trends. WLTP uses a more straightforward methodology and the simulations capture well the trends. The thermal management is less relevant in these cycles due to higher velocities and longer duration. Instead, driving range is mainly depending on air, roll, grade and inertia resistance which is based on vehicle parameters specified in the model, thus variations are low. EPA is a bit more complex with weighting factors for range prediction not completely available for general public and manufacturers can choose different methods to test their BEVs. It is however noticeable that the simulation results for all Tesla models deviate for EPA while being very close to the official data for WLTP. At the same time they have an almost identical range for WLTP and EPA while for other BEV models WLTP-range is higher than their EPA rated range. It is interesting that one manufacturer (Tesla) clearly deviates from the others and one possible explanation to this is the fact that Tesla has "been in the game a longer time" and knows how to optimize for these tests. Besides for the Tesla vehicles the Amesim model is suitable for simulating a hypothetical standard vehicle and TM concepts.

In the comparison of the AAA-test designed to test how well the TMS represents reality there are also good results from the simulations. An important factor affecting the result is that **very few manufacturers are transparent with their thermal management strategy**, causing difficulties while making comparisons since information such as target temperatures and operating ranges can vary significantly. It is also a problem that input data or maps containing efficiency maps on components such as the electric motor, battery, pumps and the compressor where the model utilizes the same maps for all models which naturally is not the case. **If efficiency maps and characteristics of components in different BEVs were available, a more detailed and accurate result could be achieved.** With this in mind, the comparison with the AAA-study shows that the model manages to identify the overall trends with some differences that most likely could be explained by differences in components and overall strategies implemented in each BEV.

7.2 Cycles, conditions and concepts

The driving cycles and conditions affect the performance of BEVs as presented in chapter 6.2. The components are clearly consuming varying amounts of energy depending on which scenario is considered. In these simulations the strategy implemented with the TMS is important, another allowed operating range, efficiency and dimension can impact the results but since all scenarios have the same setup with the standard vehicle the trends are trustworthy. Another factor to consider is the control strategy in the HVAC-loop where PID-controllers, multiple input signals and functions are utilized in many different ways. There were lots of time spent on tweaking, adjusting and optimizing this control system with parameters in the function, PID-controllers and temperature ranges that is not presented to a representative extent in the report. For some of the concepts such as Peak-I and BEM the control strategy could be further optimized to achieve better results, **however the focus of this thesis concerns the TMS, not the control systems.**

In the energy per distance test it is evident how much colder ambient temperatures affect driving range, mainly due to the lack of regenerative braking and increased energy consumption by the auxiliary systems. In city cycles regenerative braking is a crucial feature that separates BEVs from conventional vehicles, which is further investigated in the re-gen concept. The graphs shown in figures 58 and 59 clearly visualize how the same standard vehicle can have different range depending of which of the two official driving cycle testing methods is applied. Additionally, they illustrate how differences in ambient temperatures result in significant changes in driving range. Regenerative braking is as already mentioned crucial and the strategy used in this case is that full power is available above 0°C, which leads to longer range compared to reality in the conditions of 0 to 15°C. The simulations show good agreement with the official data for driving range at -15°C, overestimate the range between 0-15°C, good prediction again between 15-30°C and overestimation again in hot conditions. The overestimation may be due to higher efficiency in the system, a lower demanded target temperature, different TM strategy or other behaviour which is difficult to imitate in the simulations.

Preconditioning proved to be a highly efficient method to save energy, especially in very cold temperatures while driving short city cycles. By connecting the BEV to a charger during parking and consuming small amounts of energy to sustain optimal temperatures of the components a lot of energy from the battery can be saved avoiding losing up to 65% range. In warmer conditions the effects were not as significant mainly due to regenerative braking still being available. This approach might not be comparable to other TM strategies since it puts responsibility on the infrastructure and customers instead of the manufacturer. Other types of vehicles also benefits from preconditioning while the effects are not as significant as for BEVs. The charging infrastructure is today lagging behind even if comprehensive investments are planned, depends largely on where the customer lives, works and drives and how available preconditioning is. Since the effects are so significant at demanding conditions it is in the interest of all involved parts to make charging and preconditioning more available. Especially considering BEVs are expected to increase the overall market share in the future.

Peak-I as a concept is very interesting from a technical point of view. Limiting power consumption at auxiliary systems during higher load is used to even out the output currents and reduce the current peaks. Power-losses are exponentially depending on the current and thus the strategy can result in increased efficiency especially for higher load scenarios. It also increases demands on the control system and can interfere with the PID-controllers and functions with higher fluctuations and reduced benefits as a result. Based on the results there are some issues with the control system since efficiency is increased up to 2% in some scenarios and reduced by 3% in the other. The results are as expected with lower battery losses due to lower currents, but due to the low part of total energy consumption battery losses accounts for, the effects are limited. If the controllers are optimized further it could deliver more stable results depending on the scenario.

Heating for re-gen as a concept is highlighting the importance and key aspects behind regenerative braking. By creating an efficiency map for the maximum battery power based on SOC and battery temperature it can be investigated whether investing energy to heat up the battery and make regenerative braking available is worth it. The results show it depends on starting temperature, target temperature, driving cycle and SOC. Longer driving cycles such as WLTP, especially at low SOC and ΔT proved beneficial while HWFET at 70% SOC at colder initial temperatures was not as efficient. The concept is built on the assumption that the trip ahead is known, for instance from the gps-system it could be calculated if energy should be withdrawn from the battery to heat it up or not. If a driver travels the same distance every day and cannot use preconditioning, the BEV could compute the efficiency based on input parameters. The concepts also relies on the regen-map specific to Tesla Model 3, which are not available from other manufacturers. However, the theory and literature prove that temperature and SOC affects maximum charging power, but how the map looks can vary significantly between different BEVs. A BEV could change the map to suit the conditions and from a system perspective be beneficial, the vehicle can also heat up the battery before stopping for charging to increase maximum power and this strategy is already used by some BEVs. The battery thermal mass is also of great importance, a larger battery requires more energy to heat up and this can change the efficiency.

The BEM concept connects the TM circuit of the electric motor and battery to increase the efficiency of the system. According to the theory, battery losses might decrease slightly, similar for electric motor losses which instead can result in a few percent decreased overall losses. This depends on the load since copper losses inside the motor increase with the load and milder driving cycles might not benefit from the concept as much with tiny savings in the low voltage auxiliary system. The simulations proves this to be correct with up to 1.5% range increase in the high-load Artemis highway cycle while resulting in less than 0.5% in WLTP and EPA. For higher temperatures it was not efficient since the battery became too warm and required more cooling from the compressor which eliminated the saving in copper losses. This is seen in figure 74 where compressor power increased, it was also noticed that copper losses decreased leading to the range increase, which is in line with theory. One key aspect of this concept is that high loads for long time result in battery temperature reaching levels where cooling is required thus decreasing the efficiency. In case of a long drive session the efficiency might not be as high due to the warm battery. The balance between load and time is crucial for BEM to work, during commutes shorter than one hour it should be beneficial but for high load driving it might not work as well. Battery thermal mass is also important where a larger battery can absorb more energy to cool down the motors and result in a high efficiency for longer time. The advantage is that the 4-way valve can switch and connect the two circuits in parallel if this occurs, which shows the potential of the concept. The consistency of the concept is another advantage for the BEM concept where it delivers increased range in a controlled manner unlike Peak-I that seemed to be more dependent on the control system. By having this in mind it was investigated if a combination of the two concepts can deliver a good result, and it did deliver some synergy effects where the combined concept has both consistency and good cold temperature performance.

In summary it is important to highlight that **the tests were performed for drive cycles that**

represent certain distances, the difference in energy consumption in the test was interpolated and used to calculate the driving range. If simulations would be performed from a fully charged battery to a drained one the benefits with simulations would be lost. Since temperature of the components stabilize after certain time, the difference in energy consumption might decrease if the battery is completely drained. For instance, the effect of preconditioning would reduce in a full discharge cycle, but most driving is conducted in shorter periods of time, thus making drive cycle results relevant. The saved energy from the concepts can be used to increase range or reduce charging times, but since range is the desired property from the saved energy, that is where the focus of this work was.

8 Conclusion

In this chapter the conclusions are made based on results and discussion, further recommendations on the subject are also discussed providing answers to the aims and purposes previously mentioned.

Ambient conditions affect efficiency of a BEV by reducing its range in demanding conditions such as cold or warm temperatures. The three main subsystems consisting of the battery, electric motor and passenger compartment require a certain temperature interval that is provided by the TMS which consumes energy. Under these demanding conditions auxiliary systems draw more power and **can consume a majority of the total energy during some scenarios**. Total driving range proved to differ by 50% in cold climates and about 20% in warm climates from the simulation results, which is also in line with previous studies.

The driving cycles used in this thesis include a range of city, urban and highway cycles with different characteristics that suit BEVs to different extents. Highway cycles with high velocities are not affecting the performance as much as city/urban cycles where regenerative braking makes it possible to BEVs to save significant amount of energy otherwise lost during mechanical braking. Keeping regenerative braking available is crucial for maintaining a sufficient range for a BEV and is affected by both SOC and ambient temperature. Drive cycles with more accelerations and higher loads generate more losses in a BEV and makes the TMS even more important for keeping components within optimal operating range.

The variations in range from the different drive cycles and scenarios show how difficult range-prediction can be where a wide variety of factors affect the result. The official claims on driving range are not the same for all testing methods and this was investigated by imitating the tests and analyzing how well the results correlate to reality. The results showed that the model managed to identify the trends in driving range estimations for different BEVs and predicted the range with high accuracy for WLTP and EPA cycles. The TMS was tested and compared with the results from other studies and investigations and its performance was well predicted with good range estimation.

The range can be increased by utilizing TM strategies such as *Preconditioning*, *Peak-I*, *Heating for regenerative braking*, *connecting battery and electric motor TM circuits*, as well as by combining the concepts and benefiting from synergy effects. It was found that **preconditioning is by far the most effective method to limit the range-drop**, by heating up or cooling down the subsystems before driving a lot of energy can be saved from the BEVs battery. Up to 65% in cold and 40% in warm conditions of range could be lost in some cycles since the energy is used by auxiliary systems. Heating up the battery using its own energy to allow regenerative braking proved to be efficient in some scenarios. Mostly in **longer cycles with much regenerative braking and with low difference in initial and final battery temperature where a return on invested energy of over 3.5 was achieved**, proving that invested energy can be returned by a factor of over 3.5 in some scenarios. At other driving cycles and especially at higher differences between initial and final temperatures the efficiency was not sufficient to motivate heating up the battery by using its own energy.

By limiting the current peaks at higher motor loads in the Peak-I concept, the range in a drive cycle could be increased by up to 2.5% but also reduced by 3.2% depending on scenario. The reduced consistency makes the result somewhat uncertain and there is room for improvement within the control system.

Connecting the TM circuits in the BEM-concept was the most consistent concept where **an increase in drive cycle range of 1.4% and decrease of 1.6% were found depending on scenario**. The decreases occurred in warm temperatures where more auxiliary power was consumed than saved in copper losses and higher load driving resulted in the largest savings in range.

A combination of Peak-I and BEM concepts gave good results and **can be considered to be the most consistent and effective concept in increasing driving cycle range with stable increases up to 2.1%**. The reason for increased range is a combination of reduced copper losses in the electric motor and reduced battery losses due to lower current peaks, leading to less energy consumed and thus longer range.

In the list below a range of suggested future topics that could be investigated further is presented.

- **Control systems:** In this thesis the focus was on TMS of a BEV rather than optimizing the control system of the various strategies. By conducting further work within this area to provide better control of the system, higher efficiencies and increased stability can most likely be achieved.
- **Involve more components in the holistic approach:** in this thesis the battery and electric motor TM circuits were connected and thus utilized holistic synergy effects. There are more components that could be included and even more energy to take into account such as passengers compartment heat in sunny days to heat up other components.
- **Conduct more thorough and detailed analysis on a component level:** This thesis focused on a system perspective rather than on a detailed component level. By looking closer at construction and manufacturing of certain components the TM could be improved ever further, such as engineering internal solutions in the electric motor or battery.
- **Validating models with real values provided by manufacturers:** A major limiting factor in this thesis was lack of experimental data and manufacturer efficiency maps, by utilizing real data a higher accuracy can be achieved. Implementing actual TM strategies from manufacturers in the Amesim model and validate would also be interesting to see how it affects the end result.

The results from the concepts on TM strategies shows the importance and the role of the TMS in a BEV. The Amesim simulation model proved to provide trustworthy results in the comparisons and while used to test the concepts it showed that one of the most crucial features of BEVs, the driving range, can be improved and uncertainties reduced. In the world where the BEVs become increasingly common with a growing interest due to stringent legislation and climate change optimizing the TMS is of great importance.

By implementing different strategies a higher performance can be achieved, especially at the otherwise uncertain situations concerning demanding ambient conditions and different driving cycles. A holistic approach where energy-flow is optimized between the components in a BEV has proven to be of great importance due to the potential for increasing efficiency and range. The approach will hopefully be implemented in future BEV-models for a wide range of customers living in all sorts of environments.

References

- [1] Boerboom M. (2012). *Electric Vehicle Blended Braking maximizing energy recovery while maintaining vehicle stability and maneuverability*, Master's Thesis, Chalmers University of Technology, Gothenburg. URL: <https://publications.lib.chalmers.se/records/fulltext/155034.pdf1>.
- [2] European Environment Agency (2015). *Evaluating 15 years of transport and environmental policy integration*. URL: http://www.eea.europa.eu/publications/term-report-2015/at_download/file.
- [3] Amnesty International (2016). *DEMOCRATIC REPUBLIC OF CONGO: "THIS IS WHAT WE DIE FOR": HUMAN RIGHTS ABUSES IN THE DEMOCRATIC REPUBLIC OF THE CONGO POWER THE GLOBAL TRADE IN COBALT*. URL: <https://www.amnesty.org/en/documents/afr62/3183/2016/en/>.
- [4] EPA (2017). *EPA Test Procedures for Electric Vehicles and Plug-in Hybrids*. URL: <https://www.fueleconomy.gov/feg/pdfs/EPA%20test%20procedure%20for%20EVs-PHEVs-11-14-2017.pdf>. (accessed: 15.05.2021).
- [5] Evans, P (2018). *Heat Pump Guide*. URL: <https://theengineeringmindset.com/heat-pump-guide/>. (accessed: 07.05.2021).
- [6] IPCC (2018). *Special Report Global Warming of 1.5deg C*. URL: <https://www.ipcc.ch/sr15/>.
- [7] Tracy, D (2018). *The Tesla Model 3 'Superbottle' Easter Egg Is a Fascinating Packaging Solution*. URL: <https://jalopnik.com/the-tesla-model-3s-superbottle-easter-egg-is-a-fascin-1830992728>. (accessed: 09.05.2021).
- [8] American Automobile Association (2019). *AAA ELECTRIC VEHICLE RANGE TESTING AAA proprietary research into the effect of ambient temperature and HVAC use on driving range and MPGe*. URL: <http://www.aaa.com/AAA/common/AAR/files/AAA-Electric-Vehicle-Range-Testing-Report.pdf>. (accessed: 21.04.2021).
- [9] European Environment Agency (2019). *Emissions of air pollutants from transport*. URL: <https://www.eea.europa.eu/data-and-maps/indicators/transport-emissions-of-air-pollutants-8/transport-emissions-of-air-pollutants-8>. (accessed: 30.04.2021).
- [10] IEA (2019). *Global EV Outlook 2019*, IEA, Paris. URL: <https://www.iea.org/reports/global-ev-outlook-2019>.
- [11] Moloughney, T (2019). *Cold Weather Electric Car Tips: Maximize Your EV For Winter*. URL: <https://insideevs.com/features/342917/cold-weather-electric-car-tips-maximize-your-ev-for-winter/>. (accessed: 17.05.2021).
- [12] Rebecca Bertram (2019). *Is Latin America's lithium industry sustainable? Environmental costs of the new white gold*. URL: <https://energytransition.org/2019/06/latin-americas-lithium-industry/>.
- [13] Bower, G (2020). *Tesla Model Y Heat Pump Details Infrequently Discussed By The Media*. URL: <https://insideevs.com/news/452464/tesla-model-y-heat-pump-system-details/>. (accessed: 09.05.2021).
- [14] Choksey, S. J (2020). *Electric Vehicle Range Testing: UNDERSTANDING NEDC VS. WLTP VS. EPA*. URL: <https://www.jdpower.com/cars/shopping-guides/electric-vehicle-range-testing-understanding-nedc-vs-wltp-vs-epa>. (accessed: 14.05.2021).
- [15] European Environment Agency (2020). *Greenhouse gas emissions from transport in Europe*. URL: <https://www.eea.europa.eu/data-and-maps/indicators/transport-emissions-of-greenhouse-gases/transport-emissions-of-greenhouse-gases-12>.

- [16] Field. K (2020). *Tesla's Octovalve Enabled A Staggering 10% Increase In Range For The Model Y*. URL: <https://cleantechnica.com/2020/08/03/teslas-octovalve-enabled-a-staggering-10-increase-in-range-for-the-model-y/>. (accessed: 09.05.2021).
- [17] Green Car Congress (2020). *Hyundai and Kia continuing to develop heat pump technology for EVs*. URL: <https://www.greencarcongress.com/2020/06/20200610-hyundaikia.html>. (accessed: 08.05.2021).
- [18] Henze V. (2020). *Battery Pack Prices Cited Below \$100/kWh for the First Time in 2020, While Market Average Sits at \$137/kWh*. URL: <https://about.bnef.com/blog/battery-pack-prices-cited-below-100-kwh-for-the-first-time-in-2020-while-market-average-sits-at-137-kwh/>.
- [19] IEA (2020). *Global EV Outlook 2020*, IEA, Paris. URL: <https://www.iea.org/reports/global-ev-outlook-2020>.
- [20] Irvine M. Rivaldo M. (2020). *TESLA'S BATTERY DAY AND THE ENERGY TRANSITION*. URL: <https://www.dnv.com/feature/tesla-battery-day-energy-transition.html>.
- [21] Klender. J (2020). *Tesla's Model 3 Heat Pump is a game changer compared to its old system*. URL: <https://www.teslarati.com/tesla-model-3-heat-pump-test-video/>. (accessed: 07.05.2021).
- [22] Lombardo. T (2020). *Hyundai/Kia's new EV heat pump technology*. URL: <https://chargedevs.com/newswire/hyundai-kias-new-ev-heat-pump-technology/>. (accessed: 07.05.2021).
- [23] Loveday. S (2020). *Tesla Model Y Range: Battery Preconditioning Makes A Huge Difference*. URL: <https://insideevs.com/news/461178/video-tesla-model-y-battery-preconditioning-range/>. (accessed: 17.05.2021).
- [24] Polestar. (2020). *Polestar 2 LCA*. URL: <https://www.polestar.com/dato-assets/11286/1600176185-20200915polestarlcafinala.pdf>.
- [25] Rebecca Lindsey (2020). *Climate Change: Atmospheric Carbon Dioxide*. URL: <https://www.climate.gov/news-features/understanding-climate/climate-change-atmospheric-carbon-dioxide>.
- [26] Reuters (2020). *Fossil fuel-based vehicle bans across the world*. URL: <https://www.reuters.com/article/climate-change-britain-factbox-idINKBN27Y19F>. (accessed: 25.04.2021).
- [27] Ritchie H. (2020). *Cars planes trains: where do CO2 emissions from transport come from?* URL: <https://ourworldindata.org/co2-emissions-from-transport>.
- [28] Ritchie H. (2020). *Sector by sector: where do global greenhouse gas emissions come from?* URL: <https://ourworldindata.org/ghg-emissions-by-sector>.
- [29] Ritchie H. Roser M. (2020). *Future greenhouse gas emissions*. URL: <https://ourworldindata.org/future-emissions>.
- [30] Ronald Li (2020). *What are Tipping Points in the Climate Crisis?* URL: <https://earth.org/what-are-tipping-points-in-the-climate-crisis/>.
- [31] Ruffo G. H. (2020). *How Much Does The Powertrain Represent Out Of Total Cost For An EV?* URL: <https://insideevs.com/features/396979/how-much-powertrain-cost-ev/>.
- [32] Sciencealert (2020). *We've Officially Passed The Threshold of 1.1 Degree Celsius Warming*. URL: <https://www.sciencealert.com/the-last-five-years-were-the-warmest-ever-recorded-again>.
- [33] Vanderverp. D (2020). *The Secret Adjustment Factor Tesla Uses to Get Its Big EPA Range Numbers*. URL: <https://www.caranddriver.com/features/a33824052/adjustment-factor-tesla-uses-for-big-epa-range-numbers/>. (accessed: 14.05.2021).

- [34] Walton R. (2020). *Electric vehicle models expected to triple in 4 years as declining battery costs boost adoption*. URL: <https://www.utilitydive.com/news/electric-vehicle-models-expected-to-triple-in-4-years-as-declining-battery/592061/>.
- [35] Adler K. IHS markit (2021). *IHS Markit forecasts global EV sales to rise by 70% in 2021*. URL: <https://ihsmarkit.com/research-analysis/ihm-markit-forecasts-global-ev-sales-to-rise-by-70-percent.html>.
- [36] BOSCH (2021). *Efficiency and comfort for electric vehicles*. URL: <https://www.bosch-mobility-solutions.com/en/solutions/thermal-management/thermal-management-for-hybrid-systems-and-electric-drives/>. (accessed: 09.05.2021).
- [37] CurrentResults (2021). *Weather Averages for European Cities*. URL: <https://www.currentresults.com/Weather/Europe/Cities/average-european-city-weather.php>. (accessed: 15.05.2021).
- [38] EV-database (2021). *About EV Database*. URL: <https://ev-database.uk/>. (accessed: 22.04.2021).
- [39] Dieselnet (2021). *Federal Test Procedure (FTP-75)*. URL: <https://dieselnet.com/standards/cycles/ftp75.php>. (accessed: 13.05.2021).
- [40] Dieselnet (2021). *Highway fuel economy test cycle (HWFET)*. URL: <https://dieselnet.com/standards/cycles/hwfet.php>. (accessed: 14.05.2021).
- [41] Dieselnet (2021). *New York City Cycle (NYCC)*. URL: <https://dieselnet.com/standards/cycles/nycc.php>. (accessed: 14.05.2021).
- [42] Dieselnet (2021). *Worldwide harmonized light vehicles testing procedure (WLTP)*. URL: <https://dieselnet.com/standards/cycles/wltp.php>. (accessed: 14.05.2021).
- [43] EPA (2021). *Automotive Trends Report*. URL: <https://www.epa.gov/automotive-trends/about-automotive-trends-data>. (accessed: 14.05.2021).
- [44] European Commision (2021). *CO₂ emission performance standards for cars and vans*. URL: https://ec.europa.eu/clima/policies/transport/vehicles/regulation_en. (accessed: 29.04.2021).
- [45] European Commision (2021). *EU climate action and the European Green Deal*. URL: https://ec.europa.eu/clima/policies/eu-climate-action_en. (accessed: 29.04.2021).
- [46] European Commision (2021). *Mobility Strategy A fundamental transport transformation: Commission presents its plan for green, smart and affordable mobility*. URL: https://ec.europa.eu/transport/themes/mobilitystrategy_en. (accessed: 29.04.2021).
- [47] ev specifications (2021). *Electric vehicle brands*. URL: <https://www.evspecifications.com/>. (accessed: 30.05.2021).
- [48] IEA (2021). *Global Energy Review: CO₂ Emissions in 2020, IEA, Paris*. URL: <https://www.iea.org/articles/global-energy-review-co2-emissions-in-2020>.
- [49] IEA (2021). *Global EV Outlook 2021, IEA, Paris*. URL: <https://www.iea.org/reports/global-ev-outlook-2021>.
- [50] Kane. M (2021). *Global Plug-In Electric Car Sales December 2020: Over 570,000 Sold*. URL: <https://insideevs.com/news/485298/global-plugin-car-sales-december-2020/>. (accessed: 16.05.2021).
- [51] MAHLE (2021). *MAHLE thermal management*. URL: <https://www.mahle.com/en/products-and-services/emobility/thermal-management/>. (accessed: 09.05.2021).
- [52] Nasa (2021). *The Effects of Climate Change*. URL: <https://climate.nasa.gov/effects/>.
- [53] Sunday times driving (2021). *CAR MAKERS ELECTRIC VEHICLE PLANS — A BRAND-BY-BRAND GUIDE*. URL: <https://www.driving.co.uk/news/new-cars/current-upcoming-pure-electric-car-guide-updated/>. (accessed: 25.04.2021).

- [54] UNFCCC (2021). *The Paris Agreement*. URL: <https://unfccc.int/process-and-meetings/the-paris-agreement/the-paris-agreement>.
- [55] Voelcker J. (2021). *Range Anxiety Is Very Real, New J.D. Power EVs Survey Finds*. URL: <https://www.forbes.com/wheels/news/range-anxiety-very-real-jd-power-evs-survey/>.
- [56] Wagner I. (2021). *Automotive industry worldwide - statistics facts*. URL: <https://www.statista.com/topics/1487/automotive-industry/>.
- [57] US Geological Survey. (2021). *Major countries in worldwide cobalt mine production from 2010 to 2020 (in metric tons) [Graph]*. URL: <https://www.statista.com/statistics/264928/cobalt-mine-production-by-country/>.
- [58] Argue C. (May 2020). *To what degree does temperature impact EV range?* (accessed: 24.04.2021).
- [59] AlixPartners (October 2021). *INTERNATIONAL ELECTRIC-VEHICLE CONSUMER SURVEY, Are battery electric vehicles here to stay?* URL: <https://www.alixpartners.com/media/13453/ap-electric-vehicle-consumer-study-2019.pdf>.
- [60] Doerr J. Attensperger T. Wittmann L. et al. "The New Electric Axle Drives from Audi." In: *ATZ Elektron Worldw* 13 (2018), pp. 16–23. DOI: <https://doi.org/10.1007/s38314-018-0040-y>.
- [61] Michel André. "The ARTEMIS European driving cycles for measuring car pollutant emissions". In: *Science of The Total Environment* 334-335 (2004). Highway and Urban Pollution, pp. 73–84. ISSN: 0048-9697. DOI: <https://doi.org/10.1016/j.scitotenv.2004.04.070>. URL: <https://www.sciencedirect.com/science/article/pii/S0048969704003584>.
- [62] Virtual Institute of Applied Science. *Stray load loss*. URL: http://www.vias.org/kimberlyee/ee_14_05.html. (accessed: 06.05.2021).
- [63] Arfa Grunditz. E (2014). *BEV Powertrain Component Sizing With Respect to Performance, Energy Consumption and Driving Patterns, Lic thesis, Chalmers Univeristy of Technology, Gothenburg*. URL: <http://www.chalmers.se/SiteCollectionDocuments/Energi%5C%20och%5C%20milj%5C%C3%5C%B6/Elteknik/EmmasLicReport.pdf%7D>.
- [64] Aurich J. Baumgart R (2018). *Comparison and Evaluation of different A/C Compressor Concepts for Electric Vehicles, International compressor engineering conference*. URL: <https://docs.lib.purdue.edu/cgi/viewcontent.cgi?article=3607&context=icec>.
- [65] Barnitt. R, Brooker. A, Ramroth. L, John Rugh, Kandler A. Smith (2010). *Analysis of Off-Board Powered Thermal Preconditioning in Electric Drive Vehicles*. URL: <https://www.nrel.gov/docs/fy11osti/49252.pdf>.
- [66] "Battery warm-up methodologies at subzero temperatures for automotive applications: Recent advances and perspectives". In: *Progress in Energy and Combustion Science* 77 (2020), p. 100806. ISSN: 0360-1285. DOI: <https://doi.org/10.1016/j.pecs.2019.100806>. URL: <https://www.sciencedirect.com/science/article/pii/S0360128519301169>.
- [67] BatteryUniversity. *Charging at High and Low Temperatures*. URL: https://batteryuniversity.com/learn/article/charging_at_high_and_low_temperatures. (accessed: 03.05.2021).
- [68] BatteryUniversity. *Discharging at High and Low Temperatures*. URL: https://batteryuniversity.com/learn/article/discharging_at_high_and_low_temperatures. (accessed: 03.05.2021).
- [69] BatteryUniversity. *How to Prolong Lithium-based Batteries*. URL: https://batteryuniversity.com/index.php/learn/article/how_to_prolong_lithium_based_batteries. (accessed: 05.05.2021).
- [70] BatteryUniversity. *What Causes Li-ion to Die?* URL: https://batteryuniversity.com/index.php/learn/article/bu_808b_what_causes_li_ion_to_die. (accessed: 05.05.2021).
- [71] Bengt Jacobson et al. *Vehicle Dynamics Compendium*. URL: https://research.chalmers.se/publication/520229/file/520229_Fulltext.pdf. (accessed: 04.05.2021).

- [72] Bjorn Nyland (2020 February 18). *How battery temperature affects performance [Youtube Video]*. URL: <https://www.youtube.com/watch?v=dfSTR6i5H8k>.
- [73] Lars-Henrik Björnsson and Sten Karlsson. "The potential for brake energy regeneration under Swedish conditions". In: *Applied Energy* 168 (2016), pp. 75–84. ISSN: 0306-2619. DOI: <https://doi.org/10.1016/j.apenergy.2016.01.051>. URL: <https://www.sciencedirect.com/science/article/pii/S0306261916300319>.
- [74] April 9) Buysse C. Miller J. (2021). *Transport could burn up the EU's entire carbon budget. ICCT staff blog*. URL: <https://theicct.org/blog/staff/eu-carbon-budget-apr2021>.
- [75] Dafen Chen et al. "Comparison of different cooling methods for lithium ion battery cells". In: *Applied Thermal Engineering* 94 (2016), pp. 846–854. ISSN: 1359-4311. DOI: <https://doi.org/10.1016/j.applthermaleng.2015.10.015>. URL: <https://www.sciencedirect.com/science/article/pii/S1359431115010613>.
- [76] Qiaoyan Chen et al. "A simply designed and universal sliding mode observer for the SOC estimation of Lithium-ion batteries". In: *IET Power Electronics* 10 (Jan. 2017). DOI: 10.1049/iet-pel.2016.0095.
- [77] International Council on Clean Transportation. *The role of the European Union's vehicle CO₂ standards in achieving the European Green Deal*. URL: <https://theicct.org/sites/default/files/publications/EU-vehicle-standards-green-deal-mar21.pdf>.
- [78] International Council on Clean Transportation. *A strategy to decarbonize the global transport sector by mid-century*. URL: https://theicct.org/sites/default/files/publications/ICCT_Vision2050_sept2020.pdf.
- [79] Climate and Clean Air Coalition. *What are short-lived climate pollutants?* URL: <https://www.ccacoalition.org/en/slcps/black-carbon>. (accessed: 30.04.2021).
- [80] M.Atshaya Mohan Dr.A.Sheela. "Design Of Permanent Magnet Synchronous Motor For Electric Vehicle Application Using Finite Element Analysis". In: *INTERNATIONAL JOURNAL OF SCIENTIFIC TECHNOLOGY RESEARCH* 9.03 (2020), pp. 523–524. URL: <http://www.ijstr.org/final-print/mar2020/Design-Of-Permanent-Magnet-Synchronous-Motor-For-Electric-Vehicle-Application-Using-Finite-Element-Analysis.pdf>.
- [81] Earthcharts. *Emissions sources*. URL: <http://earthcharts.org/emissions-sources/%7D>. (accessed: 04.05.2021).
- [82] electrnoisnotes. *Li-ion Lithium Ion Battery Charging*. URL: https://www.electronics-notes.com/articles/electronic_components/battery-technology/li-ion-lithium-ion-charging.php. (accessed: 03.05.2021).
- [83] EngineeringToolBox. *Air - Density, Specific Weight and Thermal Expansion Coefficient at Varying Temperature and Constant Pressures*. URL: https://www.engineeringtoolbox.com/air-density-specific-weight-d_600.html. (accessed: 05.05.2021).
- [84] Fardad Niknam (2019). *The Science Behind Rolling Resistance in Passenger Tires*. URL: <https://www.tirereview.com/science-behind-rolling-resistance-passenger-tires/>. (accessed: 05.05.2021).
- [85] Allen A. Fawcett et al. "Can Paris pledges avert severe climate change?" In: *Science* 350.6265 (2015), pp. 1168–1169. ISSN: 0036-8075. DOI: 10.1126/science.aad5761. eprint: <https://science.sciencemag.org/content/350/6265/1168.full.pdf>. URL: <https://science.sciencemag.org/content/350/6265/1168>.
- [86] Globalgoals. *THE GLOBAL GOALS*. URL: <https://www.globalgoals.org/>.
- [87] Greg Goetchius. *Leading the Charge – The Future of Electric Vehicle Noise Control*. URL: <http://www.sandv.com/downloads/1104goet.pdf>. (accessed: 05.05.2021).

- [88] Wolf-Heinrich Hucho. "Chapter 1 - Introduction to automobile aerodynamics". In: *Aerodynamics of Road Vehicles*. Ed. by Wolf-Heinrich Hucho. Butterworth-Heinemann, 1987, pp. 1–46. ISBN: 978-0-7506-1267-8. DOI: <https://doi.org/10.1016/B978-0-7506-1267-8.50005-1>. URL: <https://www.sciencedirect.com/science/article/pii/B9780750612678500051>.
- [89] Jandaud. P-O, Le Besnerais. J (2017). *Heat transfer in electric machines, [Webinar]*, URL: <https://www.slideshare.net/sustenergy/cooling-of-electric-motors>.
- [90] S. Lam A. et al. Knobloch F. Hanssen. "Net emission reductions from electric cars and heat pumps in 59 world regions over time." In: *Nat Sustain* 3, 437-447 (2020). (). DOI: <https://doi.org/10.1038/s41893-020-0488-7>.
- [91] Larsson. J, Lindström. M (2019). *Development and Evaluation of Internal PMSM Cooling for Electrified Vehicles, MSc thesis, Chalmers Univeristy of Technology, Gothenburg*. URL: <https://publications.lib.chalmers.se/records/fulltext/200046/200046.pdf>.
- [92] Andrzej Lebkowski. "Temperature, Overcharge and Short-Circuit Studies of Batteries used in Electric Vehicles". In: *Przegląd Elektrotechniczny* 1 (May 2017). DOI: 10.15199/48.2017.05.13.
- [93] Li.J, Zhu.Z (2014). *Battery Thermal Management Systems of Electric Vehicles, MSc thesis, Chalmers Univeristy of Technology, Gothenburg*. URL: <https://publications.lib.chalmers.se/records/fulltext/200046/200046.pdf>.
- [94] Kaizhi Liang et al. "Data-Driven Ohmic Resistance Estimation of Battery Packs for Electric Vehicles". In: *Energies* 12 (Dec. 2019). DOI: 10.3390/en12244772.
- [95] Ziyue Ling et al. "A hybrid thermal management system for lithium ion batteries combining phase change materials with forced-air cooling". In: *Applied Energy* 148 (2015), pp. 403–409. ISSN: 0306-2619. DOI: <https://doi.org/10.1016/j.apenergy.2015.03.080>. URL: <https://www.sciencedirect.com/science/article/pii/S0306261915003827>.
- [96] Kai Liu et al. "Materials for lithium-ion battery safety". In: *Science Advances* 4 (June 2018), eaas9820. DOI: 10.1126/sciadv.aas9820.
- [97] Shuai Ma et al. "Temperature effect and thermal impact in lithium-ion batteries: A review". In: *Progress in Natural Science: Materials International* 28.6 (2018), pp. 653–666. ISSN: 1002-0071. DOI: <https://doi.org/10.1016/j.pnsc.2018.11.002>. URL: <https://www.sciencedirect.com/science/article/pii/S1002007118307536>.
- [98] Asma Mohamad Aris and Bahman Shabani. "An Experimental Study of a Lithium Ion Cell Operation at Low Temperature Conditions". In: *Energy Procedia* 110 (Mar. 2017), pp. 128–135. DOI: 10.1016/j.egypro.2017.03.117.
- [99] Office of Energy Efficiency Renewable Energy. *How Does a Lithium-ion Battery Work?* URL: <https://www.energy.gov/eere/articles/how-does-lithium-ion-battery-work?>. (accessed: 02.05.2021).
- [100] Myeong Hyeon Park and Sung Kim. "Heating Performance Enhancement of High Capacity PTC Heater with Modified Louver Fin for Electric Vehicles". In: *Energies* 12 (July 2019), p. 2900. DOI: 10.3390/en12152900.
- [101] Polestar. *Polestar 2 [press kit]*. URL: <https://www.polestar.com/bynder-assets/m/3b46df57d0e5580c>.
- [102] B. Sakhdari and N.L. Azad. "An Optimal Energy Management System for Battery Electric Vehicles". In: *IFAC-PapersOnLine* 48.15 (2015). 4th IFAC Workshop on Engine and Powertrain Control, Simulation and Modeling E-COSM 2015, pp. 86–92. ISSN: 2405-8963. DOI: <https://doi.org/10.1016/j.ifacol.2015.10.013>. URL: <https://www.sciencedirect.com/science/article/pii/S2405896315018893>.

- [103] Schellnhuber Hans Joachim; Whiteman Gail; Rockström Johan; Hobley Anthony; Rahmstorf Stefan. “Three years to safeguard our climate”. In: *Nature* 546.7660 (2017), pp. 593–595. ISSN: 0028-0836. DOI: 10.1038/546593a. URL: <https://www.nature.com/news/three-years-to-safeguard-our-climate-1.22201>.
- [104] Bengt Sundén. “Chapter 6 - Thermal management of batteries”. In: *Hydrogen, Batteries and Fuel Cells*. Ed. by Bengt Sundén. Academic Press, 2019, pp. 93–110. ISBN: 978-0-12-816950-6. DOI: <https://doi.org/10.1016/B978-0-12-816950-6.00006-3>. URL: <https://www.sciencedirect.com/science/article/pii/B9780128169506000063>.
- [105] Sundén. B (2020). *Battery Thermal Management Systems BTMS, [Lecture Notes], Hydrogen, batteries and fuel cells TFRD60, Lund Univeristy, Delivered 10 August 2020*.
- [106] tec-science. *Drag coefficient (friction and pressure drag)*. URL: <https://www.tec-science.com/mechanics/gases-and-liquids/drag-coefficient-friction-and-pressure-drag/>. (accessed: 05.05.2021).
- [107] Technische Universitaet Muenchen (2014). *Lithium-ion batteries: Phenomenon of 'lithium plating' during the charging process observed, ScienceDaily*. URL: <https://www.sciencedaily.com/releases/2014/09/140903105638.htm>. (accessed: 05.05.2021).
- [108] Transport and Environment. (2020). *How clean are electric cars? TE's analysis of electric car lifecycle CO₂ emissions*. URL: <https://www.transportenvironment.org/sites/te/files/downloads/T%26E%E2%80%99s%20EV%20life%20cycle%20analysis%20LCA.pdf>.
- [109] Transport and Environment. (2017 October 26). *Electric cars emit less CO₂ over their lifetime than diesels even when powered with dirtiest electricity – study [press release]*. URL: <https://www.transportenvironment.org/press/electric-cars-emit-less-co2-over-their-lifetime-diesels-even-when-powered-dirtiest-electricity>.
- [110] November 19) United Nations Framework Convention on Climate Change. (2019). *Cut Global Emissions by 7.6 Percent Every Year for Next Decade to Meet 1.5°C Paris Target - UN Report [press release]*. URL: <https://unfccc.int/news/cut-global-emissions-by-76-percent-every-year-for-next-decade-to-meet-15degc-paris-target-un-report>.
- [111] Mario Vražić, Oriana Barić, and Peter Virtic. “Auxiliary systems consumption in electric vehicle”. In: *Przegląd Elektrotechniczny* 12 (Dec. 2014), pp. 172–175. DOI: 10.12915/pe.2014.12.42.
- [112] Wappelhorst S. International Council on Clean Transportation (March 2021). *On the electrification path: Europe's progress towards clean transportation*. URL: <https://www.eafo.eu/sites/default/files/2021-03/EAF0%20Europe%20on%20the%20electrification%20path%20March%202021.pdf>.
- [113] WeberAuto (2018 December 11). *Chevrolet Bolt EV Coolant System Loops [Youtube Video]*. URL: https://www.youtube.com/watch?v=_ILkLUE3Zxc.
- [114] Wesley D. (November 2017). *How Electric Cars Work*. URL: <https://www.quote.com/auto-insurance/electric-cars/>. (accessed: 25.04.2021).
- [115] Wikner. E (2017). *Lithium ion Battery Aging: Battery Lifetime Testing and Physics-based Modeling for Electric Vehicle Applications, LIC thesis, Chalmers Univeristy of Technology, Gothenburg*. URL: <https://publications.lib.chalmers.se/records/fulltext/249356/249356.pdf>.
- [116] Steve Windsor. “Real World Drag Coefficient – Is It Wind Averaged Drag?” In: Oct. 2014. ISBN: 9780081001998. DOI: 10.1533/9780081002452.1.3.
- [117] Shaoshen Xue et al. “A New Iron Loss Model for Temperature Dependencies of Hysteresis and Eddy Current Losses in Electrical Machines”. In: *IEEE Transactions on Magnetics* 54.1 (2018), pp. 1–10. DOI: 10.1109/TMAG.2017.2755593.

- [118] Jianfeng Yu, Ting Zhang, and Jianming Qian. “6 - Testing methods for electric motors”. In: *Electrical Motor Products*. Ed. by Jianfeng Yu, Ting Zhang, and Jianming Qian. Woodhead Publishing, 2011, pp. 95–172. ISBN: 978-0-85709-077-5. DOI: <https://doi.org/10.1533/9780857093813.95>. URL: <https://www.sciencedirect.com/science/article/pii/B9780857090775500062>.

Appendice A - Amesim

In this section additional figures from Amesim are presented, including simulation results and full scale figures of the model.

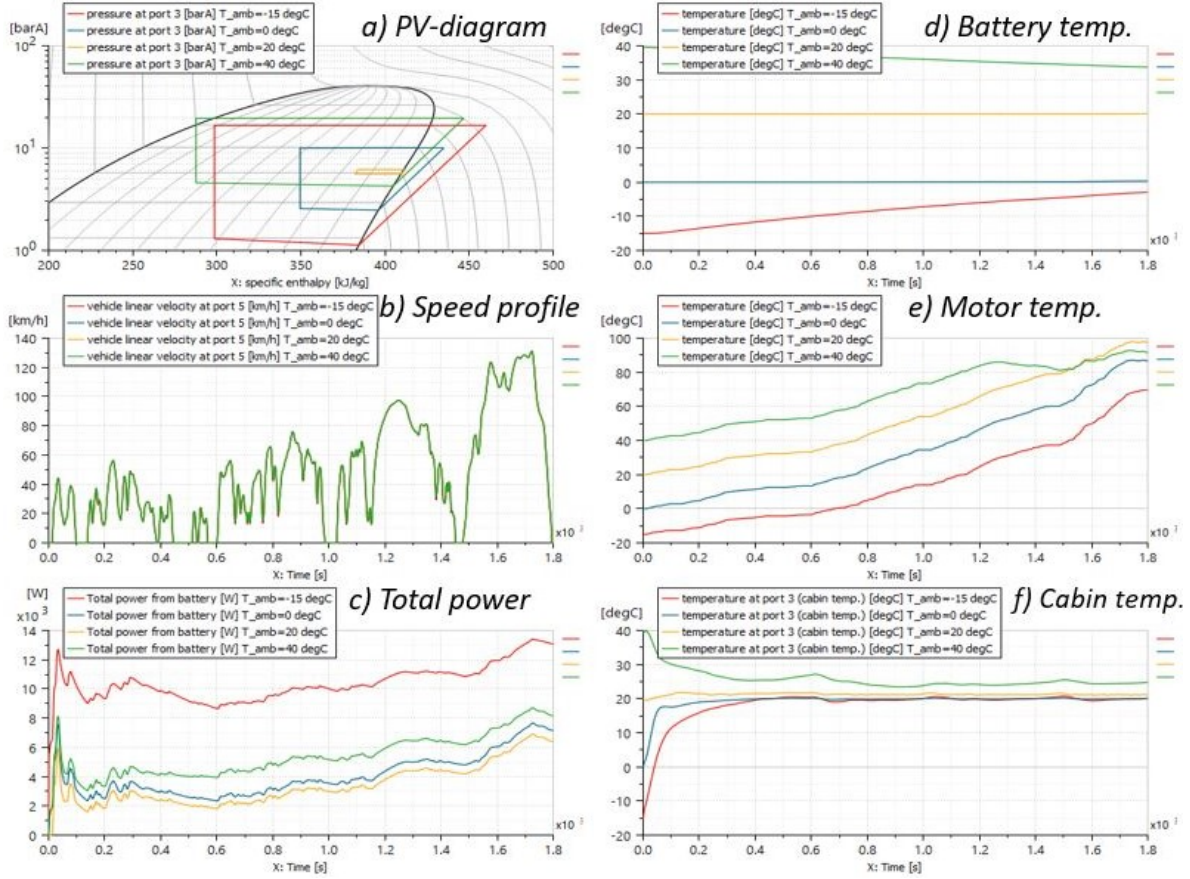


Figure 78: WLTP simulation result parameters from Amesim

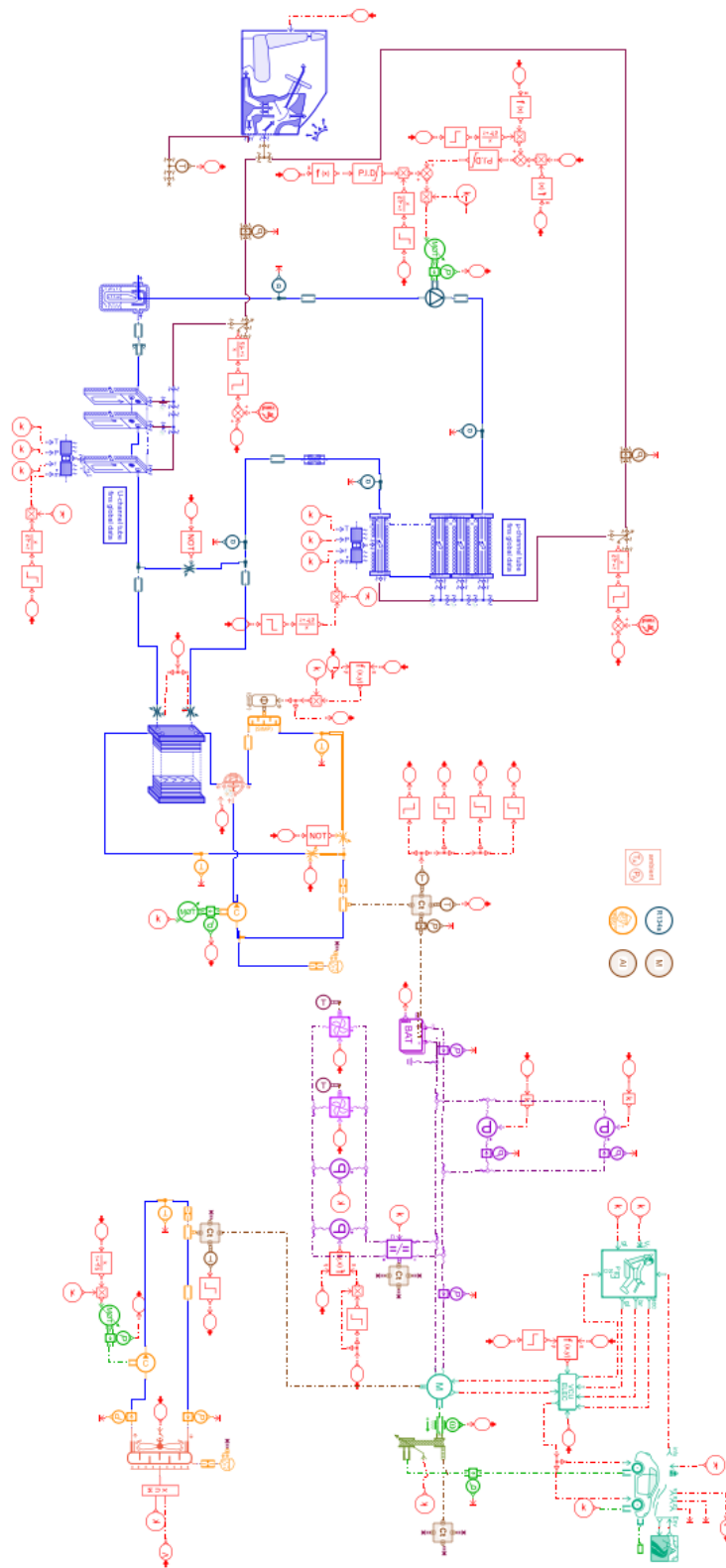


Figure 79: Amesim model V.5

Appendice B - Vehicle Parameters

In this section the vehicle parameters used in the validation process is presented. The parameters are gathered from [38], [47] and official webpages from the manufacturers.

Table 15: Mazda mx30 parameters

Model	Mazda mx30
Curb weight	1765 kg
Battery (cell) mass	142 kg
Battery capacity (usable)	35.5 (30) kWh
Battery voltage, architecture	350V, 96s3p
Power, torque and speed	107 kW, 271 Nm, 11000 RPM
Tire dimensions [W/H-R]	215/55-R18
Cd, A	0.29, 2.35 m^2
Gear ratio	10.3

Table 16: Honda e parameters

Model	Honda e
Curb weight	1514 kg
Battery (cell) mass	142 kg
Battery capacity (usable)	35 (29.5) kWh
Battery voltage, architecture	350V, 96s3p
Power, torque and speed	100 kW, 315 Nm, 10000 RPM
Tire dimensions [W/H-R]	205/55-R16
Cd, A	0.27, 2.25 m^2
Gear ratio	8.2

Table 17: Peugeot 208e parameters

Model	Peugeot 208e
Curb weight	1564 kg
Battery (cell) mass	200 kg
Battery capacity (usable)	50 (45) kWh
Battery voltage, architecture	350V, 96s3p
Power, torque and speed	100 kW, 260 Nm, 10000 RPM
Tire dimensions [W/H-R]	205/45-R17
Cd, A	0.29, 2.1 m^2
Gear ratio	7.75

Table 18: Renault zoe parameters

Model	Renault zoe
Curb weight	1577 kg
Battery (cell) mass	219 kg
Battery capacity (usable)	54.7 (52) kWh
Battery voltage, architecture	350V, 96s2p
Power, torque and speed	100 kW, 245 Nm, 11000 RPM
Tire dimensions [W/H-R]	215/55-R16
Cd, A	0.32, 2.3 m^2
Gear ratio	9.6

Table 19: Volkswagen ID.3 parameters

Model	Volkswagen ID.3
Curb weight	1806 kg
Battery (cell) mass	248 kg
Battery capacity (usable)	62 (58) kWh
Battery voltage, architecture	350V, 96s3p
Power, torque and speed	150 kW, 310 Nm, 16000 RPM
Tire dimensions [W/H-R]	215/55-R18
Cd, A	0.267, 2.35 m^2
Gear ratio	10

Table 20: Volvo xc40 recharge parameters

Model	Volvo xc40 recharge (AWD)
Curb weight	2188 kg
Battery (cell) mass	312 kg
Battery capacity (usable)	78 (75) kWh
Battery voltage, architecture	400V, 108s3p
Power, torque and speed	150+150 kW, 330+330 Nm, 12000 RPM
Tire dimensions [W/H-R]	235/45-R20
Cd, A	0.34, 2.5 m^2
Gear ratio	9.02

Table 21: Tesla model 3 SR+ parameters

Model	Tesla model 3 SR+
Curb weight	1611 kg
Battery (cell) mass	215 kg
Battery capacity (usable)	53.6 (51) kWh
Battery voltage, architecture	360V, 99s31p
Power, torque and speed	211 kW, 375 Nm, 18000 RPM
Tire dimensions [W/H-R]	235/45-R19
Cd, A	0.23, 2.22 m^2
Gear ratio	9.0

Table 22: Tesla model Y LR parameters

Model	Tesla model Y LR (AWD)
Curb weight	2003 kg
Battery (cell) mass	296 kg
Battery capacity (usable)	75 (72.5) kWh
Battery voltage, architecture	350V, 96s46p
Power, torque and speed	150+150 kW, 275+275 Nm, 18000 RPM
Tire dimensions [W/H-R]	255/45-R19
Cd, A	0.23, 2.3 m^2
Gear ratio	9.1

Table 23: Volkswagen ID.4 parameters

Model	Volkswagen ID.4
Curb weight	2049 kg
Battery (cell) mass	328 kg
Battery capacity (usable)	82 (77) kWh
Battery voltage, architecture	350V, 96s3p
Power, torque and speed	150 kW, 310 Nm, 16000 RPM
Tire dimensions [W/H-R]	255/45-R20
Cd, A	0.28, 2.5 m^2
Gear ratio	10

Table 24: Hyundai kona parameters

Model	Hyundai kona
Curb weight	1685 kg
Battery (cell) mass	270 kg
Battery capacity (usable)	67.5 (64) kWh
Battery voltage, architecture	356V, 98s3p
Power, torque and speed	150 kW, 395 Nm, 10500 RPM
Tire dimensions [W/H-R]	215/55-R17
Cd, A	0.29, 2.3 m^2
Gear ratio	7.98

Table 25: Audi e-tron parameters

Model	Audi e-tron 55 (AWD)
Curb weight	2595 kg
Battery (cell) mass	380 kg
Battery capacity (usable)	95 (86.5) kWh
Battery voltage, architecture	396V, 108s4p
Power, torque and speed	165+135 kW, 355+309 Nm, 12000 RPM
Tire dimensions [W/H-R]	255/55-R19
Cd, A	0.29, 2.75 m^2
Gear ratio	9.2

Table 26: Tesla model X parameters

Model	Tesla model X (AWD)
Curb weight	2554 kg
Battery (cell) mass	400 kg
Battery capacity (usable)	100 (95) kWh
Battery voltage, architecture	400V, 110s64p
Power, torque and speed	193+193 kW, 330+30 Nm, 16000 RPM
Tire dimensions [W/H-R]	265/45-R20
Cd, A	0.25, 2.9 m^2
Gear ratio	9.3

Table 27: Mercedes EQS 450+ parameters

Model	Mercedes EQS 450+
Curb weight	2480 kg
Battery (cell) mass	245 kg
Battery capacity (usable)	115 (108) kWh
Battery voltage, architecture	395V, 108s3p
Power, torque and speed	245 kW, 568 Nm, 12000 RPM
Tire dimensions [W/H-R]	265/45-R20
Cd, A	0.2, 2.75 m^2
Gear ratio	8.2

